# The Identification of the mTOR-Regulated Phosphoproteome and a Mediator of Feedback Inhibition to PI3K-Akt



by

Peggy Ping Hsu

A.B. Molecular Biology
Princeton University, 2003

SUBMITTED TO THE DEPARTMENT OF BIOLOGY IN PARTIAL FULFULLMENT OF THE REQUIREMENTS FOR THE DEGREE OF

DOCTOR OF PHILOSOPHY IN BIOLOGY
AT THE
MASSACHUSETTS INSTITUTE OF TECHNOLOGY



JUNE 2011



Signature of Author: ___

Department of Biology
April 27, 2011

Certified by: _____

David M. Sabatini
Associate Professor of Biology
Member, Whitehead Institute for Biomedical Research
Thesis Supervisor

Accepted by: _____

Stephen P. Bell
Professor of Biology
Co-Chair, Committee for Graduate Students

The Identification of the mTOR-Regulated Phosphoproteome and a Mediator of Feedback Inhibition to PI3K-Akt

by

Peggy Ping Hsu

Submitted to the Department of Biology on April 27, 2011 in Partial Fulfillment of the Requirements for the Degree of Doctor of Philosophy in Biology

## ABSTRACT

The mTOR protein kinase nucleates two complexes, mTORC1 and mTORC2. Collectively, the two complexes regulate processes important for cell growth and proliferation, including protein synthesis, autophagy, metabolism, and cytoskeletal maintenance. Despite this diverse array of cellular functions, few mTOR substrates are known. To address this deficit, we defined the mTOR-regulated phosphoproteome by quantitative mass spectrometry and characterized the primary sequence motif specificity of mTOR using positional scanning peptide libraries. We found that the phosphorylation response to insulin is largely mTOR-dependent and that mTOR regulates the phosphorylation of many proteins not presently appreciated to be linked to mTOR signaling. The mTOR kinase, moreover, exhibits a preference for proline, hydrophobic, and aromatic residues at the +1 position which is unique among all kinases previously profiled. Grb10 is an adaptor protein and negative regulator of growth factor signaling identified as an mTORC1 substrate that mediates the inhibition of PI3K typical of cells lacking TSC2, a tumor suppressor and negative regulator of mTORC1. Phosphorylation of Grb10 is important for its inhibitory function as well as for its stability. While acute mTORC1 inhibition results in changes in Grb10 and IRS1 phosphorylation which partially reactivates Akt in TSC2-null cells, chronic mTORC1 inhibition causes Grb10 destabilization, IRS protein stabilization, and a complete resensitization of Akt to insulin and IGF-1. These changes in Grb10 and IRS protein abundance are likely to be the most important effects of mTOR inhibitors to consider in their clinical use. Finally, the discovery of Grb10 as an mTORC1 substrate validates our phosphoproteomic approach and suggests that the other potential downstream effectors we identified may also serve as starting points for new areas of investigation in mTOR biology.

Thesis Supervisor: David M. Sabatini
Title: Associate Professor of Biology, MIT; Member, Whitehead Institute for Biomedical Research

For my parents

## Acknowledgments

I cannot sufficiently express my gratitude and respect for my advisor, David Sabatini. He is the scientist that I could only wish to become: insightful, creative, intelligent, fearless, and efficient. I especially appreciate that David gave me the freedom to follow my own path while focusing me when I had wandered astray.

I am also grateful to have had Mike Yaffe and Mike Hemann on my thesis committee for the past few years. I have learned quite a bit from them in both my formal meetings as well as in casual conversations. I must also thank Brendan Manning, whose work I have long admired, and Piyush Gupta for being on my defense committee.

David has built a lab of bright, fun, and ambitious people, and I have enjoyed working with every single one of them. Siraj first introduced me to the lab, and Dos showed me how to properly Western blot. The graduate students who came before me - Shomit, Tim, and Yasemin - inspired me with their hard work and independence. Tony has been a fantastic collaborator, and from him I learned how to be a more efficient experimentalist. I have enjoyed conversations with Dudley over coffee, and Do and Yoav in tissue culture. Carson has also become a close friend in the lab. He is a person whose scientific advice I value enormously and also someone who I have enjoyed getting to know over the past few years. I respect him not only for his intellect but also the manner in which he lives his life.

I especially want to acknowledge Kathleen and Heather. I do not know what I did to deserve Kathleen's help, but I have immensely enjoyed working with her. Her thirst for learning and self-improvement are inspiring. She has given me great life advice and constant encouragement. And Heather has been a great friend in the lab. I too admire her for her independence and assertiveness, but also for her loyalty to friends and excitement about both the little and small things in life. I have really enjoyed coming to work knowing that I have a friend as a baymate.

I would like to thank my PhD classmates, MD classmates, the many amazing people working at the Whitehead, and friends I have met along the way for their

support. Lauren and Derek have been amazing friends, and in Lauren I am so thankful to have found a friend with whom I can share all aspects of the MD PhD journey. I also have to thank Renuka, Jasper, Vincent, and Michelle for their help, friendship, and commiseration.

Through it all, Dan has been my best friend, and I have enjoyed sharing life and science with him. I admire the ways he thinks about scientific problems and his generous, patient, and caring nature. I do not know what I would do without him, or how I would have finished this thesis!

Finally, I would like to thank my family. While they were not part of the day-to-day aspects of the PhD, knowing that they believed in me and were there for me no matter what was a great source of strength and comfort. I see myself in them, and know that I would not be where I am without them.

# Table of Contents

## Appendix

### Cancer Cell Metabolism: Warburg and Beyond

# Chapter 1

# Introduction

## Summary

Beginning with the fortuitous discovery of the macrolide antibiotic rapamycin isolated from bacteria inhabiting the soil of Easter Island, the study of the target of rapamycin, TOR, has led to a greater understanding of the diverse processes cumulatively integrated into cell growth. TOR is a highly conserved serine-threonine kinase, and the mammalian orthologue, mTOR, is the catalytic component of two multi-protein complexes, mTOR complex 1 and mTOR complex 2. mTORC1 and mTORC2 are both regulated by growth factors while mTORC1 is additionally regulated by amino acids, hypoxia, and energetic stress. The two complexes exhibit distinct substrate repertoires, with mTORC1 phosphorylating key factors for translation initiation and autophagy and mTORC2 acting on regulators of cellular survival and proliferation.

Dysregulation of the mTOR pathway has been implicated in genetic hamartoma syndromes exemplified by outgrowths, which, while generally benign, cause significant morbidity and can occasionally lead to cancerous lesions. mTOR hyperactivation has also been implicated in spontaneous cancers, and the role of mTOR in metabolic processes central to diabetes is now appreciated to be multi-faceted and complex.

Given its disease relevance, there has been much interest in finding ways to modulate mTOR function by targeting specific components upstream, downstream, and at the level of the kinase. While the allosteric inhibitor rapamycin is the founding member of mTOR inhibitors now employed widely as immunosuppressants and lucratively as anti-stenosis agents in drug-eluting stents, it is now appreciated that rapamycin only partially - both qualitatively and quantitatively - inhibits mTORC1. Therefore, the recent development of kinase domain inhibitors of mTOR that inhibit both complexes has increased the likelihood of more effective anti-mTOR agents in the clinic.

In this introductory chapter, the current understanding of the complicated signaling network with mTOR at its center will be reviewed. Emphasis will be placed on the aspects of the pathway most relevant to the work described in subsequent chapters.

## Rapamycin and its molecular target

### The discovery of the target of rapamycin

Rapamycin is a macrocyclic polyketide isolated from *Streptomyces hygroscopicus* inhabiting the soil of Easter Island, also known in Polynesian as Rapa Nui, or "Big Rapa" (Abraham and Wiederrecht, 1996). While it was originally appreciated to have antifungal properties (Sehgal et al., 1975), its potent anti-proliferative effects on cells of the immune system were noticed and rapamycin was developed as an immunosuppressant (Morris et al., 1990).

The identification of the target of rapamycin was accomplished genetically in yeast and biochemically in mammalian cells – a common theme in the history of the field. In *Saccharomyces cerevisiae*, rapamycin causes a profound G1 arrest and was used in genetic screens to identify genes whose mutations led to resistance to the arrest caused by rapamycin. Mutations in the gene encoding the peptidyl-prolyl cis-trans isomerase FKBP12 (also known as FPR or RBP1) rendered yeast cells indifferent to the effects of rapamycin (Heitman et al., 1991; Koltin et al., 1991).

Rapamycin, FK506, and cyclosporin A are all immunosuppressants and share a unique mechanism of action despite inhibiting different steps in T-cell activation (Abraham and Wiederrecht, 1996). Rapamycin and FK506 are macrolides while cyclosporin A is a cyclic peptide. Before their direct targets were known, it had been appreciated that FK506 and cyclosporin A both inhibited transcription downstream of the transcription factor NFAT while rapamycin blocked a later step in T-cell activation: proliferation in response to the interleukin-2 cytokine. All three drugs bind to intracellular proline isomerases called immunophilins. Cyclosporin A binds cyclophilin A while FK506 and rapamycin both bind FKBP12.

Binding of rapamycin, FK506, and cyclosporin A to their respective immunophilins inhibited proline isomerase activity (Abraham and Wiederrecht, 1996). However, several

pieces of evidence suggested that it was not the inhibition of the immunophilin which caused the cellular effects of these drugs, but that it was the drug: immunophilin complex which was toxic. First, the drugs are toxic at concentrations which do not saturate immunophilin binding (Bierer et al., 1990a). Second, both FK506 and rapamycin bind FKBP12 but affect different steps of T cell activation (Bierer et al., 1990a). Third, related compounds which inhibit isomerase activity do not result in arrest (Bierer et al., 1990b). Finally, as the absence of the immunophilin does not phenocopy drug treatment (Heitman et al., 1991), it was determined that they were not the real targets. Rather, in the case of rapamycin, rapamycin binds to FKBP12 and together the two form a complex that inhibits the cellular target responsible for the proliferation arrest. In addition to FKBP12, mutations in two genes, TOR1 and TOR2, named for the target of rapamycin, were also found to render yeast cells resistant to rapamycin (Heitman et al., 1991). While TOR1 and TOR2 were suspected to be the true targets of rapamycin, direct evidence awaited biochemical verification.

Given that rapamycin-FKBP12 were thought to bind and inhibit the true target of rapamycin, several groups concurrently purified mammalian TOR, mTOR, (also known as FKBP12-rapamycin associated protein (FRAP) and rapamycin and FKBP12 target 1 (RAFT1)) using the rapamycin-FKBP12 complex as a biochemical handle (Brown et al., 1994; Sabatini et al., 1994; Sabers et al., 1995). mTOR belongs to the phosphatidylinositol-3 kinase-related kinase (PIKK) family, along with the DNA damage kinases ataxia-telangiectasia mutated (ATM), ataxia- and Rad3-related (ATR), and DNA-dependent protein kinase (DNA-PK), suppressor of morphogenesis in genitalia (SMG1) which is involved in nonsense-mediated mRNA decay and transformation/transcription domain-associated protein (TRRAP) (Lempiainen and Halazonetis, 2009) (Fig. 1). While they share a homologous domain to the lipid kinase phosphatidylinositide-3-kinase (PI3K), except for TRRAP, they are all protein kinases which phosphorylate serine and threonine. The adaptor protein TRRAP shares homology with the other members but lacks kinase activity.

All PIKK family members are large, with mTOR being a zaftig 289 kDa. The

family members share several common domains. A FRAP, ATM, and TRRAP (FAT) domain is always accompanied by a C-terminal FAT-C domain (Lempiainen and Halazonetis, 2009). Both are required for mTOR kinase activity through unclear mechanisms (Bosotti et al., 2000). The kinase domain of mTOR, like the other members of the PIKK family, is more homologous to lipid kinases than to protein kinases (Manning et al., 2002b). The PIKK regulatory domain is required for activity but deletion of parts of the domain can lead to increased kinase activity (Sekulic et al., 2000). Finally, the FBKP12-rapamycin binding (FRB) domain of mTOR is situated between its FAT and kinase domain (Chen et al., 1995; Choi et al., 1996; Stan et al., 1994), and two stretches of HEAT (huntingtin, elongation factor 3, the A subunit of protein phosphatase 2A, and TOR) repeats present in the N-terminus mediate protein-protein interactions (Perry and Kleckner, 2003).

ATM, ATR, DNA-PK, and SMG-1 are all involved in nucleotide repair and share a similar phosphoacceptor motif: (S*/T*)Q (where * indicates the phosphoacceptor residue) (Abraham, 2002). A consensus motif for mTOR however has not been described. In known substrates, mTOR either phosphorylates a hydrophobic motif (HM) present in AGC kinases or proline-directed sites (proline in the +1 position relative to the phosphoacceptor residue) (Fig. 2) (Brunn et al., 1997a; Burnett et al., 1998; Isotani et al., 1999). How mTOR can phosphorylate these distinct motifs is the subject of a later chapter.

**Two mTOR complexes**

Yeast have two TOR genes, TOR1 and TOR2. TOR1 is inessential, while TOR2 is essential (Kunz et al., 1993). In yeast, it was discovered that the TOR proteins form two distinct complexes, TOR complex 1 (TORC1) and TOR complex 2 (TORC2) (Loewith et al., 2002). Yeast TORC1 is sensitive to inhibition by rapamycin and consists of either Tor1p or Tor2p, kontroller of growth 1 (Kog1p), and lethal with SEC13 protein 8 (Lst8p). Yeast TORC2 is rapamycin-insensitive and consists of Tor2p, adheres voraciously to TOR2 1 (Avo1p), Avo2p, Avo3p, and Lst8p.

The two complex organization is conserved from yeast to man. Although the mammalian TOR protein is encoded by one gene, mTOR still nucleates two complexes (Fig. 3). mTOR complex 1 (mTORC1) consists of regulatory associated protein of mTOR (raptor), mammalian LST8 (mLST8), proline-rich Akt substrate of 40 kDa (PRAS40), and DEP domain containing mTOR-interacting protein (DEPTOR). mTOR complex 2, mTORC2, consists of mTOR, rapamycin-insensitive companion of mTOR (rictor), mammalian stress-activated protein kinase interacting protein 1 (mSIN1), proline-rich protein 5 or protein associated with rictor 1 (PRR5/PROTOR1) or PRR5L (also known as PROTOR2), DEPTOR, and mLST8. mTORC1 was originally deemed the rapamycin sensitive complex while mTORC2 was considered rapamycin-insensitive. However, it is now appreciated that these stereotypes do not necessarily hold true. Several functions of mTORC1 are rapamycin-resistant (Choo et al., 2008; Feldman et al., 2009; Thoreen et al., 2009), and mTORC2 assembly is inhibited in certain cell types with chronic treatment of rapamycin (Sarbassov et al., 2006). The mTOR complex components can be divided into core members that are required for complex activity and/or integrity and accessory proteins which modulate but are not essential for mTORC activity (Fig. 3). At this point, it is likely that the essential mTOR complex components have all been discovered.

Raptor is the orthologue of yeast Kog1p and a founding member of mTORC1. A 150 kDa protein, raptor contains an N-terminal conserved (RNC) domain which is present in all raptor orthologues, and HEAT repeats and WD-40 domains for protein-protein interactions (Hara et al., 2002; Kim et al., 2002). Raptor is required for the phosphorylation of mTORC1 substrates in cells. Several lines of evidence indicate that raptor may be required for substrate binding or proper localization of mTOR with its activators. Raptor is thought to interact with a TOR signaling (TOS) motif present in several, but not all, mTORC1 substrates (Nojima et al., 2003; Schalm and Blenis, 2002; Schalm et al., 2003). Mutation of the TOS motif prevents efficient phosphorylation by mTORC1. More recently, it has shown that raptor is required for the proper localization and therefore activation of mTORC1 to the lysosome, where mTORC1, as described in

more detail later, is activated (Sancak et al., 2010; Sancak et al., 2007).

mLST8, the orthologue of yeast LST8, is a small protein consisting of WD-40 repeats and is stably present in both mTORC1 and mTORC2 (Kim et al., 2003; Sarbassov et al., 2004). Acute RNAi-mediated knockdown of mLST8 disrupts mTORC1 activity and integrity, and therefore it was considered to be a core component of mTORC1 (Kim et al., 2003). It was a great surprise however that in vivo loss of mLST8 was dispensable for mTORC1 signaling while still required for mTORC2 activity (Guertin et al., 2006). The reason for this discrepancy is a mystery.

The remaining mTORC1 complex components are not essential for activity but modulate its function. While it was known that mTORC1 activity in cells was regulated by growth factors, this regulation was difficult to replicate in vitro as mTORC1 activity purified both from cells deprived of serum or from cells stimulated with growth factors was constitutively hyperactive (Sancak et al., 2007). Regulation was regained with reduction of the salt concentration in the buffers used to isolate and wash the kinase. Thus, it was postulated that a salt-sensitive inhibitor was responsible for mediating the growth factor signal to mTORC1. PRAS40 (also known as AKT1S1) was identified as that inhibitor (Fonseca et al., 2007; Oshiro et al., 2007; Sancak et al., 2007; Vander Haar et al., 2007; Wang et al., 2007). As its name suggests, it is phosphorylated by Akt on T246 (Kovacina et al., 2003) such that the growth factor signal is transmitted to PI3K, Akt, PRAS40 and then mTORC1 (Fig. 4). The phosphorylation then inhibits PRAS40, releasing it from mTORC1 and leading to mTORC1 activation. PRAS40 can also be phosphorylated by mTORC1 on S183, and this site may also be important for the inhibitory function of the protein (Oshiro et al., 2007).

DEPTOR was identified as an mTOR interacting protein which is present in both mTOR complexes (Peterson et al., 2009). While not an essential member of either complex, DEPTOR was found to be an inhibitor of mTOR activity. DEPTOR expression is negatively regulated at both the mRNA and protein levels by mTORC1. DEPTOR was found to be highly expressed in a subset of multiple myelomas. While one might expect that DEPTOR overexpression would lead to a suppression of mTORC1 and

mTORC2, due to the feedback inhibition of PI3K-Akt by mTORC1 and S6K1 which will be described in more detail later, DEPTOR overexpression chronically leads to PI3K-mTORC2-Akt activation. Multiple myeloma cells which express high amounts of DEPTOR exhibit hyperactive Akt signaling in the absence of PTEN or PI3K mutations (Peterson et al., 2009).

Turning to mTORC2, rictor, the orthologue of yeast Avo3p, is a 200 kDa protein (Jacinto et al., 2004; Sarbassov et al., 2004). While it is absolutely required for mTORC2 activity in vitro and in vivo, its molecular function is unclear. mSin1 binds rictor and is required for a productive rictor-mTOR interaction (Frias et al., 2006; Jacinto et al., 2006; Yang et al., 2006). mSin1 exists in multiple splice isoforms. Interestingly, mSin1 has a putative pleckstrin homology (PH) domain, perhaps responsible for lipid binding and mTORC2 localization at membranes (Schroder et al., 2007a). The isoform lacking the PH domain is insensitive to growth factor regulation (Frias et al., 2006), leading to the possibility that proper localization of mTORC2 is required for its regulation and also that distinct mTORC2s with differential regulation may exist. In yeast, TORC2 localization to the plasma membrane is required for cell viability and is dependent on the yeast mSin1 homolog, Avo1p (Berchtold and Walther, 2009). mSin1 also has a putative Ras-binding domain (Schroder et al., 2007b).

PRR5/Protor is a more recently described member of mTORC2 which also exists in two isoforms (PRR5 or Protor1 and PRR5L or Protor2) enforcing the idea that different mTORC2 complexes with different combinations of Protor and mSin1 may exist in the cell (Pearce et al., 2007). It also may be important for PDGFR expression (Woo et al., 2007). While originally not thought to be required for mTORC2 activity, recent evidence, as discussed later, suggests that it might be important for phosphorylation of some, but not all, mTORC2 substrates (Pearce et al., 2011).

## Upstream signaling: mTOR senses the nutrient and metabolic state of the cell

The two mTOR complexes maintain cellular homeostasis by sensing a variety of intracellular and extracellular signals (Fig. 4) and ensuring that downstream, energy-consuming processes are matched to the state of the cell.

### The TSC1/2 complex: an integrating platform

Tuberous sclerosis complex is a rare, autosomal dominant disease which affects about 1 in 6000 live births and is marked by hamartomatous outgrowths which can affect many organs, but most notably the skin, kidneys, and brain (Crino et al., 2006; Montagne et al., 2001). While the outgrowths tend to be benign, they can cause significant morbidity, and the presence of cortical tubers can stunt normal childhood development. The disease is due to loss of function mutations in hamartin (TSC1) and tuberin (TSC2) which together form a heterodimeric GTPase activating protein (GAP) for the small Ras-like G-protein Ras homologue expressed in brain (Rheb), an activator of mTORC1. Loss of TSC1/2 results in hyperactive mTORC1 signaling and repressed Akt activity (Garami et al., 2003; Inoki et al., 2003; Tee et al., 2003; van Slegtenhorst et al., 1997; van Slegtenhorst et al., 1998; Zhang et al., 2003b). Rheb was identified in a Drosophila screens for growth regulators (Saucedo et al., 2003; Stocker et al., 2003). For a while it was not known how Rheb activated mTORC1, but it has now been shown that the activation occurs directly (Sancak et al., 2007).

The TSC1/2 complex serves as a platform by which upstream signals are integrated and sensed by mTOR. Many of these signals are downstream of the major growth factor pathways. Extracellular signal-regulated knase (ERK) (Ma et al., 2005), Akt (Inoki et al., 2002; Manning et al., 2002a; Potter et al., 2002), and RSK (Roux et al., 2007) all inhibit TSC2. The regulation occurs via a series of phosphorylations which inhibit and/or destabilize TSC2, thereby leading to increased GTP-bound Rheb, activation of mTORC1. GSK3β does the opposite; its phosphorylation activates TSC1/2

(Inoki et al., 2006).

While growth factors can signal through TSC2 to mTORC1, they can also signal directly to the mTORC1 complex through Akt-mediated phosphorylation of PRAS40 (Sancak et al., 2007; Vander Haar et al., 2007), an mTORC1 component described above.

**mTORC1 senses cellular energetic status and oxygen levels**

mTORC1 senses energetic depletion, as under glucose or nutrient deprivation through direct (Dennis et al., 2001) and indirect mechanisms. AMP-activated protein kinase (AMPK) is activated by a high AMP: ATP ratio and subsequently phosphorylates TSC2, activating it, and leading to decreased GTP-bound Rheb (Corradetti et al., 2004; Inoki et al., 2006; Shaw et al., 2004). AMPK can directly inhibit mTORC1 phosphorylation through raptor phosphorylation, affecting its binding to 14-3-3 proteins (Gwinn et al., 2008).

mTORC1 senses oxygen levels indirectly through AMPK but more directly through regulated in development and DNA damage response 1 (REDD1) whose expression is increased under hypoxia (Brugarolas et al., 2004; Reiling and Hafen, 2004). REDD1 promotes TSC1/2 activity by binding inhibitory 14-3-3 proteins which bind and inhibit TSC2 (DeYoung et al., 2008), thereby activating the inhibitory function of TSC2.

**Amino acid regulation of mTORC1**

The mechanism by which mTOR sensed amino acids was until recently a complete mystery. The signal was known to be sensed independently of TSC1 or 2 as TSC2-null cells, while insensitive to serum deprivation, are still sensitive to amino acid starvation (Smith et al., 2005). The heterodimeric Rag proteins consisting of either RagA or Rag B bound to Rag C or Rag D are homologous to the yeast Gtr1p and Gtr2p and were found to relay the amino acid signal (Kim et al., 2008; Sancak et al., 2008). Knockdown of the Rag proteins prevented mTORC1 activation by amino acids

while overexpression of an activating RagB mutant caused mTORC1 to be insensitive to amino acid starvation. Rags act by regulating mTORC1 localization (Sancak et al., 2008). mTORC1 is diffuse in the cytoplasm in the absence of amino acids and subsequently recruited to the lysosome by the Rag proteins. Under nutrient replete conditions, RagA and RagB are GTP-loaded while Rag C and RagD are GDP-loaded, allowing interaction with raptor and recruitment of mTORC1 to the lysosome where the Rag proteins are located, tethered by the heterotrimeric p14, p18, MAPK scaffold protein 1 (MP1) Ragulator complex (Sancak et al., 2010). At the lysosome, mTORC1 can then be activated by GTP-bound Rheb.

These results explain several observations of amino acid signaling. First, it explains how amino acids are a necessary requirement for growth factor activation of mTORC1 (Hara et al., 1998; Wang et al., 1998). Even if Rheb is GTP-bound, it cannot activate mTORC1 if the complex is not at the lysosome. Moreover, it suggests that one of the primary roles of raptor is to localize mTORC1 to its activators, perhaps explaining how mTOR can phosphorylate some of its substrates in vitro in the absence of raptor but cannot do so in the cell (Burnett et al., 1998; Yip et al., 2010). How the actual sensing of amino acids occurs is unclear, but one can hypothesize that lysosomal amino acids are the pool of amino acids being sensed, or that the sensor senses some lysosomal parameter dependent on amino acids (Korolchuk et al., 2011).

### Growth factor regulation of mTORC2

mTORC2 is regulated by growth factors and is downstream of the receptor tyrosine kinase - PI3K pathway (Sarbassov et al., 2005). The mechanism by which mTORC2 is regulated by growth factors is a mystery, although it was recently shown that mTORC2 binding to the ribosome is involved in its activation (Zinzalla et al., 2011). A ribosome biogenesis factor was found to be required for yeast TORC2 and mTORC2 activity, and growth factor stimulation resulted in recruitment of mTORC2 to the ribosome.

Given that mTORC1 is directly activated by the small G-protein Rheb, one

might wonder if a G-protein is also required for mTORC2 activation. Accordingly, a Ras homologue (RasC) in Dictylostelium seems to be important for TORC2 activity and chemotaxis, a TORC2-regulated process in the organism (Charest et al., 2010; Lee et al., 2005)

## Downstream functions: mTOR is the master regulator of cell growth

Cell growth is an accumulation in mass, in contrast to cell proliferation, which is an increase in cell number. While we refer to mTOR as the master regulator of cell growth, mTORC1 is traditionally considered to be the growth-regulating complex while mTORC2 is thought to regulate cell surivival and proliferation. Cell growth is required for cell division (Johnston et al., 1977) and the two are tightly linked processes, both contributing to the determination of organismal size (Conlon and Raff, 1999). Inactivation of the TOR pathway by pharmacologic inhibitors, genetic loss of key components, or nutrient starvation results in decreased cell size in a variety of organisms (Fingar et al., 2002; Montagne et al., 1999; Oldham et al., 2000; Zhang et al., 2000). Activation of mTORC1 results in increased cell size (Ito and Rubin, 1999; Stocker et al., 2003). Attesting to its importance in many processes involved in cell growth, mice without mTOR die very early in embryonic development (e12.5) (Gangloff et al., 2004; Murakami et al., 2004).

### mTORC1 and protein synthesis

4 high-energy phosphate bonds are hydrolyzed with each peptide bond forged during mRNA translation: 2 from ATP for tRNA charging, 1 from GTP for tRNA binding, and an additional GTP molecule for translocation. Coupled to the cost of biogenesis of the ribosomal machinery itself, protein synthesis is an energetically expensive process. Not surprisingly, the regulation of translation is tightly linked to the nutrient and metabolic state of the cell. mTORC1 plays an important role in regulating translation through its substrates, S6K1 and 4E-BP1.

**S6K1.** S6 is a component of the 40S ribosomal subunit. Highly abundant in the cell, it was the among the first serine-threonine phosphorylations shown to be regulated by rapamycin (Chung et al., 1992; Kuo et al., 1992). The kinases for S6 were identified through biochemical purification (Blenis et al., 1987; Price et al., 1989). There are two

S6 Kinases, S6K1 and S6K2. S6K1 is additionally present in two splice isoforms (p70 and p85), one of which (p85) is present in the nucleus. p70 S6K1 was subsequently shown to be a direct substrate of mTOR (Burnett et al., 1998; Isotani et al., 1999).

S6K is a member of the Protein Kinase A, G, and C (AGC) family of kinases. Several AGC kinases, such as S6K, Akt, and SGK, are downstream of PI3K (Pearce et al., 2010). Phosphorylation of two AGC kinase sites is required for their activity. The first, the activation loop or T-loop site, is phosphorylated by 3-phosphoinositide-dependent protein kinase 1 (PDK1) (Mora et al., 2004). PDK1 is itself also an AGC kinase. While the PDK1 sites are regulated by PI3K and growth factor signaling, the activity of PDK1 itself is not regulated. Rather, the regulation occurs at the level of the substrate (Pearce et al., 2010). In the case of S6K, the phosphorylation of its C-terminal hydrophobic motif by mTOR serves as a docking motif for PDK1. mTOR phosphorylation of the T389 hydrophobic motif residue by mTORC1 is therefore essential for S6K1 activity (Burnett et al., 1998).

S6K1 in turn regulates many substrates involved in translation. The phosphorylation of the S6 subunit of the 40S ribosome had been correlated with active translation initiation complexes (Duncan and McConkey, 1982; Thomas et al., 1982). However, cells in which S6 is replaced with an S6 in which the phosphorylation sites have been mutated to alanines, while smaller, did not have defects in global protein synthesis or in the translation of a subset of 5' terminal oligopyrimidine tract mRNAs described later in this section (Ruvinsky et al., 2005). Thus, despite being a highly abundant phosphorylation event and a marker of mTORC1 and S6K1 activity, the phosphorylation of S6 is of unclear significance.

S6K1, however, additionally regulates translation through several other substrates. S6K1 binds and phosphorylates S6K1 Aly/REF-like target (SKAR) which is present at the exon-junction complexes (Ma et al., 2008). Together, SKAR and S6K1 increase the efficiency of newly-spliced mRNAs. S6K1 also phosphorylates eIF4B which is important for its ability to stimulate the translation initiation helicase eIF4A (Raught et al., 2004). Programmed cell death protein 4 (PDCD4) is another S6K1 substrate,

and it inhibits eIF4A (Dorrello et al., 2006). Phosphorylation by S6K1 leads to PDCD4 ubiquitination by SCF (βTRCP) and its proteasomal destruction. S6K1 also increases translation elongation by phosphorylating elongation factor 2 kinase (eEF2K) (Wang et al., 2001).

**4E-BP1.** In addition to S6K1, the other canonical mTORC1 substrates are the eIF-4E binding proteins (4E-BP1 and 4E-BP2) on which mTOR phosphorylates several proline-directed sites (T37, T46, S65, T70) (Brunn et al., 1997b; Hara et al., 1997). Phosphorylation of 4E-BP1 has been known to be rapamycin-sensitive (Beretta et al., 1996). However, it is now appreciated that 4E-BP1 contains both rapamycin-sensitive and -insensitive mTORC1 sites (Choo et al., 2008; Feldman et al., 2009; Thoreen et al., 2009; Wang et al., 2005). T37 and 46 are rapamycin-insensitive and less well-regulated by serum while S65 is rapamycin-sensitive and highly serum-regulated.

The translation of the majority of mRNAs is cap-dependent. The 5' 7-methyl-guanosine cap is recognized by the translation initiation factor eIF4E. eIF4E subsequently recruits the scaffold protein eIF4G which in turn binds the poly-A binding protein at the 3' end of the mRNA and leads to mRNA circularization (Ma and Blenis, 2009). The eIF4A RNA helicase is the third component of the eIF4F translation initiation complex. The entire eIF4F complex must be assembled before the small ribosomal subunit can be recruited and begin scanning. The 4E-BPs are negative regulators of translation by binding the 7-methyl-GTP cap binding protein eIF4E, preventing it from binding eIF4G and forming a translation-competent initiation complex (Haghighat et al., 1995). Phosphorylation of the 4E-BPs releases eIF4E and allows it to incorporate into eIF4F. Mice lacking both 4E-BP1 and 4E-BP2 are viable with increased cell size in adipocytes (Le Bacquer et al., 2007). Recent work also suggests 4E-BP1 and 2 -null cells do not have defects in cell size but have effects primarily on proliferation through translational regulation of several pro-proliferative mRNAs encoded by the ornithine decarboxylase (ODC), cyclin D3, and vascular endothelial growth factor (VEGF) genes (Dowling et al., 2010a).

mTORC1 has other effects on translation which are independent of S6K1 and the

4E-BPs. While much of the support for this occurs in yeast, mammalian TOR increases the production of ribosomes through regulating the activity and localization of the regulatory protein TIF-1A, which is a required cofactor for RNA polymerase I responsible for the transcription of rRNA genes (Mayer et al., 2004).

Many mRNAs encoding ribosomal proteins or other components of the translational machinery have a tract of oligopyrimidines in their 5' UTRs (Levy et al., 1991). Rapamycin was shown to inhibit the translation of 5' terminal oligopyrimidine tract (5' TOP) mRNAs, and this inhibition was thought to be a mechanism by which mTOR regulated translation (Jefferies et al., 1994; Terada et al., 1994). However, the mechanism by which mTOR regulates these mRNAs is unknown as 5' TOP mRNAs are regulated in the absence of S6K and phosphorylateable S6 (Pende et al., 2004; Ruvinsky et al., 2005).

**mTORC1 and autophagy**

Macroautophagy is the process by which organelles and cytosol are sequestered in a double-membrane compartment, called the autophagosome, and then degraded and recycled when the autophagosome fuses with the lysosome (Rabinowitz and White, 2010; Yang and Klionsky, 2010). Autophagosome formation is conserved from yeast to mammalian cells and is orchestrated by several important complexes. The unc-51-like kinases (ULK1 and ULK1, equivalent to yeast Atg1p) are key regulators of autophagy induction. Beclin-1 (yeast Atg6p) recruits VPS34 which produces phosphatidylinositol-3-phosphate. Extension of the autophagosome involves two ubiquitin-like protein conjugation systems with two ubiquitin-like proteins, Atg12 and LC3 (yeast ATG8). LC3 is cleaved, lipidated, and inserted into the autophagosome membrane, a key marker for autophagy but a relatively late step in autophagy induction. The autophagosome subsequently fuses with the lysosome to form the autolysosome resulting in degradation and recycling of the macromolecules contained within. A basal level of autophagy is important for cellular homeostasis, especially in the maintenance of terminally differentiated cells. However, under conditions of starvation or stress, autophagy can be

upregulated as an adaptive survival mechanism to provide a source of nutrients. While TOR/mTOR has been known to be a negative regulator of autophagy (Rabinowitz and White, 2010; Yang and Klionsky, 2010), its relevant substrates were not elucidated until recently.

**ULK1 and ATG13.** In mammalian cells, ULK1, mammalian ATG13, and FAK family kinase-inhibitory protein (FIP200) are in a complex with mTORC1 under nutrient replete conditions (Ganley et al., 2009; Hosokawa et al., 2009; Jung et al., 2009). mTORC1 phosphorylates ULK1 and ATG13, resulting in inhibition of autophagosome formation. Under starvation conditions, mTORC1 is released allowing for autophagy to occur. While autophagy in mammalian cells has traditionally been probed with rapamycin, mTOR catalytic domain inhibitors result in a stronger induction of autophagy (Thoreen et al., 2009), suggesting that other rapamycin-insensitive mechanisms may exist. The degradation of macromolecules in the autolysosomes leads to a reactivation of mTOR which subsequently leads to a termination of autophagy and the reformation of lysosomes (Yu et al., 2010).

### mTORC1 and metabolism

In a cell-autonomous manner, mTOR senses the nutrient and energy status of the cell and coordinates downstream processes accordingly. In multicellular organisms, mTOR also has roles in whole-body sensing of nutrients and coordinates organismal metabolism. While the molecular mechanisms involved are often unknown, the physiological consequences can be quite profound.

In a transcriptional screen for metabolic regulators downstream of mTORC1, it was found that mTORC1 hyperactivation led to increased processing of sterol regulatory element-binding protein (SREBP1) which is a key regulator of lipid and cholesterol biosynthesis and increased expression of genes involved in lipid metabolism (Duvel et al., 2010). The increase in processed SREBP was dependent on the mTORC1 substrate S6K1. It has also been shown that regulation of SREBP1 is important for cell growth by regulating the key enzymes in lipid synthesis, fatty acid synthase (FAS),

acetyl-CoA carboxylase (ACC), and ATP citrate lyase (ACLY) (Porstmann et al., 2008). SREBP1 knockdown resulted in decreased cell size, suggesting that mTORC1 also regulates growth through its effects on lipid metabolism.

mTORC1 regulates mitochondrial respiration and biogenesis by modulating the interaction between the transcription factor yin-yang 1 (YY1) with the peroxisome-proliferator-activated receptor coactivator (PGC)-1α (PGC-1α) (Cunningham et al., 2007). Conversely, the loss of raptor in muscle results in muscular dystrophy, decreased oxidative capacity, and decreased expression of PGC-1α transcript (Bentzinger et al., 2008). Unlike in muscle where mTORC1 activates mitochondrial respiration, in adipose tissue it seems to do the opposite. mTORC1 increases the expression of the master regulator of adipogenesis, peroxisome-proliferator-activated receptor γ (PPARγ) partly through both transcriptional and translational mechanisms (Kim and Chen, 2004; Le Bacquer et al., 2007). TSC2-null MEFs exhibit increased PPARγ levels and increased adipogenic potential (Zhang et al., 2009). Adipose-specific loss of mTORC1 results in decreased adipose tissue and resistance to diet-induced obesity due to increased mitochondrial uncoupling and fatty acid oxidation (Polak et al., 2008).

Just as mTOR initiates autophagy during periods of starvation, on an organismal level, mTOR also initiates metabolic programs required for the fasting response. The liver produces ketone bodies when glucose levels in the blood are low; these ketone bodies are then used by many tissues. mTORC1 mediates this process by negatively regulating peroxisome-proliferator-activated receptor α (PPARα) through effects on nuclear coreceptor 1 (NCoR1) (Sengupta et al., 2011). NCoR1 is constitutively in the nucleus in mice with liver-specific loss of TSC1, thereby inhibiting PPARα and resulting in attenuated ketogenesis upon starvation. Mice with liver-specific loss of raptor have the opposite phenotype with NCoR1 in the cytoplasm with constituitive activation of ketone body production.

S6K1 negatively regulates PI3K-Akt signaling. This signaling connection is referred to as the negative feedback loop and will be discussed again later in this

chapter as well as in subsequent chapters of this thesis. Mice null for S6K1 are resistant to diet-induced obesity enhanced insulin sensitivity and increased insulin receptor substrate (IRS) phosphorylation while TSC-null cells, conversely are insulin resistant (Harrington et al., 2004; Shah et al., 2004; Um et al., 2004).

Finally, caloric restriction has been shown to extend lifespan in both lower and higher eukaryotes, including *S. cerevisiae* (Kaeberlein et al., 2005; Powers et al., 2006), *C.elegans* (Eguez et al., 2005; Jia et al., 2004; Vellai et al., 2003), *D. melanogaster* (Bjedov et al., 2010; Kapahi et al., 2004) and most recently mice (Harrison et al., 2009). The mechanism by which mTOR regulates lifespan in mice is under investigation, but may involve different tissue-specific functions of mTOR signaling.

**mTORC2 and cell proliferation, survival, and glucose metabolism**

Yeast TORC2 regulates the actin cytoskeleton (Loewith et al., 2002). A cytoskeletal role for mTORC2 was initially presumed, in concordance with its role in yeast, and mTORC2 was thought to regulate PKCα (Sarbassov et al., 2004) or the Rho GTPase pathway (Jacinto et al., 2004). However, mTORC2-null MEFs do not have cytoskeletal defects (Guertin et al., 2006). Whether this discrepancy is due to the cell type examined or the differences between acute knockdown and chronic loss is unknown. However, more evidence has accumulated for mTORC2 having a key role in cell survival and proliferation, by virtue of its regulating several important mediators of these processes.

It was an investigation into a rapamycin-resistant version of S6K1 that led to the subsequent identification of mTORC2 substrates (Ali and Sabatini, 2005) (Fig. 5). When expressed in cells, a truncated form of S6K1 lacking its C-terminal autoinhibitory domain and the N-terminal TOS motif is phosphorylated on its hydrophobic motif. This phosphorylation, however, is no longer sensitive to rapamycin because it is phosphorylated by "rapamycin-resistant" mTORC2. While the C-terminal domain prevents mTORC2 from regulating the native S6K1 protein, it indicated that mTORC2 might phosphorylate other AGC kinases which possess a hydrophobic motif but lack this

C-terminal extension. This finding also suggested that the two complexes may have similar preferences for phosphoacceptor motifs but that the selectivity of substrates between the complexes is due to extracatalytic factors.

**Akt.** As PI3K and its counterpart PTEN are frequently mutated in cancers and result in Akt hyperactivation (Faivre et al., 2006), Akt has been widely studied. Like S6K, Akt is also an AGC kinase which must be phosphorylated on both its T-loop site as well as its hydrophobic motif (HM) for full activation. Unlike S6K, however, it lacks a C-terminal autoinhibitory domain. While the kinase which phosphorylated the activation loop site had long been known to be PDK1, the kinase which phosphorylated the S473 hydrophobic motif residue, deemed "PDK2," was unknown, its identity controversial. PDK1 (Balendran et al., 1999), Akt itself (Toker and Newton, 2000), DNA-PK (Feng et al., 2004), and integrin-linked kinase (ILK) (Persad et al., 2001) had all been proposed to be PDK2. However, several pieces of evidence suggested that none were the true PDK2. Drosophila haveproper phosphorylation of the Akt HM despite not possessing a DNA-PK homologue (Dore et al., 2004). DNA-PK-null mice, furthermore, do not have defects in insulin signaling (Taccioli et al., 1998). PDK1-null cells also have proper HM phosphorylation of Akt despite lacking T-loop phosphorylation (Williams et al., 2000).

The fact that mTORC2 could phosphorylate a truncated version of S6K (Ali and Sabatini, 2005) suggested that it might phosphorylate other AGC kinases. mTORC2 was found to efficiently phosphorylate the HM of Akt in vitro while mTORC1 could not (Sarbassov et al., 2005). Moreover, knockdown of mTORC2 in a variety of cell types led to the elimination of S473 phosphorylation. Finally, in mice null for mTORC2 components and MEFs derived from those mice, Akt S473 phosphorylation was completely absent (Guertin et al., 2006). The convergence of in vitro and in vivo data proved that mTORC2 was PDK2. The importance of the finding was immediately evident as it provided a marker for mTORC2 activity, tied mTORC2 to processes regulated by Akt, and indicated that pharmacologic inhibition of mTORC2 might prove to be an important anti-cancer strategy. In addition to the hydrophobic motif, mTORC2 may also regulate turn motif phosphorylation of Akt (Facchinetti et al., 2008; Ikenoue et al.,

2008).

There are 3 Akt isoforms: Akt1, Akt2, and Akt3. Given its importance in cancer, the specificity of Akt towards a specific phosphoacceptor motif, and the existence of an antibody which recognizes this motif present in Akt substrates, many Akt substrates have been identified (Manning and Cantley, 2007). These include many proteins involved in the regulation of cell survival and metabolism. Akt regulates the cell survival regulators MDM2 (Mayo and Donner, 2001; Zhou et al., 2001); FOXO1, 3A, and 4 (Brunet et al., 1999); BAD (Datta et al., 1997; del Peso et al., 1997); and caspase 9 (Cardone et al., 1998). Phosphorylation of FOXO3A retains it in the cytoplasm and prevents transcription of pro-apoptotic genes (Brunet et al., 1999). Akt also negatively regulates TSC2, thereby placing mTORC2 upstream of mTORC1 (Manning et al., 2002a).

Akt regulates nutrient uptake through the phosphorylation of AS160/TBC1D4 which controls insulin-stimulated Glut4 translocation to the plasma membrane (Eguez et al., 2005; Sano et al., 2003). Indeed, Akt plays an important role downstream of insulin signaling by increasing glucose uptake from the membrane. Under conditions of insulin resistance, Akt is not activated upon insulin or IGF, resulting in decreased glucose uptake and hyperglycemia. Akt also inhibits glycogen synthase 3 β (GSK3β) and thereby increases glycogen synthesis (Cross et al., 1995).

While TSC2 and GSK3β are considered bona fide targets of Akt, it was a great surprise when loss of mTORC2 in mice and MEFs did not impair the phosphorylation of those two substrates, while FOXO3A phosphorylation was severely impaired (Guertin et al., 2006). One explanation for this finding is that residual T-loop phosphorylation by PDK1 is sufficient to maintain enough activity to phosphorylate TSC2 and GSK3β, but not of FOXO3A T32.

**SGK1.** Serum- and glucocorticoid-induced protein kinase (SGK), of which there are 3 isoforms, SGK1-3, is another serum-regulated AGC kinase which is phosphorylated by mTORC2 (Garcia-Martinez and Alessi, 2008). SGK regulates the NEDD4-2 ubiquitin ligase which is responsible for the degradation of epithelial sodium channels (ENaC) and thereby regulates sodium transport into epithelial cells

(Debonneville et al., 2001).

The only other well-documented substrates unique to SGK are N-myc downregulated 1 (NDRG1) and NDRG2. Interestingly, as the focus of later work described in this thesis is on the identification of downstream substrates of mTOR, it's worth briefly discussing how NDRG1 and 2 were identified to be SGK substrates. The NDRG proteins were found as SGK substrates by kinase substrate tracking and elucidation (KESTREL) in which cellular or tissue extracts are fractionated and radioactive in vitro kinase assays are performed with related kinases (Murray et al., 2004). To remove background phosphorylation, the extracts are first depleted of ATP and the substrates separated from their endogenous kinases by ion-exchange chromatography. By KESTREL, it was found that NDRG1 and 2 were substrates of SGK1, but not Akt, and therefore good markers of SGK1-specific activity. NDRG is upregulated under stress (Shimono et al., 1999), upregulated with loss of N-myc (Shimono et al., 1999), and mutated in Charcot–Marie–Tooth disease type 4D (Kalaydjieva et al., 2000). However its molecular function is unknown.

SGK and Akt may share substrates. In mTORC2-null cells, Akt has residual activity, presumably because it can still be recruited to the plasma membrane through its PH domain and phosphorylated by PDK1 (Guertin et al., 2006). PDK1, however, does not phosphorylate SGK1 in the absence of mTORC2 (Garcia-Martinez and Alessi, 2008), suggesting that the hydrophobic motif phosphorylation recruits PDK1 by its PDK1-interacting fragment (PIF)-pocket, similar to S6K1. Therefore, in mTORC2-null cells SGK activity is markedly reduced. These results may explain why TSC2 and GSK3β are still phosphorylated in mTORC2-null MEFs as the residual Akt activity is sufficient to act on these substrates. SGK, however, may instead be the main regulator of FOXO3A T32 phosphorylation, and therefore in the absence of SGK activity, FOXO3A phosphorylation is then absent. Assessing the relative contributions of SGK and Akt in mTORC2 signaling is an area of great interest.

While little is known about the Protor components of mTORC2, it has recently been shown that while Protor loss does not affect phosphorylation of Akt, Protor1 and

Protor2 deficient cells have markedly diminished SGK phosphorylation, suggesting that Protor is required for substrate selection by mTORC2 (Pearce et al., 2011).

## The pathway is complex: interconnected feedback loops

Adding to the complexity of the signaling is the fact that mTORC1 and mTORC2 are both upstream and downstream of each other, highlighting the importance of coordinating cell growth and nutrient sensing with proliferation and growth factor signaling. Given that one of the focuses of the work described later is the mechanism by which mTORC1 inhibits PI3K-Akt signaling, several of the interconnections are mentioned or briefly reiterated here.

### Akt-TSC2

In a search for Akt substrates using a phosphomotif antibody recognizing the AGC kinase motif (RXRXX(S*/T*)), it was found that a large molecular weight protein was phosphorylated in response to growth factor inhibition and possessed a site corresponding to the AGC motif (Manning et al., 2002a). Based on bioinformatic predictions, the large protein was determined to be TSC2. While it had been known that Akt activated S6K1, the mechanism had not been known. Therefore, PTEN loss, PI3K activation, or growth factor stimulation results in Akt activation, TSC2 inhibition, and mTORC1 activation. Akt therefore activates cell growth in conjunction with its role in inhibiting cell survival.

### Akt-PRAS40-mTORC1

As described above, Akt phosphorylates the mTORC1 inhibitor PRAS40 and thereby also activates mTORC1 directly (Kovacina et al., 2003).

### S6K1-IRS

There are 4 insulin receptor substrate proteins (IRS1-4) (Taniguchi et al., 2006). Upon insulin or IGF-1 stimulation, the insulin and IGF-1 receptors autophosphorylate on tyrosine residues, recruiting the IRS proteins by their phosphotyrosine-binding (PTB) domain. This recruitment allows for receptor phosphorylations on tyrosine residues

which then results in recruitment of the p85 regulatory subunit of PI3K (Taniguchi et al., 2006). Active PI3K then initiates a signaling cascade which leads to increased phosphatidylinositol-3,4,5-triphosphate ($PIP_3$), Akt activation, and signal transduction cascades downstream of the receptor.

While mTORC2 and its substrate Akt are upstream of mTORC1 through TSC2 and PRAS40 phosphorylation, mTORC1 is also upstream of mTORC2 via a negative feedback loop first described in cells null for TSC1/2 (Harrington et al., 2004; Shah and Hunter, 2006; Shah et al., 2004). TSC-null cells exhibit a profound insulin and IGF-1 resistance due to increased inhibitory phosphorylation of IRS1 on serines 302, 636, and 639 as well as decreased stability of IRS1 and IRS2 proteins, thereby preventing signal transduction from the receptor to PI3K. The phosphorylation and effects on stability are thought to be mediated by S6K1, and in accordance with this hypothesis, mice null for S6K1 have increased inhibitory phosphorylation of IRS1 on S307, S636, and S639 and slightly increased IRS1 levels (Um et al., 2004). As a result, these mice are resistant to diet-induced obesity and exhibit enhanced insulin sensitivity. A more detailed investigation of this feedback loop is presented in the second part of the thesis work.

**S6K1-mTORC2**

Rictor has been shown to be phosphorylated on T1135 by S6K1 (Dibble et al., 2009; Julien et al., 2010; Treins et al., 2010). While the phosphorylation does not affect mTORC2 in vitro activity, mutation of the phosphorylation site in cells results in increased Akt phosphorylation and regulates the binding of rictor to 14-3-3 proteins.

**TSC2-mTORC2**

While the TSC1/2 complex has canonically been considered a negative regulator of mTORC1, it has been reported that TSC2 can directly bind mTORC2 and is required for its activity (Huang et al., 2008). Mutations which retain GAP activity but still bind mTORC2 may be important for separating out the functions of TSC2 towards the two complexes.

### TSC-PDGFR

mTORC1 hyperactivation leads to platelet derived growth factor (PDGF) receptor downregulation in cells null for TSC (Zhang et al., 2003a). Interestingly, however, reintroduction of PDGFR expression leads to increased sensitivity of TSC null cells not only to PDGF but also to insulin and serum. Reintroduction of the receptor also increases the tumorigenicity of TSC null tumors which are normally indolent, presumably due to repressed Akt signaling (Zhang et al., 2007).

### DEPTOR

As described above, DEPTOR is an mTOR-binding protein which interacts with both complexes (Peterson et al., 2009). While it is considered a negative regulator of both complexes, its net effect in the cells is inhibition of mTORC1 with subsequent disinhibition of PI3K-Akt signaling and activation of mTORC2 through the proposed feedback from mTORC1 and S6K to PI3K-Akt. DEPTOR is not universally expressed in different cell types (Peterson et al., 2009), and its expression may be predictive of the level of feedback activities.

## The role of mTOR in cancer

### Genetic hamartoma syndromes linked to the mTOR pathway

Genetic deregulation of mTOR-mediated growth control can result in several hereditary hamartoma syndromes. The one most proximal to mTOR is the tuberous sclerosis complex in which patients exhibit benign, yet still morbidity-causing, tubers in the brain, kidney, lung, and heart (Crino et al., 2006). TSC patients are also predisposed to angiomyolipomas and renal cell carcinomas. While the syndrome is autosomal dominant and therefore the patients are germ-line heterozygous for TSC1/2 loss of function, the patients eventually gain a second mutated copy. The mutations can either occur in TSC1, required for TSC2 stabilization, or TSC2, the active GTPase activating protein (Crino et al., 2006; Jones et al., 1999). Some patients with tuberous sclerosis complex develop lymphangiomyomatosis (LAM) (Muzykewicz et al., 2009). Affecting mostly women, LAM is marked by cysts which destroy the lung parenchyma and an infiltration of smooth muscle cells in the lung. The disease is fatal, and the cysts return even upon lung transplantation. The "LAM" cell, the causative cell of origin, is elusive, but as many LAM patients also have angiomyolipomas, one hypothesis is that LAM cells may be derived from the angiomyolipoma and then metastasize to the lung (Yu and Henske, 2010).

Other tumor suppressors upstream of mTOR also result in genetic hamartoma syndromes associated with increased risk of cancer. Cowden disease is caused by germline loss of PTEN and is marked by small hamartomas of the skin and epithelium which are also largely benign, although patients can also develop breast, prostate, and thyroid cancer (Krymskaya and Goncharova, 2009). Peutz-Jeghers is marked by polyps which affect the small intestine (Krymskaya and Goncharova, 2009). It is caused by mutations in LKB1, the kinase upstream of AMPK. Neurofibromatosis (also known as von Recklinghausen disease) is a syndrome due to mutations in Neurofibromatosis factor 1, NF1, which is the GAP for the Ras and is marked by aberrant outgrowths of neural crest-derived cells, resulting in neurofibromas and aberrant pigmentation of

the skin (McClatchey, 2007). Germline mutation of NF1 also results in an increased likelihood of meningiomas and gliomas. Birt-Hogg-Dube syndrome is caused by mutation in folliculin which leads to benign tumors of the hair follicles, cysts in both lungs, and an increased likelihood of renal cell carcinoma (Menko et al., 2009). While its molecular connection to mTOR is still unclear, the constellation of clinical manifestations of folliculin loss places it securely in the mTOR pathway.

**mTOR signaling is activated in spontaneous cancers**

Given that loss of common tumor suppressors and activation of common oncogenes can lead to increased flux through the mTOR pathway (Fig. 4), hyperactive mTOR signaling and deregulated cell growth may be a frequent event in cancer (Faivre et al., 2006; Menon and Manning, 2008). PI3K and PTEN are commonly mutated in cancers, with PTEN being the second-most frequently mutated tumor suppressor besides p53. PI3K and PTEN loss activate mTORC2 and Akt activity and lead to TSC1/2 inhibition, and mTORC1 hyperactivation. Receptor tyrosine kinases are frequently amplified or mutated, leading to downstream inhibition of TSC1/2. And mutations in Ras and Raf are also common cancer-initiating events. LKB1 mutation in cancers leads to reduced AMPK activation, thereby further increasing mTORC1 activity through its effects on TSC1/2 as well as on raptor (Gwinn et al., 2008).

Deregulated mTOR signaling results in cell growth, cell survival, and proliferation uncoupled from growth factors, nutrient, oxygen, or ATP levels. Translational control downstream of mTORC1 also seems to be an important arm of oncogenic mTOR signaling. eIF4E has emerged as an oncogene (Ruggero et al., 2004; Wendel et al., 2004). Translational upregulation may be a common feature of many tumors and phospho-4E-BP1 an adverse prognostic marker (Armengol et al., 2007). Inhibition of the 4E-BPs is pro-proliferative (Dowling et al., 2010a) and is important for tumorigenicity (Petroulakis et al., 2009; She et al., 2010). Accordingly, overexpression of 4E-BP1 in an Akt-driven lymphoma model resulted in reduction in tumor size, as did pharmacologic inhibition of mTOR (Hsieh et al., 2010).

The effects of mTOR on angiogenesis is another way in which mTOR signaling may promote tumor formation. mTOR increases the expression of hypoxia-inducible factor-1alpha (HIF-1alpha) (Duvel et al., 2010; Hudson et al., 2002; Thomas et al., 2006; Zhong et al., 2000) which results in increased fitness under hypoxic conditions through stimulation of angiogenesis and a metabolic switch to glycolysis.

## mTOR inhibitors

### Rapalogs in clinical use

Owing to its unique mechanism of inhibition, rapamycin is one of the original selective kinase inhibitors. Rapamycin analogs, also known as rapalogs, such as RAD001 (everolimus) and CCI-779 (temsirolimus), are a mainstain of organ transplantation pharmacotherapy (Yatscoff et al., 1993), and rapalogs are also widely employed in drug-eluting stents to prevent restenosis of the opened artery (Wessely, 2010).

Rapalogs have also been used for the treatment of various aspects of tuberous sclerosis complex or lymphangiomyomatosis. Rapamycin treatment resulted in a regression of associated renal angiomyolipomas, although withdrawal of the rapamycin led to a regrowth of the existing tumor (Bissler et al., 2008; Davies et al., 2008; Franz et al., 2006). Encouragingly, LAM patients on rapamycin treatment experienced some improvement in respiratory function that persisted after treatment was withdrawn (Bissler et al., 2008). Everolimus has also been shown to be helpful in patients with tuberous sclerosis complex with subependymal giant-cell astrocytomas (SEGA) with reduction in volume and seizure frequency (Krueger et al., 2010). Rapalogs may present a viable alternative to surgical resection of these tubers, the previous standard of care.

Rapalogs have now been in well over a hundred clinical trials for many different spontaneous cancers, but have yielded disappointing results (Chiang and Abraham, 2007; Dowling et al., 2010b; Faivre et al., 2006). One exception is the recent approval of CCI-779 for renal cell carcinoma where it improved the survival of patients with metastatic disease (Hudes et al., 2007). There are several reasons to explain why rapalogs have not been more effective as anti-cancer agents despite mTOR hyperactivation being fairly common in cancer. First, rapamycin does not fully inhibit mTORC1 and all of its functions, including translation (Feldman et al., 2009; Thoreen et al., 2009). Second, rapamycin does not always inhibit mTORC2, although it can prevent mTORC2 assembly in different cell types (Sarbassov et al., 2006). And third, mTORC1

inhibition can lead to activation of Akt by the aforementioned negative feedback signaling.

**Catalytic domain inhibitors of PI3K and mTOR**

Recently, ATP-competitive kinase domain inhibitors have been developed which inhibit phosphorylation downstream of both complexes by inhibiting the mTOR kinase itself (Chresta et al., 2010; Feldman et al., 2009; Garcia-Martinez et al., 2009; Thoreen et al., 2009; Yu et al., 2009), and preliminary results indicate that they are more effective than rapamycin at inhibiting tumorigenesis. The mTOR catalytic domain inhibitor PP242, but not rapamycin, was effective in reducing tumor size in an Akt-driven lymphoma model (Hsieh et al., 2010). PTEN-null xenografts (U87-MG) were inhibited profoundly with mTOR inhibitor treatment (Chresta et al., 2010). And glioma cells in vitro and glioma-derived xenografts in vivo were arrested by mTOR inhibitor treatment resulting in prolonged survival (Liu et al., 2009).

Given the homology of mTOR to PI3K, a class of mTOR inhibitors also inhibits PI3K (Fan et al., 2006; Maira et al., 2008). The advantage of such a compound is that it also inhibits phosphorylations independent of the Akt/mTORC2 arm of signaling downstream of PI3K. As Akt still has residual activity even with genetic ablation of mTORC2, these dual inhibitors may also inhibit Akt more profoundly (Guertin et al., 2006). Rapamycin, PP242 (an mTOR inhibitor), and PI-103 (a dual PI3K/mTOR inhibitor) were compared in terms of their effects on Philadelphia chromosome models of leukemia (Janes et al., 2010). PP242 caused leukemia cell death while rapamycin did not and was more effective in vivo. Most surprisingly, PP242 was less immunosuppressive than rapamycin, having less of an effect on normal hematopoietic cells. Moreover, inhibition of PI3K in addition to mTOR had much stronger immunosuppressive effects on normal B and T cells compared to the mTOR inhibitors, suggesting that some toxicity may arise with dual inhibitors.

Even though mTOR is hyperactivated in many tumor types, it is possible that inhibition of mTOR results in cell death only in certain contexts. Just as EGFR mutations,

rather than EGFR overexpression, can predict efficacy of EGFR inhibitors (Lynch et al., 2004), genetic information may be used to predict clinical response to mTOR inhibitors. A recent study of pancreatic neuroendocrine tumors (PanNET) and pancreatic ductal adenocarcenomas (PDAC) found that the two tumor types harbored distinct sets of mutations (Jiao et al., 2011). Interestingly, in PanNETS, mutations in mTOR pathway genes were found in 14% of tumors and were uncommon in PDACs. These included mutations in PTEN, PIK3CA, as well as TSC2. Ongoing sequencing of various tumors may reveal a subset of cancers with a specific genetic signature which may prove to be more sensitive to mTOR inhibitors.

## Introduction to the work presented in this thesis

The emergence of mTOR kinase domain inhibitors has reenergized the field by renewing hope in the clinical use of mTOR inhibitors as anti-cancer agents. Moreover, rapamycin-resistant functions of mTOR can now be probed, and, as illustrated by the work in this thesis, additional substrates can be systematically identified. Despite all that is known about the upstream signaling to mTOR and the many ascribed functions of the kinase, the number of well-characterized substrates remains surprisingly few. The focus of the first part of this work is therefore a multi-pronged attempt to define the mTOR-regulated phosphoproteome, candidate substrates of mTOR, and downstream effector pathways. We find that mTOR regulates a majority of the insulin-stimulated phosphoproteome and the phosphorylation of many proteins involved in aspects of cell growth as well as in processes not previously linked to the pathway. These proteins may serve as exciting starting points for new areas of investigation in mTOR biology.

The second part of the thesis is focused on the description of a novel mTORC1 substrate, Grb10, and the clarification of the negative feedback loop between mTORC1 and PI3K-Akt. We show that mTORC1 orchestrates inhibition of PI3K through two parallel signaling arms, one involving S6K1-IRS1 and the other involving Grb10. mTORC1 inhibition results in both acute effects on Grb10 and IRS1 phosphorylation as well as chronic effects on their stability. These changes in Grb10 and IRS protein levels which occur with chronic mTOR inhibition are likely to be the most important aspect of mTOR inhibitors to consider in their therapeutic use.

**Figure 1. The phosphatidylinositol-3 kinase-related kinase (PIKK) family.** Members of the PIKK family contain several conserved domains: FAT and FATC domains which flank the kinase domain and a PIKK-regulatory domain. The FKBP12-rapamycin complex binds the FRB domain of mTOR.

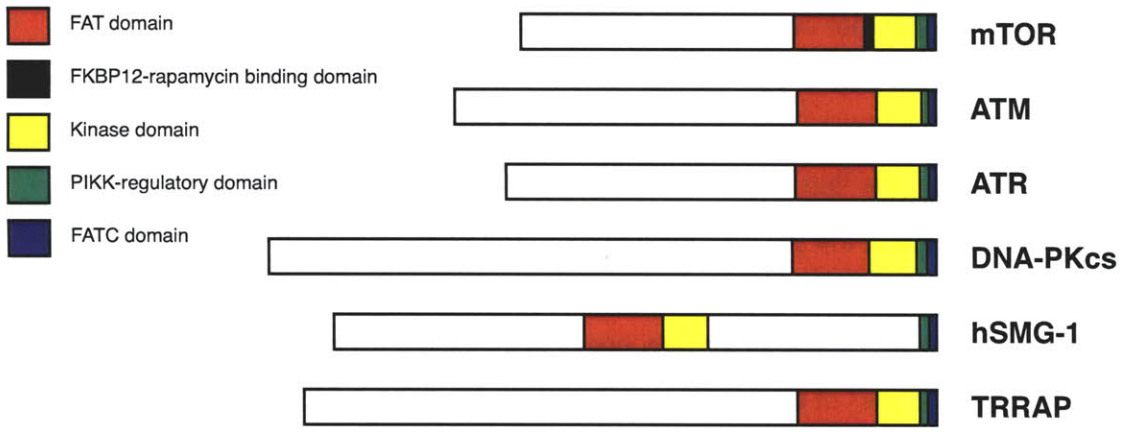

**Figure 2. mTOR phosphorylates two distinct motifs.** mTOR phosphorylates proline-directed sites present in substrates like 4E-BP1 and hydrophobic motifs present in AGC family kinases. The numbering of the positions is relative to the central phospho-acceptor serine or threonine.

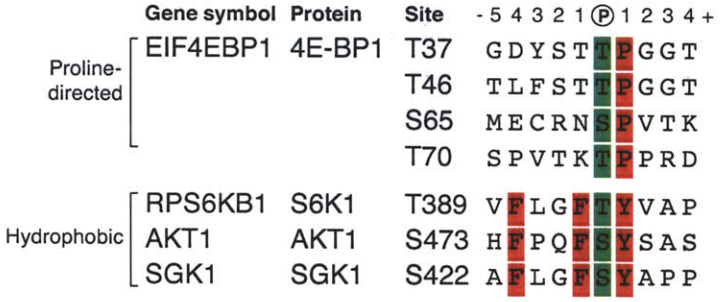

**Figure 3. The core and accessory components, inhibitor sensitivity, upstream and downstream regulation, and substrates of mTOR complex 1 and 2.**

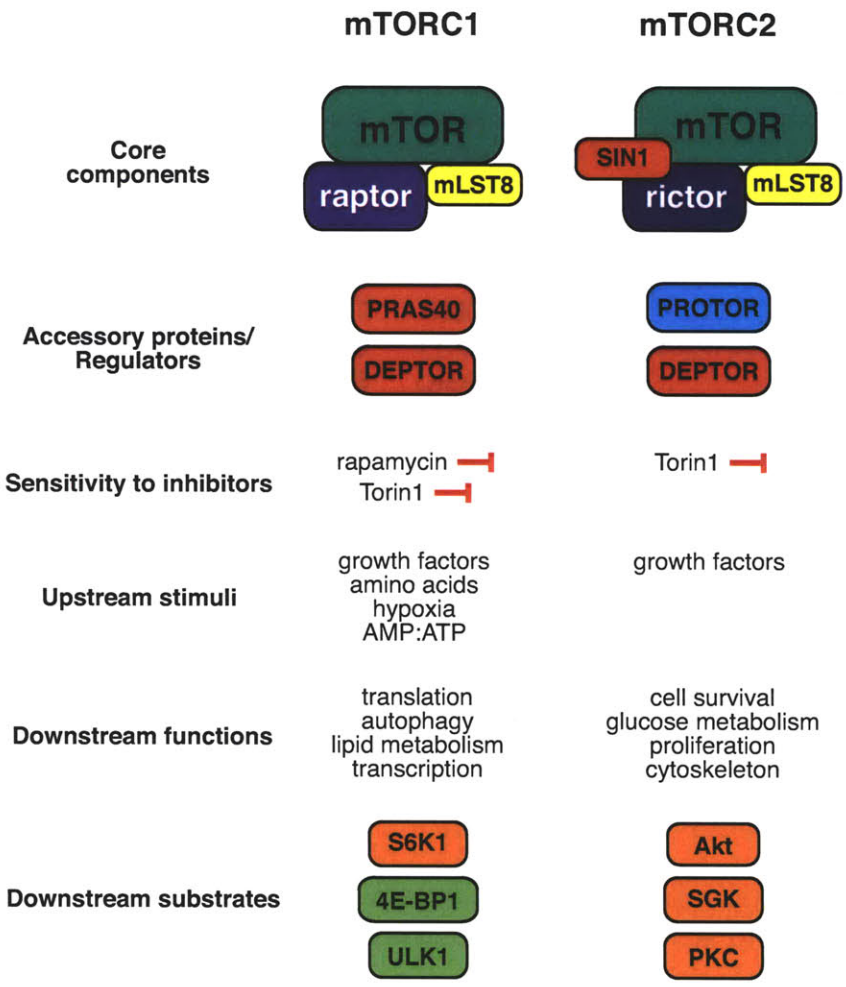

**Figure 4. An overview of the mTOR signaling pathway.** Adapted from (Laplante and Sabatini, 2009).

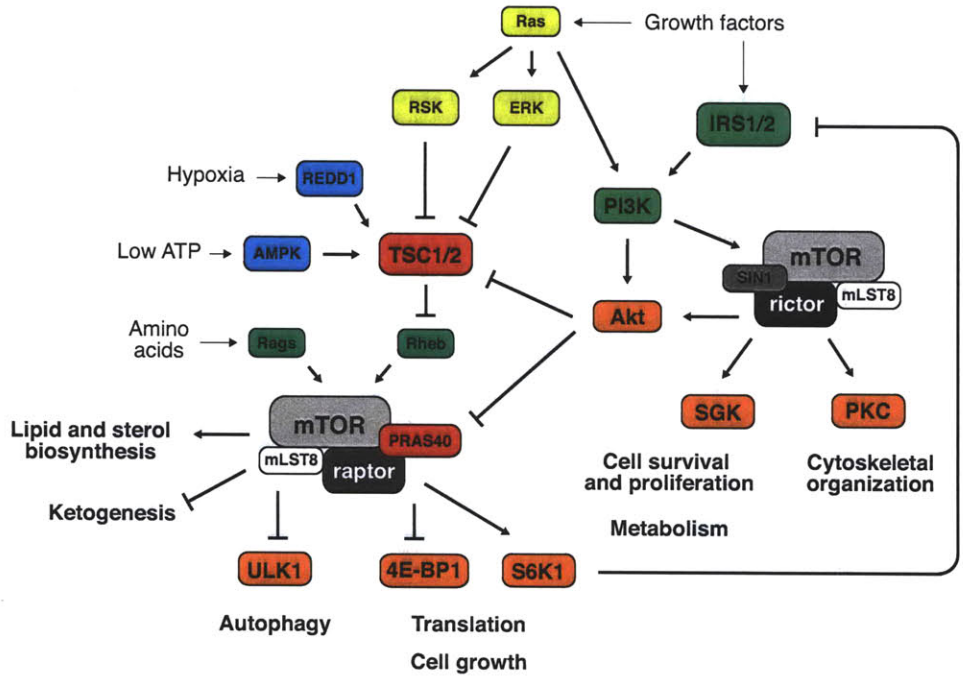

**Figure 5. mTORC1 phosphorylates S6K1 while mTORC2 phosphorylates Akt and a rapamycin-resistant form of S6K1.** mTORC1 is recruited to some substrates like S6K1 by a TOR signaling (TOS) motif, allowing for its hydrophobic motif phosphorylation on T389. mTORC2, however, cannot phosphorylate full-length S6K1 due to a C-terminal autoinhibitory domain. Truncation of the C-terminal domain allows for mTORC2 phosphorylation of S6K1 and deletion of the TOS motif prevents effective phosphorylation by mTORC1, thereby generating a "rapamycin-resistant" form of S6K1 which is phosphorylated predominantly by mTORC2 in cells. Adapted from (Ali et al, 2005).

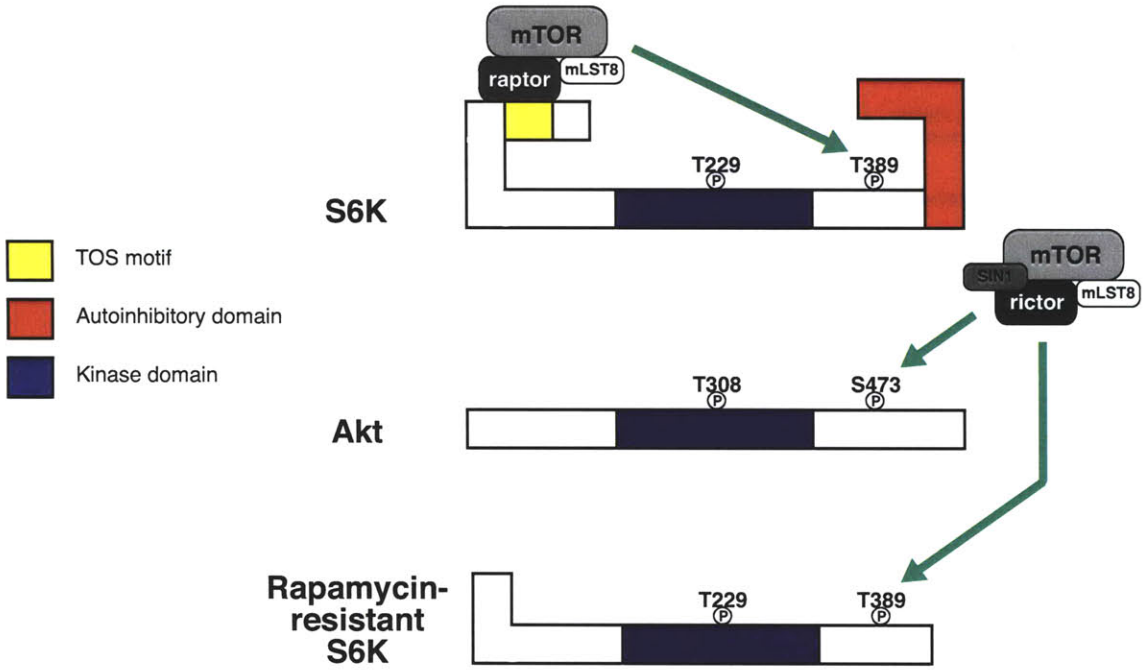

## References

Abraham, R.T. (2002). Identification of TOR signaling complexes: more TORC for the cell growth engine. Cell 111, 9-12.

Abraham, R.T., and Wiederrecht, G.J. (1996). Immunopharmacology of rapamycin. Annu Rev Immunol 14, 483-510.

Ali, S.M., and Sabatini, D.M. (2005). Structure of S6 kinase 1 determines whether raptor-mTOR or rictor-mTOR phosphorylates its hydrophobic motif site. J Biol Chem 280, 19445-19448.

Armengol, G., Rojo, F., Castellvi, J., Iglesias, C., Cuatrecasas, M., Pons, B., Baselga, J., and Ramon y Cajal, S. (2007). 4E-binding protein 1: a key molecular "funnel factor" in human cancer with clinical implications. Cancer Res 67, 7551-7555.

Balendran, A., Casamayor, A., Deak, M., Paterson, A., Gaffney, P., Currie, R., Downes, C.P., and Alessi, D.R. (1999). PDK1 acquires PDK2 activity in the presence of a synthetic peptide derived from the carboxyl terminus of PRK2. Curr Biol 9, 393-404.

Bentzinger, C.F., Romanino, K., Cloetta, D., Lin, S., Mascarenhas, J.B., Oliveri, F., Xia, J., Casanova, E., Costa, C.F., Brink, M., et al. (2008). Skeletal muscle-specific ablation of raptor, but not of rictor, causes metabolic changes and results in muscle dystrophy. Cell Metab 8, 411-424.

Berchtold, D., and Walther, T.C. (2009). TORC2 plasma membrane localization is essential for cell viability and restricted to a distinct domain. Mol Biol Cell 20, 1565-1575.

Beretta, L., Gingras, A.C., Svitkin, Y.V., Hall, M.N., and Sonenberg, N. (1996). Rapamycin blocks the phosphorylation of 4E-BP1 and inhibits cap-dependent initiation of translation. Embo J 15, 658-664.

Bierer, B.E., Mattila, P.S., Standaert, R.F., Herzenberg, L.A., Burakoff, S.J., Crabtree, G., and Schreiber, S.L. (1990a). Two distinct signal transmission pathways in T lymphocytes are inhibited by complexes formed between an immunophilin and either FK506 or rapamycin. Proc Natl Acad Sci U S A 87, 9231-9235.

Bierer, B.E., Somers, P.K., Wandless, T.J., Burakoff, S.J., and Schreiber, S.L. (1990b).

Probing immunosuppressant action with a nonnatural immunophilin ligand. Science 250, 556-559.

Bissler, J.J., McCormack, F.X., Young, L.R., Elwing, J.M., Chuck, G., Leonard, J.M., Schmithorst, V.J., Laor, T., Brody, A.S., Bean, J., et al. (2008). Sirolimus for angiomyolipoma in tuberous sclerosis complex or lymphangioleiomyomatosis. N Engl J Med 358, 140-151.

Bjedov, I., Toivonen, J.M., Kerr, F., Slack, C., Jacobson, J., Foley, A., and Partridge, L. (2010). Mechanisms of life span extension by rapamycin in the fruit fly Drosophila melanogaster. Cell Metab 11, 35-46.

Blenis, J., Kuo, C.J., and Erikson, R.L. (1987). Identification of a ribosomal protein S6 kinase regulated by transformation and growth-promoting stimuli. J Biol Chem 262, 14373-14376.

Bosotti, R., Isacchi, A., and Sonnhammer, E.L. (2000). FAT: a novel domain in PIK-related kinases. Trends Biochem Sci 25, 225-227.

Brown, E.J., Albers, M.W., Shin, T.B., Ichikawa, K., Keith, C.T., Lane, W.S., and Schreiber, S.L. (1994). A mammalian protein targeted by G1-arresting rapamycin-receptor complex. Nature 369, 756-758.

Brugarolas, J., Lei, K., Hurley, R.L., Manning, B.D., Reiling, J.H., Hafen, E., Witters, L.A., Ellisen, L.W., and Kaelin, W.G., Jr. (2004). Regulation of mTOR function in response to hypoxia by REDD1 and the TSC1/TSC2 tumor suppressor complex. Genes Dev 18, 2893-2904.

Brunet, A., Bonni, A., Zigmond, M.J., Lin, M.Z., Juo, P., Hu, L.S., Anderson, M.J., Arden, K.C., Blenis, J., and Greenberg, M.E. (1999). Akt promotes cell survival by phosphorylating and inhibiting a Forkhead transcription factor. Cell 96, 857-868.

Brunn, G.J., Fadden, P., Haystead, T.A., and Lawrence, J.C., Jr. (1997a). The mammalian target of rapamycin phosphorylates sites having a (Ser/Thr)-Pro motif and is activated by antibodies to a region near its COOH terminus. J Biol Chem 272, 32547-32550.

Brunn, G.J., Hudson, C.C., Sekulic, A., Williams, J.M., Hosoi, H., Houghton, P.J., Lawrence, J.C., Jr., and Abraham, R.T. (1997b). Phosphorylation of the translational repressor PHAS-I by the mammalian target of rapamycin. Science 277, 99-101.

Burnett, P.E., Barrow, R.K., Cohen, N.A., Snyder, S.H., and Sabatini, D.M. (1998). RAFT1 phosphorylation of the translational regulators p70 S6 kinase and 4E-BP1. Proc Natl Acad Sci U S A 95, 1432-1437.

Cardone, M.H., Roy, N., Stennicke, H.R., Salvesen, G.S., Franke, T.F., Stanbridge, E., Frisch, S., and Reed, J.C. (1998). Regulation of cell death protease caspase-9 by phosphorylation. Science 282, 1318-1321.

Charest, P.G., Shen, Z., Lakoduk, A., Sasaki, A.T., Briggs, S.P., and Firtel, R.A. (2010). A Ras signaling complex controls the RasC-TORC2 pathway and directed cell migration. Dev Cell 18, 737-749.

Chen, J., Zheng, X.F., Brown, E.J., and Schreiber, S.L. (1995). Identification of an 11-kDa FKBP12-rapamycin-binding domain within the 289-kDa FKBP12-rapamycin-associated protein and characterization of a critical serine residue. Proc Natl Acad Sci U S A 92, 4947-4951.

Chiang, G.G., and Abraham, R.T. (2007). Targeting the mTOR signaling network in cancer. Trends in molecular medicine 13, 433-442.

Choi, J., Chen, J., Schreiber, S.L., and Clardy, J. (1996). Structure of the FKBP12-rapamycin complex interacting with the binding domain of human FRAP. Science 273, 239-242.

Choo, A.Y., Yoon, S.O., Kim, S.G., Roux, P.P., and Blenis, J. (2008). Rapamycin differentially inhibits S6Ks and 4E-BP1 to mediate cell-type-specific repression of mRNA translation. Proc Natl Acad Sci U S A 105, 17414-17419.

Chresta, C.M., Davies, B.R., Hickson, I., Harding, T., Cosulich, S., Critchlow, S.E., Vincent, J.P., Ellston, R., Jones, D., Sini, P., et al. (2010). AZD8055 is a potent, selective, and orally bioavailable ATP-competitive mammalian target of rapamycin kinase inhibitor with in vitro and in vivo antitumor activity. Cancer Res 70, 288-298.

Chung, J., Kuo, C.J., Crabtree, G.R., and Blenis, J. (1992). Rapamycin-FKBP specifically blocks growth-dependent activation of and signaling by the 70 kd S6 protein kinases. Cell 69, 1227-1236.

Conlon, I., and Raff, M. (1999). Size control in animal development. Cell 96, 235-244.

Corradetti, M.N., Inoki, K., Bardeesy, N., DePinho, R.A., and Guan, K.L. (2004). Regula-

tion of the TSC pathway by LKB1: evidence of a molecular link between tuberous sclerosis complex and Peutz-Jeghers syndrome. Genes Dev 18, 1533-1538.

Crino, P.B., Nathanson, K.L., and Henske, E.P. (2006). The tuberous sclerosis complex. N Engl J Med 355, 1345-1356.

Cross, D.A., Alessi, D.R., Cohen, P., Andjelkovich, M., and Hemmings, B.A. (1995). Inhibition of glycogen synthase kinase-3 by insulin mediated by protein kinase B. Nature 378, 785-789.

Cunningham, J.T., Rodgers, J.T., Arlow, D.H., Vazquez, F., Mootha, V.K., and Puigserver, P. (2007). mTOR controls mitochondrial oxidative function through a YY1-PGC-1alpha transcriptional complex. Nature 450, 736-740.

Datta, S.R., Dudek, H., Tao, X., Masters, S., Fu, H., Gotoh, Y., and Greenberg, M.E. (1997). Akt phosphorylation of BAD couples survival signals to the cell-intrinsic death machinery. Cell 91, 231-241.

Davies, D.M., Johnson, S.R., Tattersfield, A.E., Kingswood, J.C., Cox, J.A., McCartney, D.L., Doyle, T., Elmslie, F., Saggar, A., de Vries, P.J., et al. (2008). Sirolimus therapy in tuberous sclerosis or sporadic lymphangioleiomyomatosis. N Engl J Med 358, 200-203.

Debonneville, C., Flores, S.Y., Kamynina, E., Plant, P.J., Tauxe, C., Thomas, M.A., Munster, C., Chraibi, A., Pratt, J.H., Horisberger, J.D., et al. (2001). Phosphorylation of Nedd4-2 by Sgk1 regulates epithelial Na(+) channel cell surface expression. The EMBO journal 20, 7052-7059.

del Peso, L., Gonzalez-Garcia, M., Page, C., Herrera, R., and Nunez, G. (1997). Interleukin-3-induced phosphorylation of BAD through the protein kinase Akt. Science 278, 687-689.

Dennis, P.B., Jaeschke, A., Saitoh, M., Fowler, B., Kozma, S.C., and Thomas, G. (2001). Mammalian TOR: a homeostatic ATP sensor. Science 294, 1102-1105.

DeYoung, M.P., Horak, P., Sofer, A., Sgroi, D., and Ellisen, L.W. (2008). Hypoxia regulates TSC1/2-mTOR signaling and tumor suppression through REDD1-mediated 14-3-3 shuttling. Genes Dev 22, 239-251.

Dibble, C.C., Asara, J.M., and Manning, B.D. (2009). Characterization of Rictor phosphorylation sites reveals direct regulation of mTOR complex 2 by S6K1. Molecular and

Cellular Biology 29, 5657-5670.

Dore, A.S., Drake, A.C., Brewerton, S.C., and Blundell, T.L. (2004). Identification of DNA-PK in the arthropods. Evidence for the ancient ancestry of vertebrate non-homologous end-joining. DNA Repair (Amst) 3, 33-41.

Dorrello, N.V., Peschiaroli, A., Guardavaccaro, D., Colburn, N.H., Sherman, N.E., and Pagano, M. (2006). S6K1- and betaTRCP-mediated degradation of PDCD4 promotes protein translation and cell growth. Science 314, 467-471.

Dowling, R.J., Topisirovic, I., Alain, T., Bidinosti, M., Fonseca, B.D., Petroulakis, E., Wang, X., Larsson, O., Selvaraj, A., Liu, Y., et al. (2010a). mTORC1-mediated cell proliferation, but not cell growth, controlled by the 4E-BPs. Science 328, 1172-1176.

Dowling, R.J., Topisirovic, I., Fonseca, B.D., and Sonenberg, N. (2010b). Dissecting the role of mTOR: lessons from mTOR inhibitors. Biochim Biophys Acta 1804, 433-439.

Duncan, R., and McConkey, E.H. (1982). Preferential utilization of phosphorylated 40-S ribosomal subunits during initiation complex formation. European journal of biochemistry / FEBS 123, 535-538.

Duvel, K., Yecies, J.L., Menon, S., Raman, P., Lipovsky, A.I., Souza, A.L., Triantafellow, E., Ma, Q., Gorski, R., Cleaver, S., et al. (2010). Activation of a metabolic gene regulatory network downstream of mTOR complex 1. Molecular cell 39, 171-183.

Eguez, L., Lee, A., Chavez, J.A., Miinea, C.P., Kane, S., Lienhard, G.E., and McGraw, T.E. (2005). Full intracellular retention of GLUT4 requires AS160 Rab GTPase activating protein. Cell metabolism 2, 263-272.

Facchinetti, V., Ouyang, W., Wei, H., Soto, N., Lazorchak, A., Gould, C., Lowry, C., Newton, A.C., Mao, Y., Miao, R.Q., et al. (2008). The mammalian target of rapamycin complex 2 controls folding and stability of Akt and protein kinase C. Embo J 27, 1932-1943.

Faivre, S., Kroemer, G., and Raymond, E. (2006). Current development of mTOR inhibitors as anticancer agents. Nat Rev Drug Discov 5, 671-688.

Fan, Q.W., Knight, Z.A., Goldenberg, D.D., Yu, W., Mostov, K.E., Stokoe, D., Shokat, K.M., and Weiss, W.A. (2006). A dual PI3 kinase/mTOR inhibitor reveals emergent efficacy in glioma. Cancer Cell 9, 341-349.

Feldman, M.E., Apsel, B., Uotila, A., Loewith, R., Knight, Z.A., Ruggero, D., and Shokat, K.M. (2009). Active-site inhibitors of mTOR target rapamycin-resistant outputs of mTORC1 and mTORC2. PLoS Biol 7, e38.

Feng, J., Park, J., Cron, P., Hess, D., and Hemmings, B.A. (2004). Identification of a PKB/Akt Hydrophobic Motif Ser-473 Kinase as DNA-dependent Protein Kinase. J Biol Chem 279, 41189-41196.

Fingar, D.C., Salama, S., Tsou, C., Harlow, E., and Blenis, J. (2002). Mammalian cell size is controlled by mTOR and its downstream targets S6K1 and 4EBP1/eIF4E. Genes Dev 16, 1472-1487.

Fonseca, B.D., Smith, E.M., Lee, V.H., MacKintosh, C., and Proud, C.G. (2007). PRAS40 is a target for mammalian target of rapamycin complex 1 and is required for signaling downstream of this complex. J Biol Chem 282, 24514-24524.

Franz, D.N., Leonard, J., Tudor, C., Chuck, G., Care, M., Sethuraman, G., Dinopoulos, A., Thomas, G., and Crone, K.R. (2006). Rapamycin causes regression of astrocytomas in tuberous sclerosis complex. Ann Neurol 59, 490-498.

Frias, M.A., Thoreen, C.C., Jaffe, J.D., Schroder, W., Sculley, T., Carr, S.A., and Sabatini, D.M. (2006). mSin1 is necessary for Akt/PKB phosphorylation, and its isoforms define three distinct mTORC2s. Curr Biol 16, 1865-1870.

Gangloff, Y.G., Mueller, M., Dann, S.G., Svoboda, P., Sticker, M., Spetz, J.F., Um, S.H., Brown, E.J., Cereghini, S., Thomas, G., et al. (2004). Disruption of the mouse mTOR gene leads to early postimplantation lethality and prohibits embryonic stem cell development. Mol Cell Biol 24, 9508-9516.

Ganley, I.G., Lam du, H., Wang, J., Ding, X., Chen, S., and Jiang, X. (2009). ULK1.ATG13.FIP200 complex mediates mTOR signaling and is essential for autophagy. J Biol Chem 284, 12297-12305.

Garami, A., Zwartkruis, F.J., Nobukuni, T., Joaquin, M., Roccio, M., Stocker, H., Kozma, S.C., Hafen, E., Bos, J.L., and Thomas, G. (2003). Insulin activation of Rheb, a mediator of mTOR/S6K/4E-BP signaling, is inhibited by TSC1 and 2. Mol Cell 11, 1457-1466.

Garcia-Martinez, J.M., and Alessi, D.R. (2008). mTOR complex 2 (mTORC2) controls hydrophobic motif phosphorylation and activation of serum- and glucocorticoid-induced protein kinase 1 (SGK1). Biochem J 416, 375-385.

Garcia-Martinez, J.M., Moran, J., Clarke, R.G., Gray, A., Cosulich, S.C., Chresta, C.M., and Alessi, D.R. (2009). Ku-0063794 is a specific inhibitor of the mammalian target of rapamycin (mTOR). Biochem J.

Guertin, D.A., Stevens, D.M., Thoreen, C.C., Burds, A.A., Kalaany, N.Y., Moffat, J., Brown, M., Fitzgerald, K.J., and Sabatini, D.M. (2006). Ablation in mice of the mTORC components raptor, rictor, or mLST8 reveals that mTORC2 is required for signaling to Akt-FOXO and PKCalpha, but not S6K1. Dev Cell 11, 859-871.

Gwinn, D.M., Shackelford, D.B., Egan, D.F., Mihaylova, M.M., Mery, A., Vasquez, D.S., Turk, B.E., and Shaw, R.J. (2008). AMPK phosphorylation of raptor mediates a metabolic checkpoint. Mol Cell 30, 214-226.

Haghighat, A., Mader, S., Pause, A., and Sonenberg, N. (1995). Repression of cap-dependent translation by 4E-binding protein 1: competition with p220 for binding to eukaryotic initiation factor-4E. EMBO J 14, 5701-5709.

Hara, K., Maruki, Y., Long, X., Yoshino, K., Oshiro, N., Hidayat, S., Tokunaga, C., Avruch, J., and Yonezawa, K. (2002). Raptor, a binding partner of target of rapamycin (TOR), mediates TOR action. Cell 110, 177-189.

Hara, K., Yonezawa, K., Kozlowski, M.T., Sugimoto, T., Andrabi, K., Weng, Q.P., Kasuga, M., Nishimoto, I., and Avruch, J. (1997). Regulation of eIF-4E BP1 phosphorylation by mTOR. J Biol Chem 272, 26457-26463.

Hara, K., Yonezawa, K., Weng, Q.P., Kozlowski, M.T., Belham, C., and Avruch, J. (1998). Amino acid sufficiency and mTOR regulate p70 S6 kinase and eIF-4E BP1 through a common effector mechanism. J Biol Chem 273, 14484-14494.

Harrington, L.S., Findlay, G.M., Gray, A., Tolkacheva, T., Wigfield, S., Rebholz, H., Barnett, J., Leslie, N.R., Cheng, S., Shepherd, P.R., et al. (2004). The TSC1-2 tumor suppressor controls insulin-PI3K signaling via regulation of IRS proteins. J Cell Biol 166, 213-223.

Harrison, D.E., Strong, R., Sharp, Z.D., Nelson, J.F., Astle, C.M., Flurkey, K., Nadon, N.L., Wilkinson, J.E., Frenkel, K., Carter, C.S., et al. (2009). Rapamycin fed late in life extends lifespan in genetically heterogeneous mice. Nature 460, 392-395.

Heitman, J., Movva, N.R., and Hall, M.N. (1991). Targets for cell cycle arrest by the immunosuppressant rapamycin in yeast. Science 253, 905-909.

Hosokawa, N., Hara, T., Kaizuka, T., Kishi, C., Takamura, A., Miura, Y., Iemura, S., Natsume, T., Takehana, K., Yamada, N., et al. (2009). Nutrient-dependent mTORC1 association with the ULK1-Atg13-FIP200 complex required for autophagy. Mol Biol Cell 20, 1981-1991.

Hsieh, A.C., Costa, M., Zollo, O., Davis, C., Feldman, M.E., Testa, J.R., Meyuhas, O., Shokat, K.M., and Ruggero, D. (2010). Genetic dissection of the oncogenic mTOR pathway reveals druggable addiction to translational control via 4EBP-eIF4E. Cancer Cell 17, 249-261.

Huang, J., Dibble, C.C., Matsuzaki, M., and Manning, B.D. (2008). The TSC1-TSC2 complex is required for proper activation of mTOR complex 2. Mol Cell Biol 28, 4104-4115.

Hudes, G., Carducci, M., Tomczak, P., Dutcher, J., Figlin, R., Kapoor, A., Staroslawska, E., Sosman, J., McDermott, D., Bodrogi, I., et al. (2007). Temsirolimus, interferon alfa, or both for advanced renal-cell carcinoma. N Engl J Med 356, 2271-2281.

Hudson, C.C., Liu, M., Chiang, G.G., Otterness, D.M., Loomis, D.C., Kaper, F., Giaccia, A.J., and Abraham, R.T. (2002). Regulation of hypoxia-inducible factor 1alpha expression and function by the mammalian target of rapamycin. Mol Cell Biol 22, 7004-7014.

Ikenoue, T., Inoki, K., Yang, Q., Zhou, X., and Guan, K.L. (2008). Essential function of TORC2 in PKC and Akt turn motif phosphorylation, maturation and signalling. Embo J 27, 1919-1931.

Inoki, K., Li, Y., Xu, T., and Guan, K.L. (2003). Rheb GTPase is a direct target of TSC2 GAP activity and regulates mTOR signaling. Genes Dev 17, 1829-1834.

Inoki, K., Li, Y., Zhu, T., Wu, J., and Guan, K.L. (2002). TSC2 is phosphorylated and inhibited by Akt and suppresses mTOR signalling. Nat Cell Biol 4, 648-657.

Inoki, K., Ouyang, H., Zhu, T., Lindvall, C., Wang, Y., Zhang, X., Yang, Q., Bennett, C., Harada, Y., Stankunas, K., et al. (2006). TSC2 integrates Wnt and energy signals via a coordinated phosphorylation by AMPK and GSK3 to regulate cell growth. Cell 126, 955-968.

Isotani, S., Hara, K., Tokunaga, C., Inoue, H., Avruch, J., and Yonezawa, K. (1999). Immunopurified mammalian target of rapamycin phosphorylates and activates p70 S6 kinase alpha in vitro. J Biol Chem 274, 34493-34498.

Ito, N., and Rubin, G.M. (1999). gigas, a Drosophila homolog of tuberous sclerosis gene product-2, regulates the cell cycle. Cell 96, 529-539.

Jacinto, E., Facchinetti, V., Liu, D., Soto, N., Wei, S., Jung, S.Y., Huang, Q., Qin, J., and Su, B. (2006). SIN1/MIP1 maintains rictor-mTOR complex integrity and regulates Akt phosphorylation and substrate specificity. Cell 127, 125-137.

Jacinto, E., Loewith, R., Schmidt, A., Lin, S., Ruegg, M.A., Hall, A., and Hall, M.N. (2004). Mammalian TOR complex 2 controls the actin cytoskeleton and is rapamycin insensitive. Nat Cell Biol 6, 1122-1128.

Janes, M.R., Limon, J.J., So, L., Chen, J., Lim, R.J., Chavez, M.A., Vu, C., Lilly, M.B., Mallya, S., Ong, S.T., et al. (2010). Effective and selective targeting of leukemia cells using a TORC1/2 kinase inhibitor. Nat Med 16, 205-213.

Jefferies, H.B., Reinhard, C., Kozma, S.C., and Thomas, G. (1994). Rapamycin selectively represses translation of the "polypyrimidine tract" mRNA family. Proc Natl Acad Sci U S A 91, 4441-4445.

Jia, K., Chen, D., and Riddle, D.L. (2004). The TOR pathway interacts with the insulin signaling pathway to regulate C. elegans larval development, metabolism and life span. Development 131, 3897-3906.

Jiao, Y., Shi, C., Edil, B.H., de Wilde, R.F., Klimstra, D.S., Maitra, A., Schulick, R.D., Tang, L.H., Wolfgang, C.L., Choti, M.A., et al. (2011). DAXX/ATRX, MEN1, and mTOR pathway genes are frequently altered in pancreatic neuroendocrine tumors. Science 331, 1199-1203.

Johnston, G.C., Pringle, J.R., and Hartwell, L.H. (1977). Coordination of growth with cell division in the yeast Saccharomyces cerevisiae. Experimental cell research 105, 79-98.

Jones, A.C., Shyamsundar, M.M., Thomas, M.W., Maynard, J., Idziaszczyk, S., Tomkins, S., Sampson, J.R., and Cheadle, J.P. (1999). Comprehensive mutation analysis of TSC1 and TSC2-and phenotypic correlations in 150 families with tuberous sclerosis. American journal of human genetics 64, 1305-1315.

Julien, L.A., Carriere, A., Moreau, J., and Roux, P.P. (2010). mTORC1-activated S6K1 phosphorylates Rictor on threonine 1135 and regulates mTORC2 signaling. Molecular and Cellular Biology 30, 908-921.

Jung, C.H., Jun, C.B., Ro, S.H., Kim, Y.M., Otto, N.M., Cao, J., Kundu, M., and Kim, D.H. (2009). ULK-Atg13-FIP200 complexes mediate mTOR signaling to the autophagy machinery. Mol Biol Cell 20, 1992-2003.

Kaeberlein, M., Powers, R.W., 3rd, Steffen, K.K., Westman, E.A., Hu, D., Dang, N., Kerr, E.O., Kirkland, K.T., Fields, S., and Kennedy, B.K. (2005). Regulation of yeast replicative life span by TOR and Sch9 in response to nutrients. Science 310, 1193-1196.

Kalaydjieva, L., Gresham, D., Gooding, R., Heather, L., Baas, F., de Jonge, R., Blechschmidt, K., Angelicheva, D., Chandler, D., Worsley, P., et al. (2000). N-myc downstream-regulated gene 1 is mutated in hereditary motor and sensory neuropathy-Lom. American journal of human genetics 67, 47-58.

Kapahi, P., Zid, B.M., Harper, T., Koslover, D., Sapin, V., and Benzer, S. (2004). Regulation of lifespan in Drosophila by modulation of genes in the TOR signaling pathway. Curr Biol 14, 885-890.

Kim, D.H., Sarbassov, D.D., Ali, S.M., King, J.E., Latek, R.R., Erdjument-Bromage, H., Tempst, P., and Sabatini, D.M. (2002). mTOR interacts with raptor to form a nutrient-sensitive complex that signals to the cell growth machinery. Cell 110, 163-175.

Kim, D.H., Sarbassov, D.D., Ali, S.M., Latek, R.R., Guntur, K.V., Erdjument-Bromage, H., Tempst, P., and Sabatini, D.M. (2003). GbetaL, a positive regulator of the rapamycin-sensitive pathway required for the nutrient-sensitive interaction between raptor and mTOR. Mol Cell 11, 895-904.

Kim, E., Goraksha-Hicks, P., Li, L., Neufeld, T.P., and Guan, K.L. (2008). Regulation of TORC1 by Rag GTPases in nutrient response. Nat Cell Biol 10, 935-945.

Kim, J.E., and Chen, J. (2004). Regulation of peroxisome proliferator-activated receptor-gamma activity by mammalian target of rapamycin and amino acids in adipogenesis. Diabetes 53, 2748-2756.

Koltin, Y., Faucette, L., Bergsma, D.J., Levy, M.A., Cafferkey, R., Koser, P.L., Johnson, R.K., and Livi, G.P. (1991). Rapamycin sensitivity in Saccharomyces cerevisiae is mediated by a peptidyl-prolyl cis-trans isomerase related to human FK506-binding protein. Mol Cell Biol 11, 1718-1723.

Korolchuk, V.I., Saiki, S., Lichtenberg, M., Siddiqi, F.H., Roberts, E.A., Imarisio, S., Jahreiss, L., Sarkar, S., Futter, M., Menzies, F.M., et al. (2011). Lysosomal positioning

coordinates cellular nutrient responses. Nature cell biology.

Kovacina, K.S., Park, G.Y., Bae, S.S., Guzzetta, A.W., Schaefer, E., Birnbaum, M.J., and Roth, R.A. (2003). Identification of a proline-rich Akt substrate as a 14-3-3 binding partner. J Biol Chem 278, 10189-10194.

Krueger, D.A., Care, M.M., Holland, K., Agricola, K., Tudor, C., Mangeshkar, P., Wilson, K.A., Byars, A., Sahmoud, T., and Franz, D.N. (2010). Everolimus for subependymal giant-cell astrocytomas in tuberous sclerosis. The New England journal of medicine 363, 1801-1811.

Krymskaya, V.P., and Goncharova, E.A. (2009). PI3K/mTORC1 activation in hamartoma syndromes: therapeutic prospects. Cell Cycle 8, 403-413.

Kunz, J., Henriquez, R., Schneider, U., Deuter-Reinhard, M., Movva, N.R., and Hall, M.N. (1993). Target of rapamycin in yeast, TOR2, is an essential phosphatidylinositol kinase homolog required for G1 progression. Cell 73, 585-596.

Kuo, C.J., Chung, J., Fiorentino, D.F., Flanagan, W.M., Blenis, J., and Crabtree, G.R. (1992). Rapamycin selectively inhibits interleukin-2 activation of p70 S6 kinase. Nature 358, 70-73.

Laplante, M., and Sabatini, D.M. (2009). An emerging role of mTOR in lipid biosynthesis. Curr Biol 19, R1046-1052.

Le Bacquer, O., Petroulakis, E., Paglialunga, S., Poulin, F., Richard, D., Cianflone, K., and Sonenberg, N. (2007). Elevated sensitivity to diet-induced obesity and insulin resistance in mice lacking 4E-BP1 and 4E-BP2. J Clin Invest 117, 387-396.

Lee, S., Comer, F.I., Sasaki, A., McLeod, I.X., Duong, Y., Okumura, K., Yates, J.R., 3rd, Parent, C.A., and Firtel, R.A. (2005). TOR complex 2 integrates cell movement during chemotaxis and signal relay in Dictyostelium. Mol Biol Cell 16, 4572-4583.

Lempiainen, H., and Halazonetis, T.D. (2009). Emerging common themes in regulation of PIKKs and PI3Ks. The EMBO journal 28, 3067-3073.

Levy, S., Avni, D., Hariharan, N., Perry, R.P., and Meyuhas, O. (1991). Oligopyrimidine tract at the 5' end of mammalian ribosomal protein mRNAs is required for their translational control. Proceedings of the National Academy of Sciences of the United States of America 88, 3319-3323.

Liu, T.J., Koul, D., LaFortune, T., Tiao, N., Shen, R.J., Maira, S.M., Garcia-Echevrria, C., and Yung, W.K. (2009). NVP-BEZ235, a novel dual phosphatidylinositol 3-kinase/mammalian target of rapamycin inhibitor, elicits multifaceted antitumor activities in human gliomas. Mol Cancer Ther 8, 2204-2210.

Loewith, R., Jacinto, E., Wullschleger, S., Lorberg, A., Crespo, J.L., Bonenfant, D., Oppliger, W., Jenoe, P., and Hall, M.N. (2002). Two TOR complexes, only one of which is rapamycin sensitive, have distinct roles in cell growth control. Mol Cell 10, 457-468.

Lynch, T.J., Bell, D.W., Sordella, R., Gurubhagavatula, S., Okimoto, R.A., Brannigan, B.W., Harris, P.L., Haserlat, S.M., Supko, J.G., Haluska, F.G., et al. (2004). Activating mutations in the epidermal growth factor receptor underlying responsiveness of non-small-cell lung cancer to gefitinib. The New England journal of medicine 350, 2129-2139.

Ma, L., Chen, Z., Erdjument-Bromage, H., Tempst, P., and Pandolfi, P.P. (2005). Phosphorylation and functional inactivation of TSC2 by Erk implications for tuberous sclerosis and cancer pathogenesis. Cell 121, 179-193.

Ma, X.M., and Blenis, J. (2009). Molecular mechanisms of mTOR-mediated translational control. Nat Rev Mol Cell Biol 10, 307-318.

Ma, X.M., Yoon, S.O., Richardson, C.J., Julich, K., and Blenis, J. (2008). SKAR links pre-mRNA splicing to mTOR/S6K1-mediated enhanced translation efficiency of spliced mRNAs. Cell 133, 303-313.

Maira, S.M., Stauffer, F., Brueggen, J., Furet, P., Schnell, C., Fritsch, C., Brachmann, S., Chene, P., De Pover, A., Schoemaker, K., et al. (2008). Identification and characterization of NVP-BEZ235, a new orally available dual phosphatidylinositol 3-kinase/mammalian target of rapamycin inhibitor with potent in vivo antitumor activity. Mol Cancer Ther 7, 1851-1863.

Manning, B.D., and Cantley, L.C. (2007). AKT/PKB signaling: navigating downstream. Cell 129, 1261-1274.

Manning, B.D., Tee, A.R., Logsdon, M.N., Blenis, J., and Cantley, L.C. (2002a). Identification of the tuberous sclerosis complex-2 tumor suppressor gene product tuberin as a target of the phosphoinositide 3-kinase/akt pathway. Mol Cell 10, 151-162.

Manning, G., Whyte, D.B., Martinez, R., Hunter, T., and Sudarsanam, S. (2002b). The protein kinase complement of the human genome. Science 298, 1912-1934.

Mayer, C., Zhao, J., Yuan, X., and Grummt, I. (2004). mTOR-dependent activation of the transcription factor TIF-IA links rRNA synthesis to nutrient availability. Genes Dev 18, 423-434.

Mayo, L.D., and Donner, D.B. (2001). A phosphatidylinositol 3-kinase/Akt pathway promotes translocation of Mdm2 from the cytoplasm to the nucleus. Proceedings of the National Academy of Sciences of the United States of America 98, 11598-11603.

McClatchey, A.I. (2007). Neurofibromatosis. Annu Rev Pathol 2, 191-216.

Menko, F.H., van Steensel, M.A., Giraud, S., Friis-Hansen, L., Richard, S., Ungari, S., Nordenskjold, M., Hansen, T.V., Solly, J., and Maher, E.R. (2009). Birt-Hogg-Dube syndrome: diagnosis and management. Lancet Oncol 10, 1199-1206.

Menon, S., and Manning, B.D. (2008). Common corruption of the mTOR signaling network in human tumors. Oncogene 27 Suppl 2, S43-51.

Montagne, J., Radimerski, T., and Thomas, G. (2001). Insulin signaling: lessons from the Drosophila tuberous sclerosis complex, a tumor suppressor. Sci STKE 2001, PE36.

Montagne, J., Stewart, M.J., Stocker, H., Hafen, E., Kozma, S.C., and Thomas, G. (1999). Drosophila S6 kinase: a regulator of cell size. Science 285, 2126-2129.

Mora, A., Komander, D., van Aalten, D.M., and Alessi, D.R. (2004). PDK1, the master regulator of AGC kinase signal transduction. Semin Cell Dev Biol 15, 161-170.

Morris, R.E., Wu, J., and Shorthouse, R. (1990). A study of the contrasting effects of cyclosporine, FK 506, and rapamycin on the suppression of allograft rejection. Transplant Proc 22, 1638-1641.

Murakami, M., Ichisaka, T., Maeda, M., Oshiro, N., Hara, K., Edenhofer, F., Kiyama, H., Yonezawa, K., and Yamanaka, S. (2004). mTOR is essential for growth and proliferation in early mouse embryos and embryonic stem cells. Mol Cell Biol 24, 6710-6718.

Murray, J.T., Campbell, D.G., Morrice, N., Auld, G.C., Shpiro, N., Marquez, R., Peggie, M., Bain, J., Bloomberg, G.B., Grahammer, F., et al. (2004). Exploitation of KESTREL to identify NDRG family members as physiological substrates for SGK1 and GSK3. The Biochemical journal 384, 477-488.

Muzykewicz, D.A., Sharma, A., Muse, V., Numis, A.L., Rajagopal, J., and Thiele, E.A.

(2009). TSC1 and TSC2 mutations in patients with lymphangioleiomyomatosis and tuberous sclerosis complex. J Med Genet 46, 465-468.

Nojima, H., Tokunaga, C., Eguchi, S., Oshiro, N., Hidayat, S., Yoshino, K., Hara, K., Tanaka, N., Avruch, J., and Yonezawa, K. (2003). The mammalian target of rapamycin (mTOR) partner, raptor, binds the mTOR substrates p70 S6 kinase and 4E-BP1 through their TOR signaling (TOS) motif. J Biol Chem 278, 15461-15464.

Oldham, S., Montagne, J., Radimerski, T., Thomas, G., and Hafen, E. (2000). Genetic and biochemical characterization of dTOR, the Drosophila homolog of the target of rapamycin. Genes & Development 14, 2689-2694.

Oshiro, N., Takahashi, R., Yoshino, K., Tanimura, K., Nakashima, A., Eguchi, S., Miyamoto, T., Hara, K., Takehana, K., Avruch, J., et al. (2007). The proline-rich Akt substrate of 40 kDa (PRAS40) is a physiological substrate of mammalian target of rapamycin complex 1. J Biol Chem 282, 20329-20339.

Pearce, L.R., Huang, X., Boudeau, J., Pawlowski, R., Wullschleger, S., Deak, M., Ibrahim, A.F., Gourlay, R., Magnuson, M.A., and Alessi, D.R. (2007). Identification of Protor as a novel Rictor-binding component of mTOR complex-2. Biochem J 405, 513-522.

Pearce, L.R., Komander, D., and Alessi, D.R. (2010). The nuts and bolts of AGC protein kinases. Nat Rev Mol Cell Biol 11, 9-22.

Pearce, L.R., Sommer, E.M., Sakamoto, K., Wullschleger, S., and Alessi, D.R. (2011). Protor-1 is required for efficient mTORC2-mediated activation of SGK1 in the kidney. The Biochemical journal.

Pende, M., Um, S.H., Mieulet, V., Sticker, M., Goss, V.L., Mestan, J., Mueller, M., Fumagalli, S., Kozma, S.C., and Thomas, G. (2004). S6K1(-/-)/S6K2(-/-) mice exhibit perinatal lethality and rapamycin-sensitive 5'-terminal oligopyrimidine mRNA translation and reveal a mitogen-activated protein kinase-dependent S6 kinase pathway. Mol Cell Biol 24, 3112-3124.

Perry, J., and Kleckner, N. (2003). The ATRs, ATMs, and TORs are giant HEAT repeat proteins. Cell 112, 151-155.

Persad, S., Attwell, S., Gray, V., Mawji, N., Deng, J.T., Leung, D., Yan, J., Sanghera, J., Walsh, M.P., and Dedhar, S. (2001). Regulation of protein kinase B/Akt-serine 473 phosphorylation by integrin-linked kinase: critical roles for kinase activity and amino acids

arginine 211 and serine 343. J Biol Chem 276, 27462-27469.

Peterson, T.R., Laplante, M., Thoreen, C.C., Sancak, Y., Kang, S.A., Kuehl, W.M., Gray, N.S., and Sabatini, D.M. (2009). DEPTOR is an mTOR inhibitor frequently overexpressed in multiple myeloma cells and required for their survival. Cell 137, 873-886.

Petroulakis, E., Parsyan, A., Dowling, R.J., LeBacquer, O., Martineau, Y., Bidinosti, M., Larsson, O., Alain, T., Rong, L., Mamane, Y., et al. (2009). p53-dependent translational control of senescence and transformation via 4E-BPs. Cancer Cell 16, 439-446.

Polak, P., Cybulski, N., Feige, J.N., Auwerx, J., Ruegg, M.A., and Hall, M.N. (2008). Adipose-specific knockout of raptor results in lean mice with enhanced mitochondrial respiration. Cell Metab 8, 399-410.

Porstmann, T., Santos, C.R., Griffiths, B., Cully, M., Wu, M., Leevers, S., Griffiths, J.R., Chung, Y.L., and Schulze, A. (2008). SREBP activity is regulated by mTORC1 and contributes to Akt-dependent cell growth. Cell Metab 8, 224-236.

Potter, C.J., Pedraza, L.G., and Xu, T. (2002). Akt regulates growth by directly phosphorylating Tsc2. Nat Cell Biol 4, 658-665.

Powers, R.W., 3rd, Kaeberlein, M., Caldwell, S.D., Kennedy, B.K., and Fields, S. (2006). Extension of chronological life span in yeast by decreased TOR pathway signaling. Genes Dev 20, 174-184.

Price, D.J., Nemenoff, R.A., and Avruch, J. (1989). Purification of a hepatic S6 kinase from cycloheximide-treated Rats. J Biol Chem 264, 13825-13833.

Rabinowitz, J.D., and White, E. (2010). Autophagy and metabolism. Science 330, 1344-1348.

Raught, B., Peiretti, F., Gingras, A.C., Livingstone, M., Shahbazian, D., Mayeur, G.L., Polakiewicz, R.D., Sonenberg, N., and Hershey, J.W. (2004). Phosphorylation of eucaryotic translation initiation factor 4B Ser422 is modulated by S6 kinases. Embo J 23, 1761-1769.

Reiling, J.H., and Hafen, E. (2004). The hypoxia-induced paralogs Scylla and Charybdis inhibit growth by down-regulating S6K activity upstream of TSC in Drosophila. Genes Dev 18, 2879-2892.

Roux, P.P., Shahbazian, D., Vu, H., Holz, M.K., Cohen, M.S., Taunton, J., Sonenberg, N., and Blenis, J. (2007). RAS/ERK signaling promotes site-specific ribosomal protein S6 phosphorylation via RSK and stimulates cap-dependent translation. J Biol Chem 282, 14056-14064.

Ruggero, D., Montanaro, L., Ma, L., Xu, W., Londei, P., Cordon-Cardo, C., and Pandolfi, P.P. (2004). The translation factor eIF-4E promotes tumor formation and cooperates with c-Myc in lymphomagenesis. Nat Med 10, 484-486.

Ruvinsky, I., Sharon, N., Lerer, T., Cohen, H., Stolovich-Rain, M., Nir, T., Dor, Y., Zisman, P., and Meyuhas, O. (2005). Ribosomal protein S6 phosphorylation is a determinant of cell size and glucose homeostasis. Genes & Development 19, 2199-2211.

Sabatini, D.M., Erdjument-Bromage, H., Lui, M., Tempst, P., and Snyder, S.H. (1994). RAFT1: a mammalian protein that binds to FKBP12 in a rapamycin-dependent fashion and is homologous to yeast TORs. Cell 78, 35-43.

Sabers, C.J., Martin, M.M., Brunn, G.J., Williams, J.M., Dumont, F.J., Wiederrecht, G., and Abraham, R.T. (1995). Isolation of a protein target of the FKBP12-rapamycin complex in mammalian cells. J Biol Chem 270, 815-822.

Sancak, Y., Bar-Peled, L., Zoncu, R., Markhard, A.L., Nada, S., and Sabatini, D.M. (2010). Ragulator-Rag complex targets mTORC1 to the lysosomal surface and is necessary for its activation by amino acids. Cell 141, 290-303.

Sancak, Y., Peterson, T.R., Shaul, Y.D., Lindquist, R.A., Thoreen, C.C., Bar-Peled, L., and Sabatini, D.M. (2008). The Rag GTPases bind raptor and mediate amino acid signaling to mTORC1. Science 320, 1496-1501.

Sancak, Y., Thoreen, C.C., Peterson, T.R., Lindquist, R.A., Kang, S.A., Spooner, E., Carr, S.A., and Sabatini, D.M. (2007). PRAS40 is an insulin-regulated inhibitor of the mTORC1 protein kinase. Mol Cell 25, 903-915.

Sano, H., Kane, S., Sano, E., Miinea, C.P., Asara, J.M., Lane, W.S., Garner, C.W., and Lienhard, G.E. (2003). Insulin-stimulated phosphorylation of a Rab GTPase-activating protein regulates GLUT4 translocation. The Journal of biological chemistry 278, 14599-14602.

Sarbassov, D.D., Ali, S.M., Kim, D.H., Guertin, D.A., Latek, R.R., Erdjument-Bromage, H., Tempst, P., and Sabatini, D.M. (2004). Rictor, a novel binding partner of mTOR, de-

fines a rapamycin-insensitive and raptor-independent pathway that regulates the cytoskeleton. Curr Biol 14, 1296-1302.

Sarbassov, D.D., Ali, S.M., Sengupta, S., Sheen, J.H., Hsu, P.P., Bagley, A.F., Markhard, A.L., and Sabatini, D.M. (2006). Prolonged rapamycin treatment inhibits mTORC2 assembly and Akt/PKB. Mol Cell 22, 159-168.

Sarbassov, D.D., Guertin, D.A., Ali, S.M., and Sabatini, D.M. (2005). Phosphorylation and regulation of Akt/PKB by the rictor-mTOR complex. Science 307, 1098-1101.

Saucedo, L.J., Gao, X., Chiarelli, D.A., Li, L., Pan, D., and Edgar, B.A. (2003). Rheb promotes cell growth as a component of the insulin/TOR signalling network. Nat Cell Biol 5, 566-571.

Schalm, S.S., and Blenis, J. (2002). Identification of a conserved motif required for mTOR signaling. Curr Biol 12, 632-639.

Schalm, S.S., Fingar, D.C., Sabatini, D.M., and Blenis, J. (2003). TOS motif-mediated raptor binding regulates 4E-BP1 multisite phosphorylation and function. Curr Biol 13, 797-806.

Schroder, W.A., Buck, M., Cloonan, N., Hancock, J.F., Suhrbier, A., Sculley, T., and Bushell, G. (2007a). Human Sin1 contains Ras-binding and pleckstrin homology domains and suppresses Ras signalling. Cell Signal 19, 1279-1289.

Schroder, W.A., Buck, M., Cloonan, N., Hancock, J.F., Suhrbier, A., Sculley, T., and Bushell, G. (2007b). Human Sin1 contains Ras-binding and pleckstrin homology domains and suppresses Ras signalling. Cellular Signalling 19, 1279-1289.

Sehgal, S.N., Baker, H., and Vezina, C. (1975). Rapamycin (AY-22,989), a new antifungal antibiotic. II. Fermentation, isolation and characterization. J Antibiot (Tokyo) 28, 727-732.

Sekulic, A., Hudson, C.C., Homme, J.L., Yin, P., Otterness, D.M., Karnitz, L.M., and Abraham, R.T. (2000). A direct linkage between the phosphoinositide 3-kinase-AKT signaling pathway and the mammalian target of rapamycin in mitogen-stimulated and transformed cells. Cancer Res 60, 3504-3513.

Sengupta, S., Peterson, T.R., Laplante, M., Oh, S., and Sabatini, D.M. (2011). mTORC1 controls fasting-induced ketogenesis and its modulation by ageing. Nature 468, 1100-

1104.

Shah, O.J., and Hunter, T. (2006). Turnover of the active fraction of IRS1 involves raptor-mTOR- and S6K1-dependent serine phosphorylation in cell culture models of tuberous sclerosis. Mol Cell Biol 26, 6425-6434.

Shah, O.J., Wang, Z., and Hunter, T. (2004). Inappropriate activation of the TSC/Rheb/mTOR/S6K cassette induces IRS1/2 depletion, insulin resistance, and cell survival deficiencies. Current biology : CB 14, 1650-1656.

Shaw, R.J., Bardeesy, N., Manning, B.D., Lopez, L., Kosmatka, M., DePinho, R.A., and Cantley, L.C. (2004). The LKB1 tumor suppressor negatively regulates mTOR signaling. Cancer Cell 6, 91-99.

She, Q.B., Halilovic, E., Ye, Q., Zhen, W., Shirasawa, S., Sasazuki, T., Solit, D.B., and Rosen, N. (2010). 4E-BP1 is a key effector of the oncogenic activation of the AKT and ERK signaling pathways that integrates their function in tumors. Cancer Cell 18, 39-51.

Shimono, A., Okuda, T., and Kondoh, H. (1999). N-myc-dependent repression of ndr1, a gene identified by direct subtraction of whole mouse embryo cDNAs between wild type and N-myc mutant. Mechanisms of development 83, 39-52.

Smith, E.M., Finn, S.G., Tee, A.R., Browne, G.J., and Proud, C.G. (2005). The tuberous sclerosis protein TSC2 is not required for the regulation of the mammalian target of rapamycin by amino acids and certain cellular stresses. J Biol Chem 280, 18717-18727.

Stan, R., McLaughlin, M.M., Cafferkey, R., Johnson, R.K., Rosenberg, M., and Livi, G.P. (1994). Interaction between FKBP12-rapamycin and TOR involves a conserved serine residue. J Biol Chem 269, 32027-32030.

Stocker, H., Radimerski, T., Schindelholz, B., Wittwer, F., Belawat, P., Daram, P., Breuer, S., Thomas, G., and Hafen, E. (2003). Rheb is an essential regulator of S6K in controlling cell growth in Drosophila. Nat Cell Biol 5, 559-565.

Taccioli, G.E., Amatucci, A.G., Beamish, H.J., Gell, D., Xiang, X.H., Torres Arzayus, M.I., Priestley, A., Jackson, S.P., Marshak Rothstein, A., Jeggo, P.A., et al. (1998). Targeted disruption of the catalytic subunit of the DNA-PK gene in mice confers severe combined immunodeficiency and radiosensitivity. Immunity 9, 355-366.

Taniguchi, C.M., Emanuelli, B., and Kahn, C.R. (2006). Critical nodes in signalling path-

ways: insights into insulin action. Nature reviews Molecular cell biology 7, 85-96.

Tee, A.R., Manning, B.D., Roux, P.P., Cantley, L.C., and Blenis, J. (2003). Tuberous sclerosis complex gene products, Tuberin and Hamartin, control mTOR signaling by acting as a GTPase-activating protein complex toward Rheb. Curr Biol 13, 1259-1268.

Terada, N., Patel, H.R., Takase, K., Kohno, K., Nairn, A.C., and Gelfand, E.W. (1994). Rapamycin selectively inhibits translation of mRNAs encoding elongation factors and ribosomal proteins. Proc Natl Acad Sci U S A 91, 11477-11481.

Thomas, G., Martin-Perez, J., Siegmann, M., and Otto, A.M. (1982). The effect of serum, EGF, PGF2 alpha and insulin on S6 phosphorylation and the initiation of protein and DNA synthesis. Cell 30, 235-242.

Thomas, G.V., Tran, C., Mellinghoff, I.K., Welsbie, D.S., Chan, E., Fueger, B., Czernin, J., and Sawyers, C.L. (2006). Hypoxia-inducible factor determines sensitivity to inhibitors of mTOR in kidney cancer. Nat Med 12, 122-127.

Thoreen, C.C., Kang, S.A., Chang, J.W., Liu, Q., Zhang, J., Gao, Y., Reichling, L.J., Sim, T., Sabatini, D.M., and Gray, N.S. (2009). An ATP-competitive mammalian target of rapamycin inhibitor reveals rapamycin-resistant functions of mTORC1. J Biol Chem 284, 8023-8032.

Toker, A., and Newton, A.C. (2000). Akt/protein kinase B is regulated by autophosphorylation at the hypothetical PDK-2 site. J Biol Chem 275, 8271-8274.

Treins, C., Warne, P.H., Magnuson, M.A., Pende, M., and Downward, J. (2010). Rictor is a novel target of p70 S6 kinase-1. Oncogene 29, 1003-1016.

Um, S.H., Frigerio, F., Watanabe, M., Picard, F., Joaquin, M., Sticker, M., Fumagalli, S., Allegrini, P.R., Kozma, S.C., Auwerx, J., et al. (2004). Absence of S6K1 protects against age- and diet-induced obesity while enhancing insulin sensitivity. Nature 431, 200-205.

van Slegtenhorst, M., de Hoogt, R., Hermans, C., Nellist, M., Janssen, B., Verhoef, S., Lindhout, D., van den Ouweland, A., Halley, D., Young, J., et al. (1997). Identification of the tuberous sclerosis gene TSC1 on chromosome 9q34. Science 277, 805-808.

van Slegtenhorst, M., Nellist, M., Nagelkerken, B., Cheadle, J., Snell, R., van den Ouweland, A., Reuser, A., Sampson, J., Halley, D., and van der Sluijs, P. (1998). Interaction between hamartin and tuberin, the TSC1 and TSC2 gene products. Human molecular

genetics 7, 1053-1057.

Vander Haar, E., Lee, S.I., Bandhakavi, S., Griffin, T.J., and Kim, D.H. (2007). Insulin signalling to mTOR mediated by the Akt/PKB substrate PRAS40. Nat Cell Biol 9, 316-323.

Vellai, T., Takacs-Vellai, K., Zhang, Y., Kovacs, A.L., Orosz, L., and Muller, F. (2003). Genetics: influence of TOR kinase on lifespan in C. elegans. Nature 426, 620.

Wang, L., Harris, T.E., Roth, R.A., and Lawrence, J.C., Jr. (2007). PRAS40 regulates mTORC1 kinase activity by functioning as a direct inhibitor of substrate binding. J Biol Chem 282, 20036-20044.

Wang, X., Beugnet, A., Murakami, M., Yamanaka, S., and Proud, C.G. (2005). Distinct signaling events downstream of mTOR cooperate to mediate the effects of amino acids and insulin on initiation factor 4E-binding proteins. Mol Cell Biol 25, 2558-2572.

Wang, X., Campbell, L.E., Miller, C.M., and Proud, C.G. (1998). Amino acid availability regulates p70 S6 kinase and multiple translation factors. Biochem J 334 ( Pt 1), 261-267.

Wang, X., Li, W., Williams, M., Terada, N., Alessi, D.R., and Proud, C.G. (2001). Regulation of elongation factor 2 kinase by p90(RSK1) and p70 S6 kinase. Embo J 20, 4370-4379.

Wendel, H.G., De Stanchina, E., Fridman, J.S., Malina, A., Ray, S., Kogan, S., Cordon-Cardo, C., Pelletier, J., and Lowe, S.W. (2004). Survival signalling by Akt and eIF4E in oncogenesis and cancer therapy. Nature 428, 332-337.

Wessely, R. (2010). New drug-eluting stent concepts. Nat Rev Cardiol 7, 194-203.

Williams, M.R., Arthur, J.S., Balendran, A., van der Kaay, J., Poli, V., Cohen, P., and Alessi, D.R. (2000). The role of 3-phosphoinositide-dependent protein kinase 1 in activating AGC kinases defined in embryonic stem cells. Curr Biol 10, 439-448.

Woo, S.Y., Kim, D.H., Jun, C.B., Kim, Y.M., Haar, E.V., Lee, S.I., Hegg, J.W., Bandhakavi, S., Griffin, T.J., and Kim, D.H. (2007). PRR5, a novel component of mTOR complex 2, regulates platelet-derived growth factor receptor beta expression and signaling. J Biol Chem 282, 25604-25612.

Yang, Q., Inoki, K., Ikenoue, T., and Guan, K.L. (2006). Identification of Sin1 as an essential TORC2 component required for complex formation and kinase activity. Genes

Dev 20, 2820-2832.

Yang, Z., and Klionsky, D.J. (2010). Mammalian autophagy: core molecular machinery and signaling regulation. Current Opinion in Cell Biology 22, 124-131.

Yatscoff, R.W., LeGatt, D.F., and Kneteman, N.M. (1993). Therapeutic monitoring of rapamycin: a new immunosuppressive drug. Ther Drug Monit 15, 478-482.

Yip, C.K., Murata, K., Walz, T., Sabatini, D.M., and Kang, S.A. (2010). Structure of the human mTOR complex I and its implications for rapamycin inhibition. Mol Cell 38, 768-774.

Yu, J., and Henske, E.P. (2010). mTOR activation, lymphangiogenesis, and estrogen-mediated cell survival: the "perfect storm" of pro-metastatic factors in LAM pathogenesis. Lymphat Res Biol 8, 43-49.

Yu, K., Toral-Barza, L., Shi, C., Zhang, W.G., Lucas, J., Shor, B., Kim, J., Verheijen, J., Curran, K., Malwitz, D.J., et al. (2009). Biochemical, cellular, and in vivo activity of novel ATP-competitive and selective inhibitors of the mammalian target of rapamycin. Cancer Res 69, 6232-6240.

Yu, L., McPhee, C.K., Zheng, L., Mardones, G.A., Rong, Y., Peng, J., Mi, N., Zhao, Y., Liu, Z., Wan, F., et al. (2010). Termination of autophagy and reformation of lysosomes regulated by mTOR. Nature 465, 942-946.

Zhang, H., Bajraszewski, N., Wu, E., Wang, H., Moseman, A.P., Dabora, S.L., Griffin, J.D., and Kwiatkowski, D.J. (2007). PDGFRs are critical for PI3K/Akt activation and negatively regulated by mTOR. J Clin Invest 117, 730-738.

Zhang, H., Cicchetti, G., Onda, H., Koon, H.B., Asrican, K., Bajraszewski, N., Vazquez, F., Carpenter, C.L., and Kwiatkowski, D.J. (2003a). Loss of Tsc1/Tsc2 activates mTOR and disrupts PI3K-Akt signaling through downregulation of PDGFR. J Clin Invest 112, 1223-1233.

Zhang, H., Stallock, J.P., Ng, J.C., Reinhard, C., and Neufeld, T.P. (2000). Regulation of cellular growth by the Drosophila target of rapamycin dTOR. Genes & Development 14, 2712-2724.

Zhang, H.H., Huang, J., Duvel, K., Boback, B., Wu, S., Squillace, R.M., Wu, C.L., and Manning, B.D. (2009). Insulin stimulates adipogenesis through the Akt-TSC2-mTORC1

pathway. PLoS One 4, e6189.

Zhang, Y., Gao, X., Saucedo, L.J., Ru, B., Edgar, B.A., and Pan, D. (2003b). Rheb is a direct target of the tuberous sclerosis tumour suppressor proteins. Nat Cell Biol 5, 578-581.

Zhong, H., Chiles, K., Feldser, D., Laughner, E., Hanrahan, C., Georgescu, M.M., Simons, J.W., and Semenza, G.L. (2000). Modulation of hypoxia-inducible factor 1alpha expression by the epidermal growth factor/phosphatidylinositol 3-kinase/PTEN/AKT/FRAP pathway in human prostate cancer cells: implications for tumor angiogenesis and therapeutics. Cancer Research 60, 1541-1545.

Zhou, B.P., Liao, Y., Xia, W., Zou, Y., Spohn, B., and Hung, M.C. (2001). HER-2/neu induces p53 ubiquitination via Akt-mediated MDM2 phosphorylation. Nature cell biology 3, 973-982.

Zinzalla, V., Stracka, D., Oppliger, W., and Hall, M.N. (2011). Activation of mTORC2 by Association with the Ribosome. Cell 144, 757-768.

# Chapter 2

## Characterization of the mTOR-regulated phosphoproteome

Peggy P. Hsu [1,2], Seong A. Kang [1], Jonathan Rameseder [3,4], Yi Zhang [5,6], Daniel Lim [4], Ailan Guo [8], Yongmun Choi [5,7], Roberto D. Polakiewicz [8], Michael J. Comb [8], Nathanael S. Gray [5,7], Michael B. Yaffe [2,4], Jarrod A. Marto [5,6,7], David M. Sabatini [1,2,4,9]

1 Whitehead Institute for Biomedical Research, Nine Cambridge Center, Cambridge, MA 02142, USA

2 Department of Biology, Massachusetts Institute of Technology (MIT), Cambridge, MA 02139, USA

3 Computational and Systems Biology Initiative, MIT, Cambridge, MA 02139, USA

4 David H. Koch Institute for Integrative Cancer Research at MIT, 77 Massachusetts Avenue, Cambridge, MA 02139, USA

5 Department of Cancer Biology, Dana Farber Cancer Institute (DFCI), 250 Longwood Avenue, Boston, MA 02115, USA

6 Blais Proteomics Center, DFCI, 250 Longwood Avenue, Boston, MA 02115, USA

7 Department of Biological Chemistry and Molecular Pharmacology, Harvard Medical School, 250 Longwood Avenue, Boston, MA 02115, USA

8 Cell Signaling Technology Inc., 3 Trask Lane, Danvers, MA 01923

9 Howard Hughes Medical Institute

Experiments shown in Figures 1 and 2 were performed by PPH and AG. Experiments shown in Figures 3, 4, and 5 were performed by PPH and YZ with analysis and visualization by PPH and JR. Experiments shown in Figure 6 were performed by SAK and DL with analysis by PPH and JR. The analysis shown in Figure 8 was performed by PPH and JR.

## Summary

The mTOR protein kinase is a master growth promoter that nucleates two complexes, mTORC1 and mTORC2. Despite the diverse processes controlled by mTOR, few substrates are known. In order to identify additional downstream components of the mTOR signaling pathway, we adopted a tripartite approach. First, we identified candidate AGC kinase substrates downstream of mTOR by immunoaffinity phosphopeptide isolation coupled to semiquantitative mass spectrometry. Second, we defined the mTOR-regulated phosphoproteome by quantitative mass spectrometry with isobaric mass tags. Third, we characterized the primary sequence motif specificity of mTOR using positional scanning peptide libraries. Globally, mTOR inhibition mimics serum starvation and results in the dephosphorylation of many proteins involved in processes not previously linked to the pathway. Moreover, mTOR exhibits a preference for proline, hydrophobic, and aromatic residues at the +1 position, unique among all kinases previously profiled. We classified the mTOR regulated phosphorylation sites as belonging to the mTORC1 or mTORC2 pathways and by motif as candidate direct or indirect effectors. Our results implicate mTOR in an even broader array of biological processes than presently appreciated and open new areas of investigation in mTOR biology.

## Introduction

The serine-threonine kinase mechanistic target of rapamycin (mTOR) is a major controller of growth that is deregulated in cancer and diabetes (Laplante and Sabatini, 2009; Zoncu et al., 2011). mTOR is the catalytic subunit of two multi-protein complexes, mTORC1 and mTORC2. mTORC1 is activated by growth factors and nutrients through a pathway that involves the tuberous sclerosis complex (TSC1-TSC2) tumor suppressors as well as the Rag and Rheb guanosine triphosphatases (GTPases). mTORC1 phosphorylates the translational regulators S6 Kinase 1 (S6K1) and the eIF-4E binding proteins (4E-BP1 and 4E-BP2) while mTORC2 activates Akt and serum/ glucocorticoid regulated kinase 1 (SGK1) and is part of the growth factor-stimulated phosphoinositide-3-kinase (PI3K) pathway. Collectively, mTORC1 and mTORC2 regulate cell growth, proliferation, survival, autophagy, and glucose and lipid metabolism.

The few mTOR substrates with defined phosphorylation sites likely cannot explain all processes under the control of mTOR (Laplante and Sabatini, 2009; Zoncu et al., 2011). Several reasons exist as to why more substrates have not been identified. First, mTOR only transiently interacts with several of its substrates, making biochemical isolation of a stable kinase-substrate interaction difficult. Second, unlike the other PIKK family kinases, or the AGC kinases downstream of mTOR, a consensus phosphoacceptor motif is not known, such that phosphorylation sites cannot be predicted to be, or excluded from being, mTOR-mediated. mTOR phosphorylates both the hydrophobic motif (HM) on AGC kinases, as well as proline-directed sites on substrates such as 4E-BP1 (Chapter 1, Fig. 2). Whether or not mTOR has any motif specificity is an outstanding question. Finally, the biggest challenge to the identification of mTOR substrates is that until recently it was not possible to acutely inhibit within cells all the kinase-dependent functions of mTOR. The well-known drug rapamycin is an allosteric inhibitor of mTOR that only inhibits a subset of mTORC1-mediated phosphorylations and at short treatment times does not inhibit mTORC2 (Choo et al., 2008; Feldman et

al., 2009; Thoreen et al., 2009). Thus, the recent development of potent ATP-competitive inhibitors of mTOR that block all known phosphorylations downstream of mTORC1 and mTORC2 (Feldman et al., 2009; Garcia-Martinez et al., 2009; Thoreen et al., 2009; Yu et al., 2009) has opened the door to a systematic investigation of the mTOR-regulated phosphoproteome.

Here, we adopted a three-pronged approach to identify downstream effectors of mTOR. First, we used semi-quantitative mass spectrometry and phosphospecific motif antibody enrichment to identify proline-directed phosphorylation sites and AGC kinase substrates downstream of mTOR. Second, we employed quantitative mass spectrometry with isobaric mass tags to define the mTOR-regulated phosphoproteome in cells in which mTOR signaling is hyperactivated and subsequently inhibited. Finally, we defined the consensus mTOR phospho-acceptor motif by in vitro phosphorylation of a positional scanning peptide library and used this motif to stratify the mTOR-regulated sites by likelihood of direct phosphorylation by mTOR. We found that a majority of insulin-stimulated phosphorylations are mTOR-dependent, that many Torin1-sensitive phosphorylation sites are rapamycin-resistant, and that mTOR may regulate the phosphorylation of proteins involved in processes not previously linked to it. Our results indicate that many additional mTOR substrates exist, awaiting further characterization, and may serve as starting points for new areas of investigation in mTOR biology.

## Results and Discussion

### Identification of AGC kinase substrates and proline-directed phosphorylations downstream of mTOR by immunoaffinity phosphopeptide isolation

In contrast to phosphosite-specific antibodies that recognize a specific phosphorylation site on a single protein substrate, phospho-motif antibodies are broadly reactive against consensus phosphorylation motifs that appear in substrates downstream of a kinase or kinase family (Zhang et al., 2002). Phosphopeptides can be isolated from cell lysates using these motif antibodies, and their abundances estimated across several conditions by semi-quantitative mass spectrometry (Rush et al., 2005; Stokes et al., 2007). This strategy has been successfully employed to globally profile signaling downstream of the PIKK family DNA-damage response kinases, ATM and ATR, which phosphorylate a (S*/T*)Q motif (where X can be any amino acid, and * indicates a phosphoacceptor residue) (Matsuoka et al., 2007; Stokes et al., 2007). More recently, a similar approach has been used to profile AGC kinase substrates that are recognized by a motif antibody against RXX(S*/T*), with minor selectivity for arginine at the -5 and -3 positions, downstream of activated growth factor receptors (Moritz et al., 2010). Given that mTOR is known to activate several AGC kinases, including S6K1, Akt, SGK1, and PKC$\alpha$, as well as phosphorylate proline-directed sites, we adopted this method using the same AGC kinase substrate antibody mentioned above (RXX(S*/T*)), and an antibody recognizing a T*P motif.

Human embryonic kidney (HEK)-293E cells were deprived of serum and then stimulated with insulin in the presence or absence of rapamycin or Torin1, a recently developed ATP-competitive mTOR kinase domain inhibitor that blocks all known phosphorylations downstream of mTORC1 and mTORC2 (Thoreen et al., 2009). Insulin stimulates and Torin1 inhibits both mTORC1 and mTORC2, while rapamycin only prevents a subset of mTORC1-regulated phosphorylations. With the AGC kinase motif antibody, we identified 90 phosphorylation sites on 40 proteins whose abundances were

two-fold less under Torin1 treatment ($log_2$(Torin1/Insulin) < -1) (Fig. 1). With the proline-directed motif antibody, 84 sites on 45 proteins were two-fold less abundant with mTOR inhibition (Fig. 2).

We identified several AGC kinase sites on well-known mTOR pathway components, including the S6K1 substrates PDCD4 S67, Rictor T1135, and S6 S235, S236, S240, S244, the Akt substrates TBC1D4/AS160 S588, T642 and AKT1S1/ PRAS40 T246, and the SGK1 substrates NDRG1 T328, S330, T366 and NDRG2 T330, S332 (Fig. 1). With T*P enrichment, we detected phosphorylated threonines including sites on IRS2, a known downstream effector of mTOR, as well as a few proline-directed serine phosphorylations such as S65 on the mTORC1 substrate 4E-BP1 (Fig. 2). In addition, we detected several other proline-directed phosphorylations, a subset of which could represent new mTOR substrates and require further characterization (Fig. 2).

While immunoaffinity isolation has certain advantages, including enrichment and detection of lower abundance phosphorylations, the method has certain drawbacks. First, it depends on the existence of a specific phospho-motif antibody, and on that antibody recognizing an appropriate motif. Given that a consensus motif for mTOR has not been defined, as we address later in this chapter, even a relatively nonspecific antibody like the one recognizing T*P could still exclude many relevant phosphorylations. The antibody, for example, does not recognize S*P as well, and while it is known that mTOR can phosphorylate proline-directed sites, mTOR specificity at the +1 position has never been determined, and thus the approach may fail to detect mTOR-mediated phosphorylation sites which are not proline-directed. Moreover, while it is true that several AGC kinases are activated by mTOR, other groups have already profiled many of these phosphorylations with rapamycin (Moritz et al., 2010), and the AGC kinase substrates detected by this method are one step removed from mTOR. Therefore, we turned to a motif-agnostic, quantitative approach to identify novel downstream substrates.

**Identification of the mTOR-regulated phosphoproteome by quantitative mass spectrometry**

Taking a non-motif based approach to substrate identification, we conducted a systematic investigation of the mTOR-regulated phosphoproteome using mass spectrometry and isobaric tags that permit 4-way multiplexed relative quantification of phosphopeptide abundances (iTRAQ) (Ross et al., 2004). With duplicate analyses for each, we analyzed phosphopeptides from two sets of cells in which the pathway was hyperactivated and then inhibited with Torin1, HEK-293E cells were deprived of serum and then stimulated with insulin in the presence or absence of rapamycin or Torin1 (Fig. 3A). Wild-type ($TSC2^{+/+}$) and TSC2-null ($TSC2^{-/-}$) mouse embryonic fibroblasts (MEFs), which have increased mTORC1 signaling, were also treated with or without Torin1 (Fig. 3A). Under these conditions, phosphorylation events known to be downstream of mTORC1 (e.g. rapamycin-sensitive T389 S6K1 and rapamycin-insensitive T37 and T46 4E-BP1) and mTORC2 (e.g. S473 Akt, T246 PRAS40/AKT1S1, T346 NDRG1) behaved as expected (Fig. 3B).

Cells were lysed in urea and digested, peptides labeled with iTRAQ reagent, phosphopeptides nitrilotriacetic (NTA)-$Fe^{3+}$ enriched based on their charge, and analyzed by liquid chromatography followed by tandem mass spectrometry (LC-MS/MS) with the iTRAQ reporter ion intensity values used to determine phosphopeptide abundance. By this method, we detected many phosphorylations whose abundances were affected by mTOR inhibition. From the HEK-293E cells, we identified 4256 unique phosphopeptides corresponding to 47 phosphotyrosine and 4204 phosphoserine-threonine sites on 1661 distinct proteins (FDR ~1%, Fig. 3C). Using a cutoff of 2.5 median absolute deviations (MADs) below the median $\log_2$(Torin1/Insulin ratio) (robust z-score < -2.5), 127 phosphopeptides from 93 proteins were identified as sensitive to Torin1 and designated as mTOR-regulated (Fig. 3C). From the MEFs, 7299 unique phosphopeptides corresponding to 110 phosphotyrosine and 7145 phosphoserine-threonine sites on 2406 distinct proteins were identified (FDR~1%, Fig 3D), of which 231 phosphopeptides from 174 proteins were regulated by mTOR (-2.5 MAD, $\log_2$($TSC2^{-/-}$ Torin1/$TSC2^{-/-}$ vehicle)

(Fig. 3D). By this -2.5 MAD cutoff for both the HEK-293E and MEF datasets, the mTOR-regulated sites were highly enriched in canonical mTOR pathway phosphorylations (Fisher's exact test p-value = $5.2 \times 10^{-24}$ and $6.5 \times 10^{-23}$, respectively; Fig. 3C, 3D), an indication of the predictive potential of the data to identify mTOR pathway components. We also identified sites on known mTOR substrates with less well-characterized sites (CAP-GLY domain containing linker protein 1 (CLIP1) S1158 (Choi et al., 2002), Unc-51 like kinase 1 (ULK1) S638 (Ganley et al., 2009; Hosokawa et al., 2009; Jung et al., 2009), and insulin receptor substrate 2 (IRS2) S616 (Shah et al., 2004)). Additionally, several of the proteins detected as mTOR-regulated by immunoaffinity phosphopeptide enrichment were also detected by iTRAQ in either one of the datasets to contain Torin1-sensitive sites: ACLY, AKAP12, 4E-BP1, FOXK2, HIRIP3, IRS2, KIAA0528, MAP1B, MDC1, MYCBP2, NDRG1, PDCD4, PRAS40, REPS1, RPS6, STX7, TCF12, and TMPO.

Pathway analysis of the candidate mTOR-regulated proteins revealed enrichment (FDR < 10%) in the mTOR signaling pathway (KEGG 04150) and processes known to be downstream of mTOR, such as translation (GO:0006417), regulation of cell size (GO:0008361), and aging (GO:0007568) as well as some not generally considered to be under mTOR control. These include RNA splicing (GO:0008380), DNA replication (GO:0006260), vesicle-mediated transport (GO:0016192), and regulation of mRNA processing bodies (GO:0000932), signifying a broader role for mTOR signaling than presently appreciated.

**Torin1 mimics serum deprivation and is a more complete inhibitor than rapamycin**

Global comparisons of the iTRAQ datasets revealed several interesting features. In the HEK-293E cells, phosphorylation changes resulting from Torin1 treatment were strikingly similar to those observed under serum deprivation (Spearman's $\rho = 0.66$, p-value ~ 0, Fig. 4A), revealing that insulin-regulated phosphorylations (both down- and up-) are largely mTOR-dependent. mTORC2 pathway phosphorylations, moreover, were better inhibited by serum deprivation than by Torin1 treatment while T37 and T46 phosphorylation on 4E-BP1 and 4E-BP2 were the opposite (Fig. 3B, 4A). The effects

of rapamycin and Torin1 treatment were similar (Spearman's $\rho = 0.48$, p-value ~ 0, Fig. 4B), but a subset of Torin1-sensitive sites were not rapamycin-sensitive (upper left quadrant, Fig. 4B), including T37 and T46 of 4E-BP1 and 4E-BP2 (Choo et al., 2008; Feldman et al., 2009; Thoreen et al., 2009) and the mTORC2-mediated S472 Akt3 and S330 NDRG1. These results suggest that mTOR kinase domain inhibitors may be more effective clinically than rapamycin analogs due to their greater ability to mimic serum deprivation and also confirm that substrates may have been missed previously in an era when rapamycin was the sole mTOR inhibitor available. Analysis of the MEF dataset revealed that phosphoryations that increase with TSC2 loss are more likely to be inhibited by Torin1 (Spearman's $\rho = -0.25$, p-value = $1.4 \times 10^{-130}$) (Fig. 4C).

Hierarchical clustering of the conditions and sorting of the phosphopeptide abundances in the HEK-293E cells also verified the similarity between serum starvation and Torin1 treatment (Fig. 5) and our ability to discriminate between known rapamycin-sensitive (top, Fig. 5) and -insensitive (bottom, Fig. 5) sites and showed that phosphorylations that are rapamycin-sensitive tend to be inhibited to a greater extent by Torin1 treatment than those that are not (Fig. 5).

**Definition of a consensus mTOR phospho-acceptor motif**

As the mTOR-regulated sites may be phosphorylated by mTOR or by downstream kinases we sought to distinguish direct substrates from indirect effectors by determining a consensus phospho-acceptor motif for mTOR. It is unknown if the kinase exhibits any motif specificity or if the choice of sites is entirely determined by factors beyond the primary substrate sequence (e.g. docking interactions, auxiliary scaffolding proteins, subcellular colocalization). How mTOR can phosphorylate the hydrophobic motifs of the AGC kinases as well as the quite distinct proline-directed sites of proteins such as 4E-BP1 and 4E-BP2 (Chapter 1, Fig. 2) is an outstanding mystery. A nonpolar pocket present in the substrate binding site of other proline-directed kinases and phosphatases interacts with the +1 proline but cannot satisfy the hydrogen-bonding requirement of the amide nitrogen in other amino acids (Brown et

al., 1999; Gray et al., 2003). Proline-directed specificity should therefore be mutually exclusive with hydrophobic motif specificity. Moreover, even within the AGC kinase HM, it is unclear whether certain residues present within the motif are required by mTOR for phosphorylation or are simply structural components of AGC kinases (Chapter 1, Fig. 2) (Gold et al., 2006). As alluded to earlier, this lack of knowledge regarding substrate preference has partially impeded the discovery of additional mTOR substrates.

To date, a phosphorylation motif for mTOR has not been determined because previous attempts to phosphorylate peptides with mTOR have not been successful. We found that when combined with its activator, GTP-bound Rheb, highly pure and intact mTORC1 (Yip et al., 2010) robustly phosphorylated an arrayed positional scanning peptide library (PSPL), a collection of peptides in which one position is fixed to a specific amino acid relative to a central phosphoacceptor serine or threonine and all other positions in the peptides are randomized (Hutti et al., 2004) (Fig. 6A). Although mTORC1 and mTORC2 phosphorylate distinct sets of substrates, they are likely to have similar phospho-acceptor preferences because they share the same catalytic domain. A case in point is that mTORC2 can phosphorylate the HM of truncation mutants of S6K1 (Ali and Sabatini, 2005), suggesting that its inactivity towards full length S6K1 is a result of structural constraints in the intact protein rather than an inability to recognize the HM of S6K1. This unbiased assay revealed that mTOR possesses selectivity towards peptide substrates concordant with known mTOR sites (Chapter 1, Fig. 2; this chapter, Fig. 6A-C), primarily at the +1 position at which mTOR prefers proline, hydrophobic (L, V), and aromatic residues (F, W, Y). We detected minor selectivity at other positions, including glycine at the -1, hydrophobic residues at the -5, and prolines at the -1 and -2 positions (Fig. 6A-C). mTOR also phosphorylates serines in a specific register, indicating a preference to act on serines spaced two apart (-2, +2) (Fig. 6A). This pattern of specificity, especially at the +1 position, is unique amongst all kinases previously profiled by this method (Mok et al., 2010).

These data suggest that mTOR inherently prefers proline residues and are less consistent with mTOR activating a proline-directed kinase or regulating a proline-directed

phosphatase (Alessi et al., 2009). These findings also indicate that within the HM of the AGC kinases (Chapter 1, Fig. 2) the -4 and -1 hydrophobic residues are dispensable for mTOR recognition and rather are required for AGC kinase function. Indeed, other AGC kinases (e.g. PKA) have truncated hydrophobic motifs lacking the phosphorylatable and following +1 hydrophobic residue but still have hydrophobic residues in the –4 and –1 position. Structural information will be required to resolve how mTOR can phosphorylate two very distinct motifs and more detailed biochemical characterization with model peptides will be helpful in determining whether the consensus motif represents only one motif or a conflation of two or more.

**Classification of the mTOR-regulated phosphoproteome**

Combining our approaches, we classified the mTOR-regulated phosphorylation sites as determined by iTRAQ, first by rapamycin sensitivity (HEK-293E -2.5 MAD $\log_2$(Rapamycin/Insulin) or by increased phosphorylation in cells lacking TSC2 (MEFs, +2.5 MAD $\log_2$($TSC2^{-/-}$ vehicle/$TSC2^{+/+}$ vehicle) (Fig. 7, 8). Rapamycin-sensitive sites or those upregulated in $TSC2^{-/-}$ cells are likely mTORC1-regulated while the remaining could be downstream of either complex. Second, we scored the sites by motif into the following categories: (1) candidate direct mTOR sites as scored by the Scansite algorithm using a scoring matrix derived from the quanititation of our in vitro PSPL results (Obenauer et al., 2003), (2) candidate AGC kinase substrates containing an (R/K) X(R/K)XX(S*/T*) sequence, or (3) mTOR-regulated but by an undetermined mechanism (Fig. 7, 8).

Of the 127 phoshopeptides regulated by mTOR in HEK-293E cells, only 34 met the cut-off for rapamycin sensitivity and are likely mTORC1-phosphorylated, while the remaining could be downstream of either complex. 20 and 16 phosphopeptides contained putative mTOR and AGC kinase phosphorylation sites, respectively (Fig. 7). In the MEFs, 25 of the mTOR-regulated phosphopeptides were confidently upregulated in TSC2-null MEFs compared to wild-type cells, and 47 and 34 of the mTOR-regulated phosphopeptides matched the consensus mTOR and AGC kinase motifs, respectively

(Fig. 8).

Several candidate mTOR substrates implicate mTOR in new aspects of growth control. For example, the molecular mechanisms through which mTORC1 regulates autophagy remain unclear. WD repeat domain, phosphoinositide interacting 2 (WIPI2) (Fig. 8), a sparsely characterized orthologue of the yeast Atg18p, is a potential mTOR substrate and recent work suggests it is required for early events in autophagosome formation (Polson et al., 2010). We also found the translation initiation factor eIF4G1 to be a candidate mTOR substrate (Fig. 8). Others have previously shown that eIF4G1 depletion strongly phenocopies nutrient deprivation or raptor loss and result in induction of autophagy, and that mTORC1 can phosphorylate eIF4G1 directly (Ramirez-Valle et al., 2008). Their and our data indicate that mTOR may control translation through the regulation of multiple components. In addition, the candidate substrates protein associated with topoisomerase II homolog 1 (PATL1) (Fig. 7, 8) and La ribonucleoprotein domain family member 1 (LARP1) (Fig. 7, 8) bind RNA, localize to P-bodies, and control mRNA stability (Nykamp et al., 2008; Parker and Sheth, 2007). A recent proteomic effort identified yeast Pat1p phosphorylation as rapamycin-sensitive in yeast (Huber et al., 2009), and Pat1p deficient yeast do not repress mRNA translation upon amino acid withdrawal (Coller and Parker, 2005), suggesting that the regulation of mRNA degradation may be important for mTOR-dependent growth control.

Other potential substrates point to nascent, clinically-relevant areas of mTOR biology. mTOR putatively regulates the phosphorylation of Nestin (Fig. 8), the AP-1 transcription factor c-Jun (Fig. 8), and forkhead box K1 (FoxK1) (Fig. 8). While little is known about the function of the intermediate filament protein Nestin, it is widely used as a marker of neural stem cells (Singh et al., 2004). c-Jun is a pleiotropic transcription factor involved in proliferation, apoptosis, and responses to hypoxia and is thought to play a role in various cancers (Rowe et al., 2010; Shaulian, 2010). FoxK1 expression is greatly enriched in myogenic stem cells, and mice lacking FoxK1 have impaired satellite cell function and muscle atrophy (Garry et al., 2000).

These and other candidate substrates may prompt future work into the role of

mTOR in cellular processes in which it has not yet been implicated and open new areas of investigation in mTOR biology. In the following chapter, we describe the detailed molecular characterization of one of the candidate substrates identified by these phosphoproteomic approaches.

## Figure 1

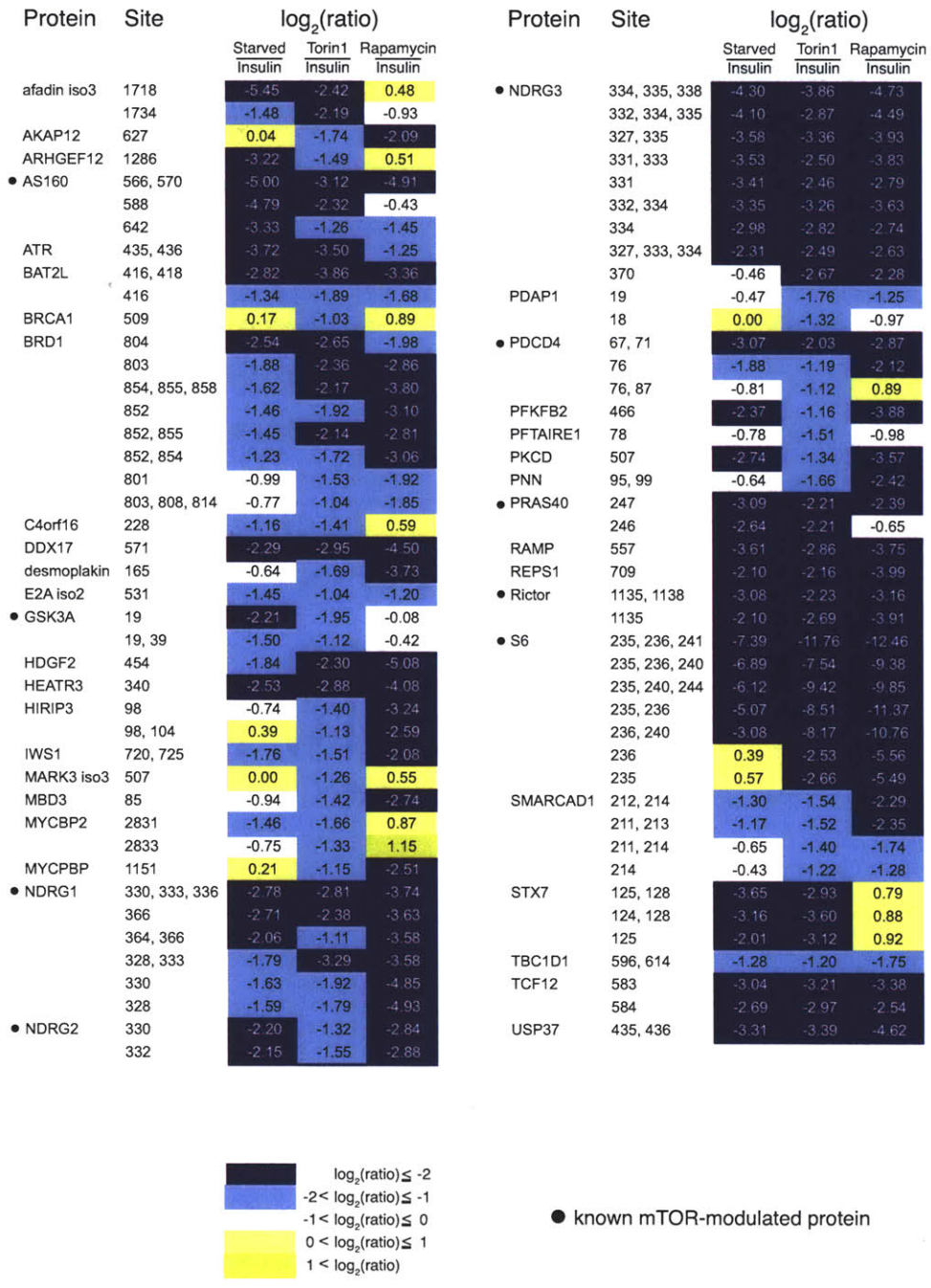
Protein
Site
log2(ratio)
Starved / Insulin
Torin1 / Insulin
Rapamycin / Insulin
afadin iso3 1718 -5.45 -2.42 0.48
1734 -1.48 -2.19 -0.93
AKAP12 627 0.04 -1.74 -2.09
ARHGEF12 1286 -3.22 -1.49 0.51
• AS160 566, 570 -5.00 -3.12 -4.91
588 -4.79 -2.32 -0.43
642 -3.33 -1.26 -1.45
ATR 435, 436 -3.72 -3.50 -1.25
BAT2L 416, 418 -2.82 -3.86 -3.36
416 -1.34 -1.89 -1.68
BRCA1 509 0.17 -1.03 0.89
BRD1 804 -2.54 -2.65 -1.98
803 -1.88 -2.36 -2.86
854, 855, 858 -1.62 -2.17 -3.80
852 -1.46 -1.92 -3.10
852, 855 -1.45 -2.14 -2.81
852, 854 -1.23 -1.72 -3.06
801 -0.99 -1.53 -1.92
803, 808, 814 -0.77 -1.04 -1.85
C4orf16 228 -1.16 -1.41 0.59
DDX17 571 -2.29 -2.95 -4.50
desmoplakin 165 -0.64 -1.69 -3.73
E2A iso2 531 -1.45 -1.04 -1.20
• GSK3A 19 -2.21 -1.95 -0.08
19, 39 -1.50 -1.12 -0.42
HDGF2 454 -1.84 -2.30 -5.08
HEATR3 340 -2.53 -2.88 -4.08
HIRIP3 98 -0.74 -1.40 -3.24
98, 104 0.39 -1.13 -2.59
IWS1 720, 725 -1.76 -1.51 -2.08
MARK3 iso3 507 0.00 -1.26 0.55
MBD3 85 -0.94 -1.42 -2.74
MYCBP2 2831 -1.46 -1.66 0.87
2833 -0.75 -1.33 1.15
MYCPBP 1151 0.21 -1.15 -2.51
• NDRG1 330, 333, 336 -2.78 -2.81 -3.74
366 -2.71 -2.38 -3.63
364, 366 -2.06 -1.11 -3.58
328, 333 -1.79 -3.29 -3.58
330 -1.63 -1.92 -4.85
328 -1.59 -1.79 -4.93
• NDRG2 330 -2.20 -1.32 -2.84
332 -2.15 -1.55 -2.88
• NDRG3 334, 335, 338 -4.30 -3.86 -4.73
332, 334, 335 -4.10 -2.87 -4.49
327, 335 -3.58 -3.36 -3.93
331, 333 -3.53 -2.50 -3.83
331 -3.41 -2.46 -2.79
332, 334 -3.35 -3.26 -3.63
334 -2.98 -2.82 -2.74
327, 333, 334 -2.31 -2.49 -2.63
370 -0.46 -2.67 -2.28
PDAP1 19 -0.47 -1.76 -1.25
18 0.00 -1.32 -0.97
• PDCD4 67, 71 -3.07 -2.03 -2.87
76 -1.88 -1.19 -2.12
76, 87 -0.81 -1.12 0.89
PFKFB2 466 -2.37 -1.16 -3.88
PFTAIRE1 78 -0.78 -1.51 -0.98
PKCD 507 -2.74 -1.34 -3.57
PNN 95, 99 -0.64 -1.66 -2.42
• PRAS40 247 -3.09 -2.21 -2.39
246 -2.64 -2.21 -0.65
RAMP 557 -3.61 -2.86 -3.75
REPS1 709 -2.10 -2.16 -3.99
• Rictor 1135, 1138 -3.08 -2.23 -3.16
1135 -2.10 -2.69 -3.91
• S6 235, 236, 241 -7.39 -11.76 -12.46
235, 236, 240 -6.89 -7.54 -9.38
235, 240, 244 -6.12 -9.42 -9.85
235, 236 -5.07 -8.51 -11.37
236, 240 -3.08 -8.17 -10.76
236 0.39 -2.53 -5.56
235 0.57 -2.66 -5.49
SMARCAD1 212, 214 -1.30 -1.54 -2.29
211, 213 -1.17 -1.52 -2.35
211, 214 -0.65 -1.40 -1.74
214 -0.43 -1.22 -1.28
STX7 125, 128 -3.65 -2.93 0.79
124, 128 -3.16 -3.60 0.88
125 -2.01 -3.12 0.92
TBC1D1 596, 614 -1.28 -1.20 -1.75
TCF12 583 -3.04 -3.21 -3.38
584 -2.69 -2.97 -2.54
USP37 435, 436 -3.31 -3.39 -4.62
log2(ratio) ≤ -2
-2 < log2(ratio) ≤ -1
-1 < log2(ratio) ≤ 0
0 < log2(ratio) ≤ 1
1 < log2(ratio)
• known mTOR-modulated protein

**Figure 1. Immunoaffinity phosphopeptide isolation and semi-quantitative mass spectrometry identifies RXX(S*/T*) sites regulated by mTOR.**

HEK-293E cells were deprived of serum for 4 hrs, treated with 100 nM rapamycin, 250 nM Torin1, or vehicle control for 1 hr, and then stimulated with 150 nM insulin for 20 min. Phosphopeptide enrichment with a phospho-motif antibody recognizing RXX(S*/T*) with minor preferences for R in the -5 and -3 positions was followed by semi-quantitative mass spectrometry to determine those phosphopeptides whose abundances decreased upon Torin1 treatment. Those phosphorylation sites whose $\log_2$(Torin1/Insulin) were less than -1 are shown here. The relevant $\log_2$(ratios) and known mTOR-regulated proteins are all indicated.

## Figure 2

| Protein | Site | $\log_2$(ratio) Starved / Insulin | Torin1 / Insulin | Rapamycin / Insulin |
|---|---|---|---|---|
| ● 4E-BP1 | 65 | -0.79 | -3.70 | 0.82 |
| ACLY | 447, 451, 453 | -3.15 | -5.34 | -3.23 |
| | 446, 451 | -1.29 | -2.52 | 0.28 |
| | 447, 451, 455 | -3.26 | -1.54 | 0.91 |
| AMPKG2 | 162, 164 | -1.21 | -2.01 | -0.71 |
| anillin | 621, 628 | 0.23 | -1.30 | -1.28 |
| ATF7 | 112 | -1.03 | -1.17 | -1.82 |
| BAZ1A | 1367 | -2.02 | -1.87 | -1.17 |
| BRSK2 | 509, 512 | 0.11 | -5.13 | -0.06 |
| C15orf42 | 1360 | 0.30 | -1.72 | -0.82 |
| C17orf49 | 146, 161 | 0.95 | -1.61 | 1.79 |
| Cdc25C | 122, 130 | -0.16 | -3.89 | -0.19 |
| CDC5L | 410, 415, 424 | -0.53 | -1.70 | -0.94 |
| CHD-3 | 1591, 1600, 1611, 1616 | -0.59 | -1.40 | -2.86 |
| | 1600, 1608, 1616 | -0.78 | -1.69 | -2.65 |
| CHED | 494 | 0.24 | -3.62 | -2.37 |
| DACH1 | 582 | -0.96 | -1.58 | -1.45 |
| DBN1 | 338, 344 | -0.43 | -1.60 | -1.95 |
| | 342, 345 | 0.76 | -1.84 | -1.51 |
| DKFZP547B1415 | 155 | -1.28 | -2.18 | -1.72 |
| ESYT2 | 705 | 0.25 | -2.68 | -2.32 |
| | 701, 704 | 0.55 | -1.81 | -1.59 |
| EZH2 | 367 | -1.20 | -1.52 | -1.36 |
| | 366 | -1.15 | -1.65 | -1.04 |
| FAM117A | 299 | -0.34 | -1.70 | -0.97 |
| FOXK2 | 381, 389 | -2.62 | -2.35 | -2.54 |
| | 389 | -1.22 | -2.27 | -1.93 |
| GRAMD1B | 56 | 0.44 | -7.61 | -0.88 |
| HN1 | 54 | -0.07 | -1.37 | -1.71 |
| ● IRS-2 | 518, 520, 527 | -3.16 | -4.18 | -2.73 |
| | 518, 527 | -2.26 | -3.04 | -2.37 |
| | 518, 520 | -2.42 | -2.27 | -2.27 |
| | 520, 527 | -2.97 | -3.20 | -2.14 |
| | 520 | -0.16 | -1.07 | -0.41 |
| KHSRP | 100 | 0.37 | -3.21 | -3.65 |
| KIAA0528 | 284, 285 | -0.65 | -1.49 | -1.05 |
| MAP1B | 1785, 1788 | 0.58 | -2.04 | -1.31 |
| MDC1 | 1563, 1567 | -0.31 | -1.03 | -0.03 |
| | 1564, 1567 | 0.22 | -4.60 | 0.12 |
| MIG-6 | 126 | -0.23 | -1.41 | -1.65 |
| MLP | 178 | 0.00 | -1.73 | -2.70 |
| MYCBP | 56 | 0.58 | -4.21 | -5.96 |
| NIFK | 223, 227, 230, 240 | -1.83 | -2.08 | -0.95 |
| | 218, 234, 238 | -1.67 | -1.36 | -0.49 |
| | 223 | 0.33 | -1.04 | -0.27 |
| p66A | 600 | 0.45 | -1.38 | -1.16 |
| POGZ | 1364, 1368 | 0.63 | -5.12 | -0.05 |
| polybromo 1 | 28 | -0.49 | -1.12 | -1.06 |
| POM121C | 445 | 0.49 | -1.33 | -0.73 |
| PTPN14 | 579 | 1.11 | -1.52 | -1.52 |
| | 577 | 0.71 | -1.50 | -1.16 |
| PUM1 | 209 | -1.50 | -1.97 | -0.15 |
| RIP | 154 | 0.62 | -1.65 | -1.58 |
| RIP140 | 553 | -0.96 | -1.30 | -1.06 |
| RPRC1 | 811 | -0.76 | -1.88 | -0.52 |
| SIPA1L2 | 1520 | -1.16 | -1.64 | -0.51 |
| TCF8 | 700 | -0.30 | -1.33 | -0.60 |
| Tel | 18, 22, 29 | -0.98 | -2.86 | -2.17 |
| Tiam2 | 150, 158 | -1.03 | -1.67 | -1.23 |
| TMPO | 158 | -0.07 | -1.55 | -0.09 |

$\log_2(\text{ratio}) \leq -2$
$-2 < \log_2(\text{ratio}) \leq -1$
$-1 < \log_2(\text{ratio}) \leq 0$
$0 < \log_2(\text{ratio}) \leq 1$
$1 < \log_2(\text{ratio})$

● known mTOR-modulated protein

**Figure 2. Immunoaffinity phosphopeptide isolation and semi-quantitative mass spectrometry identifies T*P sites regulated by mTOR.**

HEK-293E cells were deprived of serum for 4 hrs, treated with 100 nM rapamycin, 250 nM Torin1, or vehicle control for 1 hr, and then stimulated with 150 nM insulin for 20 min. Phosphopeptide enrichment with a phospho-motif antibody recognizing T*P was followed by semi-quantitative mass spectrometry to determine those phosphopeptides whose abundances decreased upon Torin1 treatment. Those phosphorylation sites whose $\log_2$(Torin1/Insulin) were less than -1 are shown here. The relevant $\log_2$(ratios) and known mTOR-regulated proteins are all indicated.

**Figure 3**

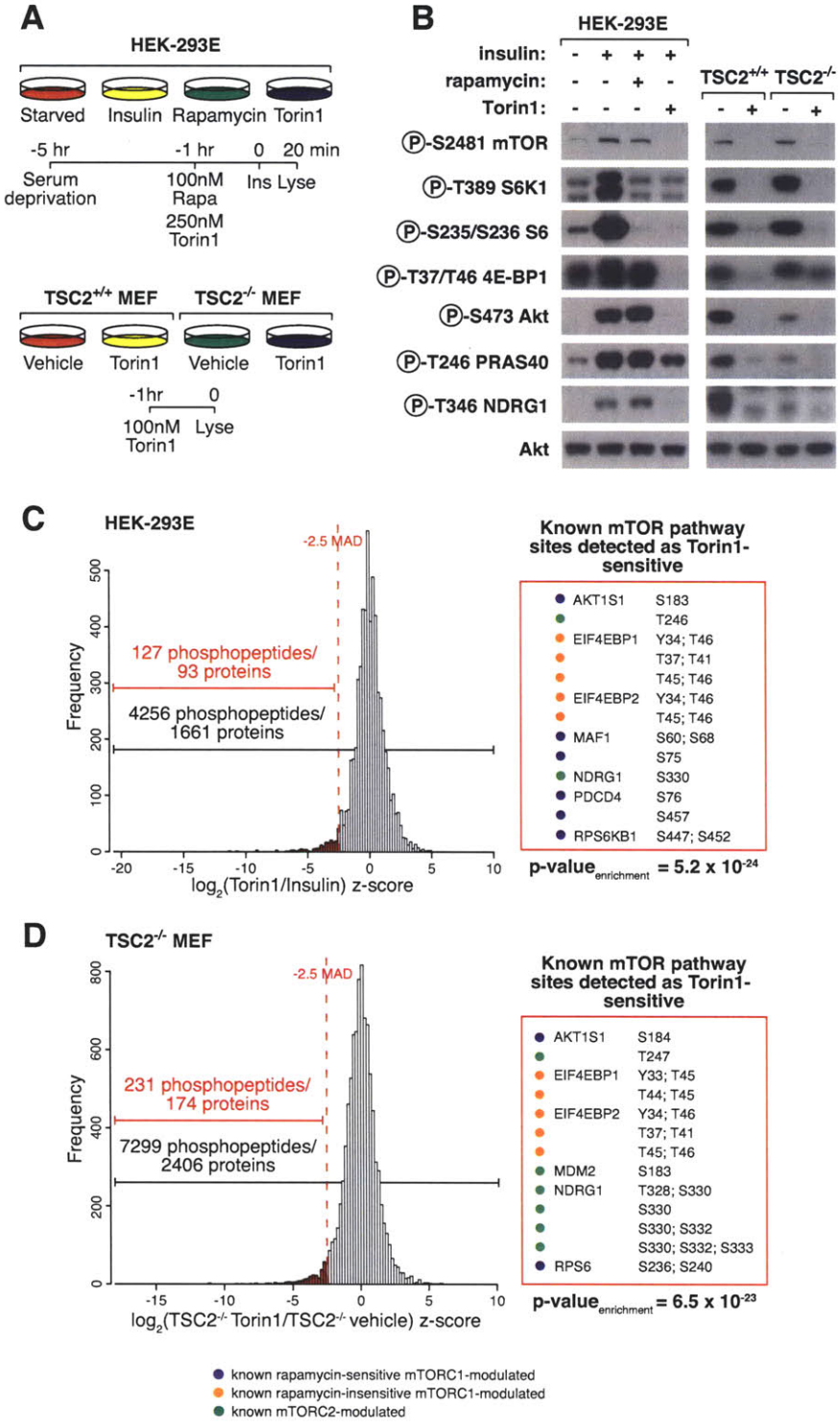
A
HEK-293E
Starved
Insulin
Rapamycin
Torin1
-5 hr
-1 hr
0
20 min
Serum deprivation
100nM Rapa
250nM Torin1
Ins Lyse
TSC2+/+ MEF
TSC2-/- MEF
Vehicle
Torin1
Vehicle
Torin1
-1hr
0
100nM Torin1
Lyse
B
HEK-293E
insulin:
rapamycin:
Torin1:
TSC2+/+
TSC2-/-
Ⓟ-S2481 mTOR
Ⓟ-T389 S6K1
Ⓟ-S235/S236 S6
Ⓟ-T37/T46 4E-BP1
Ⓟ-S473 Akt
Ⓟ-T246 PRAS40
Ⓟ-T346 NDRG1
Akt
C
HEK-293E
-2.5 MAD
127 phosphopeptides/ 93 proteins
4256 phosphopeptides/ 1661 proteins
Frequency
log2(Torin1/Insulin) z-score
Known mTOR pathway sites detected as Torin1-sensitive
AKT1S1 S183
T246
EIF4EBP1 Y34; T46
T37; T41
T45; T46
EIF4EBP2 Y34; T46
T45; T46
MAF1 S60; S68
S75
NDRG1 S330
PDCD4 S76
S457
RPS6KB1 S447; S452
p-value enrichment = 5.2 x 10-24
D
TSC2-/- MEF
-2.5 MAD
231 phosphopeptides/ 174 proteins
7299 phosphopeptides/ 2406 proteins
Frequency
log2(TSC2-/- Torin1/TSC2-/- vehicle) z-score
Known mTOR pathway sites detected as Torin1-sensitive
AKT1S1 S184
T247
EIF4EBP1 Y33; T45
T44; T45
EIF4EBP2 Y34; T46
T37; T41
T45; T46
MDM2 S183
NDRG1 T328; S330
S330
S330; S332
S330; S332; S333
RPS6 S236; S240
p-value enrichment = 6.5 x 10-23
known rapamycin-sensitive mTORC1-modulated
known rapamycin-insensitive mTORC1-modulated
known mTORC2-modulated

**Figure 3. Identification of the mTOR-regulated phosphoproteome by quantitative mass spectrometry with isobaric mass tags.**

(A) Phosphopeptide abundances were determined using isobaric tags for relative and absolute quantitation (iTRAQ) from two sets of samples: HEK-293E cells serum starved for 4 hrs, treated with 100 nM rapamycin, 250 nM Torin1, or vehicle control for 1 hr, and then stimulated with 150 nM insulin for 20 min and $TSC2^{+/+}$ and $TSC2^{-/-}$ MEFs treated with 100 nM Torin1 or vehicle control for 1 hr. (B) Cells treated as in (A) were analyzed by immunoblotting. (C and D) Distributions of robust z-scores (median absolute deviations (MADs) away from the median (C) $\log_2$(Torin1/Insulin) for HEK-293Es or (D) $\log_2$($TSC2^{-/-}$ Torin1/$TSC2^{-/-}$ vehicle) for MEFs). p-values associated with enrichment for known mTOR-modulated sites among the -2.5 MAD Torin1-sensitive phosphopeptides were determined by Fisher's exact test. Phosphopeptides detected in both replicates had to meet the -2.5 MAD threshold both times to be considered mTOR-regulated.

**Figure 4**

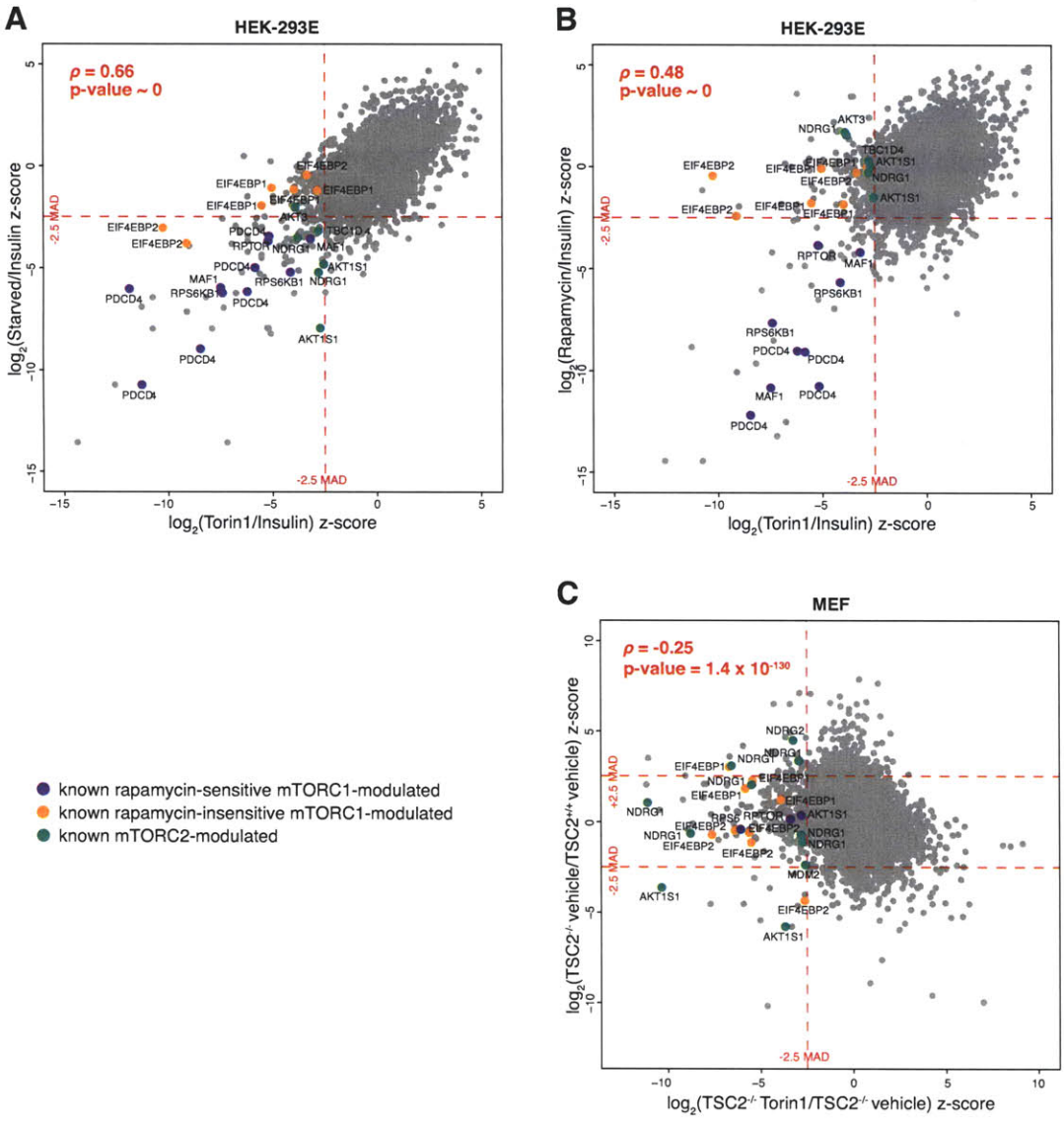
A
HEK-293E
ρ = 0.66
p-value ~ 0
log2(Starved/Insulin z-score
log2(Torin1/Insulin) z-score
-2.5 MAD
B
HEK-293E
ρ = 0.48
p-value ~ 0
log2(Rapamycin/Insulin) z-score
log2(Torin1/Insulin) z-score
-2.5 MAD
C
MEF
ρ = -0.25
p-value = 1.4 x 10-130
log2(TSC2-/- vehicle/TSC2+/+ vehicle) z-score
log2(TSC2-/- Torin1/TSC2-/- vehicle) z-score
+2.5 MAD
-2.5 MAD
known rapamycin-sensitive mTORC1-modulated
known rapamycin-insensitive mTORC1-modulated
known mTORC2-modulated

**Figure 4. Correspondence between Torin1 treatment and serum deprivation, rapamycin treatment, or TSC2 loss.**

Correspondence between (A) Torin1 treatment and serum deprivation in HEK-293Es, (B) Torin1 and rapamycin treatment in HEK-293Es, and (C) Torin1 treatment and upregulation in $TSC2^{-/-}$ MEFs. The relevant robust z-scores for both replicates, phosphopeptides corresponding to known mTOR-modulated sites, Spearman's rank correlation coefficient ($\rho$), and associated p-values are indicated. Outliers were excluded to aid in visualization.

**Figure 5**

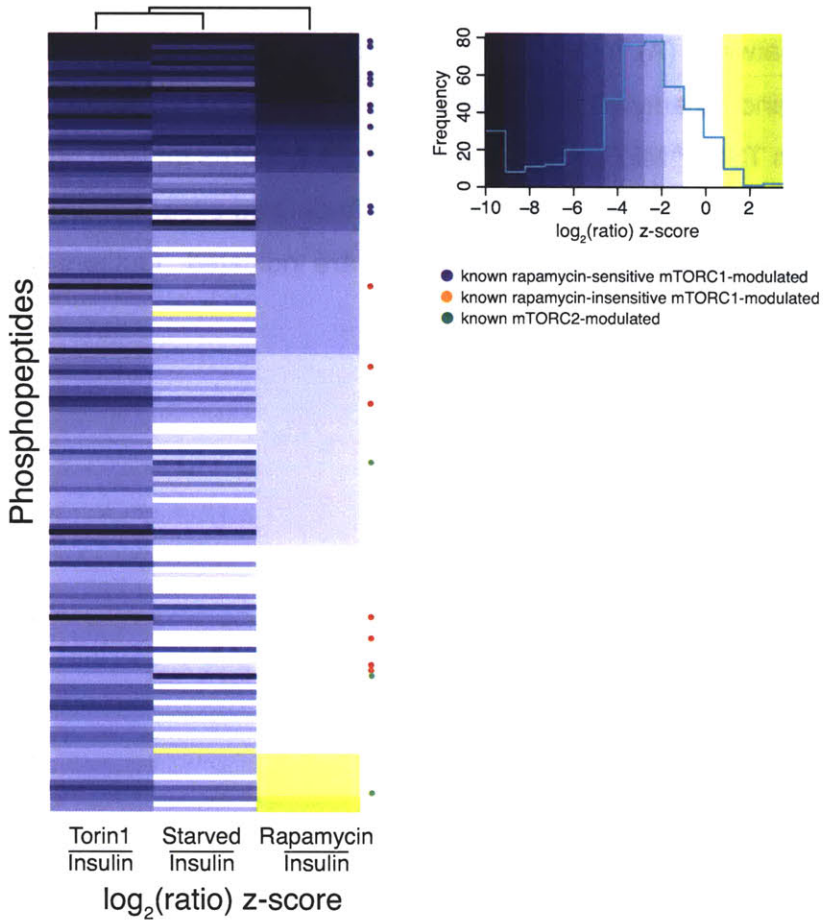
Phosphopeptides
Torin1 / Insulin
Starved / Insulin
Rapamycin / Insulin
log2(ratio) z-score
Frequency
0
20
40
60
80
−10
−8
−6
−4
−2
0
2
log2(ratio) z-score
known rapamycin-sensitive mTORC1-modulated
known rapamycin-insensitive mTORC1-modulated
known mTORC2-modulated

**Figure 5. Visualization of the phosphopeptide abundances for the HEK-293E mTOR-regulated phosphopeptides.**

Heat map visualization of the robust z-scores for the HEK-293E mTOR-regulated phosphopeptides reveals the similarity between serum starvation and Torin1 treatment, the ability to differentiate rapamycin-sensitive from -insensitive sites, and the greater extent of inhibition of rapamycin-sensitive phosphorylation sites with Torin1. Conditions were hierarchically clustered while phosphopeptides were sorted based on rapamycin-sensitivity. Yellow indicates positive z-scores, and blue indicates negative z-scores. Those z-scores less than -10 were binned together as one color for ease of visualization. Known mTOR-modulated sites are indicated.

**Figure 6**

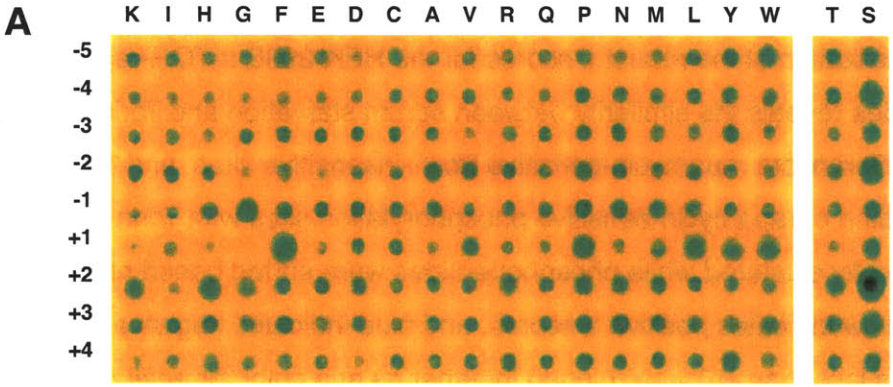


B

| | K | I | H | G | F | E | D | C | A | V | R | Q | P | N | M | L | Y | W |
|---|---|---|---|---|---|---|---|---|---|---|---|---|---|---|---|---|---|---|
| -5 | -1.4 | -0.6 | -1.2 | -0.4 | 2.9 | -0.1 | -2.4 | 1.1 | -1.6 | -1.1 | -2.6 | -1.1 | 0.4 | -1.7 | -1.6 | 1.3 | 3.9 | 5.9 |
| -4 | -0.8 | -0.6 | -1.0 | -1.7 | -0.1 | -1.9 | -1.1 | -0.2 | 0.0 | 0.3 | -1.1 | -0.8 | 2.0 | 0.9 | 0.6 | 1.3 | 2.4 | 1.8 |
| -3 | -1.3 | -0.3 | -1.6 | 0.0 | 1.0 | -0.4 | -0.4 | 0.0 | -0.8 | -1.7 | 0.1 | 0.0 | 0.9 | 1.9 | 0.9 | 0.0 | 2.6 | -0.9 |
| -2 | -2.0 | -0.9 | -4.4 | -2.6 | 0.9 | -2.8 | -1.4 | -0.8 | 4.8 | 3.3 | 1.5 | 0.0 | 3.6 | 1.5 | -0.2 | 1.5 | -0.3 | -1.7 |
| -1 | -4.5 | -4.2 | 0.7 | 7.9 | 0.9 | 0.2 | -0.1 | -0.9 | 0.4 | -3.7 | -1.4 | -0.8 | 3.8 | 3.2 | 2.8 | 0.7 | -2.3 | -2.6 |
| +1 | -11.1 | -1.6 | -6.4 | -10.7 | 15.9 | -7.5 | -1.6 | -0.4 | -6.4 | 5.8 | -5.8 | -6.1 | 14.5 | -4.7 | 1.8 | 11.4 | 5.8 | 10.0 |
| +2 | 1.2 | -3.0 | 3.4 | 0.1 | 0.4 | 0.1 | 0.4 | -2.1 | -0.9 | -0.2 | 1.3 | -0.8 | 2.0 | 1.0 | 0.6 | -0.9 | -1.1 | -1.4 |
| +3 | -1.1 | -0.7 | 0.7 | -0.5 | 1.8 | -1.0 | -0.1 | -2.1 | -0.9 | -0.5 | 0.4 | -1.1 | 1.2 | 2.5 | 0.7 | -0.3 | -0.1 | 0.8 |
| +4 | -2.4 | -0.9 | 0.5 | -0.8 | 0.1 | -0.6 | -2.5 | -0.2 | -0.8 | -0.1 | 1.4 | -0.5 | 2.1 | 0.3 | 0.9 | 0.1 | 3.2 | 0.2 |



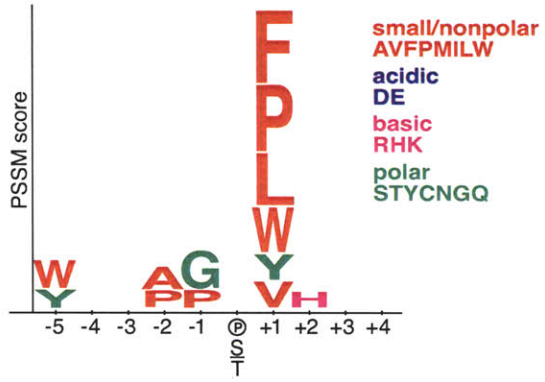

**Figure 6. Definition of a consensus mTOR motif by positional scanning peptide libraries.**

(A) In vitro phosphorylation of a positional scanning peptide library (PSPL) with mTORC1 purified from HEK-293T cells stably expressing FLAG-raptor in the presence of Rheb and radiolabeled ATP. Each reaction consists of a mixture of biotinylated peptides containing one fixed residue relative to the central phospho-acceptor and other residues randomized. Aliquots of each reaction were spotted onto a streptavidin membrane and developed by PhosphorImaging. The scan was pseudo-colored to aid in visualization. The numbering of the positions is relative to the central phospho-acceptor serine or threonine. (B) The position-specific scoring matrix (PSSM) resulting from quantification of the in vitro phosphorylation of a PSPL by mTORC1. (C) The visualized mTOR consensus motif. Letter height is proportional to the PSSM score. Only those selected residues with scores greater than a standard deviation from the average PSSM score within a row are shown.

## Figure 7

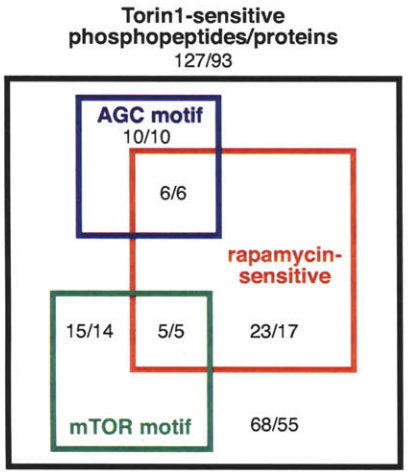


**HEK-293E**

● known mTOR-modulated sites detected as Torin1-sensitive

rapa

| | | |
|---|---|---|
| | ACIN1 | S240 |
| ● | AKT1S1 | S183 |
| | ARFGAP2 | S201 |
| | CAD | S1859 |
| | CLIP1 | S1158 |
| | GIGYF2 | S23 |
| | IBTK | S993 |
| | | Y996; S1004 |
| | LAMP1 | S69; T72; S78; S79; T85 |
| | LIMA1 | S15 |
| | | S225 |
| | | S228 |
| | | S230 |
| ● | MAF1 | S75 |
| | PCBP1 | S173 |
| ● | PDCD4 | S76 |
| | PRCC | S157; S159 |
| | PURA | S28; S30; S43 |
| ● | RPS6KB1 | S447; S452 |
| | TOR1AIP1 | S164; T166 |
| | ZFP36L2 | S490 |

AGC rapa

| | | |
|---|---|---|
| | DNAJC2 | S47; S49 |
| | GTF2F1 | T156 |
| | IBTK | S990; T1008 |
| | KIF4A | S801 |
| ● | PDCD4 | S457 |
| | ZC3H13 | S1364 |

AGC

| | | |
|---|---|---|
| ● | AKT1S1 | T246 |
| | BAT2 | S761 |
| | CCDC88A | S1417 |
| | GPI | T109 |
| | KIF4A | S801 |
| | LARP1 | S847; S849 |
| ● | NDRG1 | S330 |
| | SFRS18 | S290 |
| | SFRS2IP | S796; S802 |
| | SRRM2 | S950; S954 |

mTOR

| | | |
|---|---|---|
| | ANKRD17 | S2045; S2047 |
| | BAG3 | T285; S289 |
| | BRD9 | S492 |
| | DNMT1 | S714 |
| ● | EIF4EBP1 | T37; T41 |
| | | T41; S44 |
| | ELL | S309 |
| | FAM21A | S700; S704 |
| | LARP1 | S689; S697 |
| | MYC | S77 |
| | PATL1 | S36; S41 |
| | RPRD1B | S166 |
| | SRRM1 | T572; T574 |
| | SRRM2 | S1318; S1326; S1329 |
| | UBR4 | S2932 |

mTOR rapa

| | | |
|---|---|---|
| | EEF2K | S72; S74 |
| ● | MAF1 | S60; S68 |
| | MYC | S77 |
| | WNK1 | S2032 |
| | ZNF768 | S139 |

| | | |
|---|---|---|
| | ACLY | S455 |
| | AFAP1 | S343; T350 |
| | AKAP1 | S444 |
| | AKAP8 | S328; S339 |
| | AKAP13 | S973 |
| | ANKS1A | S677 |
| | CEP350 | S1647 |
| | CHAF1A | T949 |
| | CTNND1 | S268 |
| | DSG2 | S782 |
| | EEF1B4 | S95; S106 |
| | | S106 |
| | EEF1D | S162 |
| | EIF4B | S497 |
| ● | EIF4EBP1 | Y34; T46 |
| | | T45; T46 |
| ● | EIF4EBP2 | Y34; S44 |
| | | Y34; T46 |
| | | T45; T46 |
| | EPB41 | S149; S151; S152 |
| | ERBB2IP | S852 |
| | FAM53C | S122 |
| | FIP1L1 | T494; S496 |
| | HISPPD1 | S493; S498 |
| | KIAA0528 | S659; S662 |
| | KIAA0947 | S533 |
| | LARP1 | S766 |
| | | T769 |
| | MAP1B | S1792; Y1796 |
| | | S1793; S1797 |
| | MAP7D1 | S742 |
| | MCM6 | S689 |
| | MED1 | S1479; S1481 |
| | MSH6 | S200 |
| | NDRG1 | S367 |
| | | S332; S333 |
| | NOP14 | S146; T161 |
| | NPM1 | S70 |
| | PANK4 | S404 |
| | PCBP2 | S362 |
| | PURA | S6S8 |
| | PXN | S288 |
| | RANBP3 | S101; S108 |
| | REPS1 | S118; T121 |
| | RNASEH2A | S298 |
| | RSF1 | S1247; S1249 |
| | | T1278; Y1281; S1282 |
| | SEC16A | S1369; S1372 |
| | SET | S24 |
| | SFRS11 | S483 |
| | SFRS18 | S286 |
| | SNRNP200 | Y199 |
| | SRPK1 | S309 |
| | SRRM2 | S395; S398 |
| | | S2100; S2102 |
| | SYMPK | S1259 |
| | TCOF1 | S233 |
| | TGS1 | S405; S412 |
| | TPI1 | S21 |
| | TRA2A | T204 |
| | USP24 | S2401 |
| | ZBTB10 | S628 |
| | | S647 |
| | ZEB1 | S155 |
| | ZNF407 | S1121; S1128 |

**Figure 7. Classification of the mTOR-regulated phosphopeptides in HEK-293E cells.**

Classification of the mTOR-regulated phosphopeptides in HEK-293E cells organized by rapamycin sensitivity (-2.5 MAD ($log_2$ (Rapamycin/Insulin), consistency with the mTOR motif ($5^{th}$ percentile by Scansite) or presence of an AGC motif ((R/K)X(R/K)XX(S*/T*). The numbers before the slash represent the number of unique phosphopeptides while the numbers after the slash represent the number of unique proteins represented by those phosphopeptides within each category. The phosphorylation sites present in the phosphopeptides and the known mTOR-modulated proteins detected as Torin1-sensitive are indicated to the right.

## Figure 8

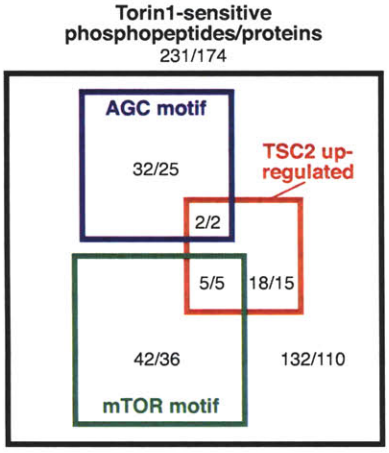


● known mTOR-modulated sites detected as Torin1-sensitive

AGC

| | | |
|---|---|---|
| | AHNAK | S5555; S5557 |
| ● | AKT1S1 | T247 |
| | ATXN1 | S751 |
| | BAT2 | S759; S761; S764 |
| | BRWD1 | S1782; S1784; S1789 |
| | CARHSP1 | S53 |
| | EHMT2 | S285 |
| | EIF4B | S174; S176 |
| | FAM178A | S318 |
| | HDGFRP2 | S450 |
| | | S450; S454 |
| | LMNA | S292 |
| | 100045983 | S983 |
| | LYSMD2 | S33 |
| ● | MDM2 | S183 |
| | MYCBP2 | S3577 |
| ● | NDRG1 | T328; S330 |
| | | S330; S332 |
| | | S330; S332; S333 |
| | PDCD11 | S1468 |
| | PLEC1 | S4245 |
| | POM121 | S367 |
| ● | RPS6 | S236; S240 |
| | SETD1A | S1176 |
| | SFRS18 | S290 |
| | SRPK2 | S488; S490 |
| | | S488; S491 |
| | TOPORS | T859; S861; S863 |
| | UTP18 | T200; S201; S202; S206 |

mTOR TSC2 up

| | | |
|---|---|---|
| | ARHGAP29 | S1040 |
| | CUX1 | S793 |
| | GRB10 | S103; S104 |
| | PHLDB2 | S17 |
| | SMCR8 | S416 |

AGC TSC2 up

| | | |
|---|---|---|
| ● | NDRG1 | S330 |
| | REEP1 | S152 |

mTOR

| | | |
|---|---|---|
| | 2810004N23. | T53; S67 |
| | AFAP1 | S665; S669 |
| | | S666; S669 |
| | AHNAK | S5525; S5536 |
| | | S5553; T5571 |
| | AKAP11 | S987 |
| | | T1092 |
| | ATXN2L | T31; S32 |
| | BC059842 | S3116 |
| | CDC42BPB | S1692 |
| | CHFR | S231 |
| | DDX18 | T101 |
| | DLG5 | S1209 |
| | DPYSL3 | S522 |
| | EHMT2 | S287 |
| ● | EIF4EBP2 | T37; T41 |
| | EIF4G1 | T212 |
| | FLNA | S1338 |
| | FOXK1 | S431 |
| | | S427; S431 |
| | FOXK2 | S547 |
| | IRS2 | S616 |
| | JUN | T242; S246 |
| | LARP1 | S1010; S1018 |
| | MCL1 | T144 |
| | MTAP1B | S1247; S1260 |
| | NES | S919 |
| | NFRKB | S351 |
| | NUMA1 | S1973; T1982 |
| | | S1974; T1982 |
| | NUP188 | T1515 |
| | PATL1 | T194 |
| | PHLDB1 | S1007; S1009 |
| | POLR2A | S1882 |
| | PTPN13 | S1073; S1077 |
| | RC3H1 | S535 |
| | ST5 | S30; S32; S42 |
| | TAF3 | S229 |
| | TBC1D10B | S382; S386; S389 |
| | TOPORS | S1016 |
| | WIPI2 | S395 |

TSC2 up

| | | |
|---|---|---|
| ● | EIF4EBP1 | T44; T45 |
| | EPB4.1L3 | T584 |
| | GORASP1 | T363; S365; S367 |
| | ITSN1 | T890 |
| | MAP4K4 | S691 |
| | MCF2L | T583 |
| | OSBP | S188; S191 |
| | PHLDB2 | T358 |
| | | S359 |
| | | T546 |
| | | S551 |
| | RPS6KC1 | S697; S708 |
| | SLK | S643; S647 |
| | SMCR8 | S413 |
| | SMTNL2 | S339 |
| | SNX18 | S20 |
| | TMEM135 | S221 |
| | TNKS1BP1 | S1437 |

| | | |
|---|---|---|
| | 4922501C03. | S451 |
| | ACIN1 | S387; S389 |
| | ADARB1 | T686 |
| | AFAP1 | S684 |
| | AKAP12 | S1645 |
| ● | AKT1S1 | S184 |
| | | S204; S213 |
| | ALAD | S215 |
| | ALS2 | S486 |
| | AMIGO3 | S257 |
| | ANKRD11 | S1829 |
| | ANXA2 | S127 |
| | ATN1 | S77 |
| | ATP2B2 | S1185 |
| | ATXN2L | S304 |
| | AW146020 | S118 |
| | BRE | S222 |
| | CCDC12 | S165 |
| | CCNL1 | S341; S344 |
| | | S344; S347 |
| | CEBPB | S183 |
| | CHD8 | S2213 |
| | CNPY2 | S115 |
| | CSNK1G3 | S367 |
| | CTPS | S575 |
| | CXCR7 | S350 |
| | DGCR8 | S377 |
| | DLK1 | S357 |
| | DTL | S654 |
| | EDC3 | S131 |
| ● | EIF4EBP1 | Y33; T45 |
| | | S34; T49 |
| | | S34; T35; T49 |
| ● | EIF4EBP2 | Y34; T46 |
| | | T45; T46 |
| | EIF5B | S184; S187 |
| | EP400 | T885; S886 |
| | EPS8 | S810; S814 |
| | F11R | S288 |
| | FAM117B | T12 |
| | FIP1L1 | S447 |
| | FNIP1 | S306 |
| | FOSL1 | S267 |
| | FOXK1 | S222; S225; S243 |
| | | S225; S229; T231 |
| | | S243 |
| | GM5780 | S534; S536 |
| | GRB10 | S99 |
| | GTF2F1 | S385 |
| | HGS | S310 |
| | HIRIP3 | S207; S208 |

| | | |
|---|---|---|
| | HNRNPF | S63 |
| | HNRNPUL2 | S166 |
| | IBTK | S994 |
| | IL1RAP | S566 |
| | KIRREL | S671; S674; S676 |
| | KTN1 | S90 |
| | LARP1 | S900; S902 |
| | | S1010; T1013 |
| | | S1108 |
| | LARP4 | S377 |
| | | S377; S379; S382 |
| | LIG1 | S922; S923 |
| | LMO7 | S1156 |
| | LOC637796 | S146; S151 |
| | LRP12 | T849 |
| | MBIP | S22 |
| | MCM2 | T25; S26; S27 |
| | MCM6 | S699 |
| | MDC1 | S168; S176 |
| | MRE11A | S686 |
| | MYADM | S22 |
| | NES | S963 |
| | | T1130 |
| | | S1860; S1861 |
| | NRADD | S226 |
| | NUMA1 | S1973 |
| | NUP133 | S40 |
| | OLFR244 | Y184; T186; T189; S190 |
| | OXR1 | T115 |
| | PDCD11 | S1470 |
| | PEX5L | S441 |
| | PLEKHG3 | S1123; S1129 |
| | PPAN | T233 |
| | PPIG | S252; S254; S255; S257 |
| | PTPN13 | S1506 |
| | PUM2 | S82 |
| | SCAP | S850 |
| | SFRS2IP | S498; S502 |
| | SLC22A14 | T346; S358 |
| | SLC4A7 | S89 |
| | SLK | S348 |
| | SNTB2 | S208; S211 |
| | SRRM2 | S971; S972 |
| | | S1243; S1247 |
| | | S1244; S1247 |
| | | T1478; S1481 |
| | | S1956 |
| | | S2548; S2550; S2552 |
| | SSRP1 | S667 |
| | SSX2IP | S313 |
| | STEAP3 | S20 |
| | STX7 | S129 |
| | SUPT6H | T1532 |
| | TBC1D5 | S561 |
| | TCF12 | S582 |
| | TCF20 | S1397 |
| | TCFAP4 | S121 |
| | TCFE3 | S413 |
| | TMPO | S384 |
| | TNS3 | S686 |
| | TOMM20 | S135 |
| | TPD52L2 | S96 |
| | TRIM28 | S596 |
| | TRIM47 | S504 |
| | TRIM68 | S388 |
| | TRIP10 | S296; S299 |
| | UBE4B | S88 |
| | UBXN7 | S367 |
| | UHRF2 | S668 |
| | ULK1 | S638 |
| | WDR33 | S1204 |
| | WDR44 | T351 |
| | WIBG | S138 |
| | ZEB1 | S681 |
| | | T680 |
| | ZFP36L1 | S334 |
| | ZFP509 | S282; S288 |

**Figure 8. Classification of the mTOR-regulated phosphopeptides in MEFs.**

Classification of the mTOR-regulated phosphopeptides in MEFs organized by upregulation in the absence of TSC2 (+2.5 MAD $\log_2$(TSC2$^{-/-}$ vehicle/TSC2$^{+/+}$ vehicle), consistency with the mTOR motif (5$^{th}$ percentile by Scansite) or presence of an AGC motif ((R/K)X(R/K)XX(S*/T*). The numbers before the slash represent the number of unique phosphopeptides while the numbers after the slash represent the number of unique proteins represented by those phosphopeptides within each category. The phosphorylation sites present in the phosphopeptides and the known mTOR-modulated proteins detected as Torin1-sensitive are indicated to the right.

## Materials and Methods

### Materials

Reagents were obtained from the following sources: antibodies to phospho-S2481 mTOR, phospho-T389 S6K1, phospho-S235/S236 S6, phospho-T37/T46 4E-BP1, phospho-S65 4E-BP1, phosho-T308 Akt, phospho-S473 Akt, phospho-T24/T32 FOXO1/3a, phospho-T246 PRAS40, phospho-T346 NDRG1, Akt from Cell Signaling Technology; an antibody to mouse Grb10 and HRP-labeled anti-mouse and anti-rabbit secondary antibodies from Santa Cruz Biotechnology; L-glutathione, FLAG M2 affinity gel, ATP, insulin from Sigma-Aldrich; [$\gamma$-$^{32}$P]ATP from Perkin-Elmer; FuGENE 6, PhosSTOP, and Complete Protease Cocktail from Roche; rapamycin from LC Laboratories, DMEM from SAFC Biosciences; Inactivated Fetal Calf Serum (IFS), Superose 6 10/300 GL and HiLoad 16/60 Superdex 200 from GE Healthcare; BCA assay reagent, protein G-sepharose and immobilized glutathione beads from Pierce; and Whatman grade P81 ion exchange chromtagraphy paper from Fisher Scientific. Torin1 was provided by Nathanael Gray (Harvard Medical School) (Thoreen et al., 2009).

### Cell lines and tissue culture

All cells (HEK-293E, MEFs) were cultured in DMEM with 10% IFS and antibiotics. HEK-293Es were generously provided by John Blenis (Harvard Medical School), TSC2$^{+/+}$ p53$^{-/-}$ and TSC2$^{-/-}$ p53$^{-/-}$ MEFs by David Kwiatkowski (Harvard Medical School).

### Immunoaffinity isolation and semi-quantitative mass spectrometry

Actively proliferating HEK-293E cells were serum starved for 4 hrs, treated with 100 nM rapamycin, 250 nM Torin1, or DMSO for 1 hr, stimulated with 150 nM insulin for 20 minutes, and then lysed. Phosphopeptide enrichment using motif antibodies (#9614 and T*P), LC-MS/MS, and semiquantitative data collection were described

previously (Moritz et al., 2010; Stokes et al., 2007). The T*P dataset was analyzed twice. Abundance estimates for phosphorylation sites detected multiple times on either the same or different peptides were averaged.

**Quantitative mass spectrometry**

*Cell lysis and protein digestion*: Actively proliferating HEK-293E cells were serum starved for 4 hrs, treated with 100 nM rapamycin, 250 nM Torin1, or DMSO for 1 hr, stimulated with 150 nM insulin for 20 minutes, and then lysed. Actively proliferating MEFs in fresh media were treated with 100nM Torin1 or DMSO for 1 hr and then lysed. Cells were lysed with 8M urea, 20mM HEPES pH 8.0, 1mM sodium orthovanadate, 2.5mM pyrophosphate, and 1mM glycerophosphate. Protein concentration was determined using the BCA assay. Proteins were reduced with 10 mM dithiothreitol for 30 min at 56°C, then alkylated with 55 mM iodoacetamide for 1 hr at room temperature in the dark. Cell lysates were diluted to a final urea concentration of 1.6M with 50 mM ammonium bicarbonate, and digested with trypsin (substrate:enzyme = 50) at 37°C overnight with end-over-end rotation. The resulting peptide solutions were acidified with 10% TFA, and desalted on a Waters C18 solid phase extraction plate. Eluted peptides were divided into ~100ug aliquots, lyophilized to complete dryness, and stored at -80°C until needed.

*iTRAQ labeling*: For both samples, duplicates were performed such that peptides were independently labeled and analyzed by LC-MS/MS twice. Desalted peptides (400µg or 800ug in total) were labeled with iTRAQ (Ross et al., 2004) 4plex or 8plex reagents according to the manufacturer's instructions. Briefly, 100 $\mu$g aliquots of dried peptides were reconstituted with 30 $\mu$L 0.5 M triethylammonium bicarbonate. One tube of iTRAQ reagent (114, 115, 116, or 117 for 4plex, 113, 114, 115, 116, 117, 118, 119, or 121 for 8plex) was reconstituted with 70 $\mu$L ethanol (4plex) or 50$\mu$l of isopropanol (8plex), and added to each peptide solution. The reaction was allowed to proceed for 1 hr (4plex) or 2 hr (8plex) at room temperature. Derivatized peptides were combined,

dried by vacuum centrifugation, and desalted on a Waters C18 solid phase extraction plate. iTRAQ labeled peptides were lyophilized to complete dryness and stored at -80°C until needed. The MEF samples were labeled with iTRAQ 4plex reagent ($TSC2^{+/+}$ Vehicle: 114; $TSC2^{+/+}$ Torin1: 115; $TSC2^{-/-}$ Vehicle: 116; $TSC2^{-/-}$ Torin1: 117). The HEK-293E samples were labeled with iTRAQ 8plex (Starved: 113; Insulin: 114; Torin: 117 or 115 for the first and second replicates, respectively; Rapamycin: 118) with the remaining channels used for other analyses not discussed here.

*Phosphopeptide enrichment*: Magnetic Ni-NTA agarose beads (100 µL of a 5% bead suspension/400 µg tryptic peptides) were treated with 400 µL of 100 mM EDTA, pH 8.0 to remove Ni(II). NTA-agarose beads were then charged with 200 µL of 100 mM aqueous FeCl3 solution (Ficarro et al., 2009). Beads were washed 4x with 400 µL 80% acetonitrile/0.1% TFA to remove excess metal ions. iTRAQ labeled peptides were reconstituted with 80% MeCN/0.1% TFA at a concentration of 1-2 µg/µL, were then mixed with the beads. The mixture was incubated for 30 min at room temperature with end-over-end rotation. After removing the supernatant, beads were washed 3x with 400 µL 80% acetonitrile/0.1% TFA, and 1x with 400ul of 0.01% acetic acid. Phosphopeptides were eluted with 50 µL of 20 mM ammonium formate buffer pH 10.

*LC-MS/MS analysis*: Enriched phosphopeptides were separated into 40 fractions by high-pH reversed phase and strong anion exchange chromatography, respectively, followed by low-pH reversed phase LC-MS/MS on a QSTAR Elite (AB Sciex, Foster City, CA) hybrid quadrupole time-of-flight mass spectrometer. The spectrometer was operated in data-dependent mode with dynamic exclusion. A precursor was selected for MS/MS when its signal intensity was at least 50 counts, and its charge state is 2+, 3+ or 4+. Up to 5 most abundant precursors in each MS scan could be selected for MS/MS, and then excluded for 20 sec. The MS/MS scan was acquired for 0.5 sec with a multiplier value of 4.

*Data processing*: MS/MS spectra from each acquisition were extracted and converted into .mgf files, and then searched against NCBI mouse and human RefSeq databases (downloaded June 2008) using Mascot. Precursor and product ion tolerances were set at 200ppm and 0.2 Da respectively. Search parameters included tyrpsin specificity with up to 2 missed cleavages, fixed carbamidomethylation on cysteine, fixed iTRAQ modification on N-terminus and lysine (8plex for HEK-293E, 4plex for MEF), variable deamidation on asparagine and glutamine, variable oxidation on methionine and variable phosphorylation on serine, threonine and tyrosine. The search results were further collated using our Multiplierz software framework (Askenazi et al., 2009; Parikh et al., 2009) for peptides above a mascot score cutoff of 25, corresponding to a FDR of ~1%. iTRAQ reporter ion intensities were extracted and corrected for isotope impurities. Results from multiple fractions were combined for each sample. iTRAQ reporter ion signals were summed for each unique phosphopeptide. A small aliquot from the supernatant of phosphopeptide enrichment was also analyzed for each sample. The intensity values of iTRAQ reporter ion were summed for each channel across all identified peptides, and were used to correct for minor variation in source protein amount in each labeled sample.

*Hit identification*: The following $\log_2$(ratios) were calculated based on the corrected ion intensities: (Starved/Insulin), (Rapamycin/Insulin), (Torin1/Insulin) for HEK-293E samples and ($TSC2^{+/+}$ Torin1/ $TSC2^{+/+}$ vehicle), ($TSC2^{-/-}$ vehicle/ $TSC2^{+/+}$ vehicle), and ($TSC2^{-/-}$ Torin1/ $TSC2^{-/-}$ vehicle) for the MEF samples. The binary logarithms were then median centered and median absolute deviation (MAD) scaled separately for each technical replicate. The mTOR-regulated phosphopeptides ("hits") were those with a robust z-score (MADs away from the median) of at least -2.5 in $\log_2$(Torin1/Insulin) or $\log_2$($TSC2^{-/-}$ Torin1/ $TSC2^{-/-}$ vehicle). Those phosphopeptides detected in both replicates had to score below the threshold both times in order to be counted among the regulated phosphopeptides. The phosphopeptides which qualified as "rapamycin-sensitive" or "TSC2-upregulated" were those whose $\log_2$(Rapamycin/Insulin) or ($TSC2^{-/-}$ vehicle/

$TSC2^{+/+}$ vehicle) met the -2.5 MAD or +2.5 MAD cutoffs, respectively. Enrichment of control peptides was determined using Fisher's Exact Test and a list of well-accepted mTOR pathway phosphorylation sites which were detected in the datasets (Table S1). Correlation of features was measured using Spearman's rank correlation coefficient and significance was tested using a ρ test. p-values ~ 0 are lower than the smallest number able to be represented computationally.

*Heat map visualization*: The HEK-293E mTOR-regulated phosphopeptides were sorted based on their $\log_2$(Rapamycin/Insulin) robust z-score and negative outliers were set to -10 in the heatmap for improved visualization. Conditions were clustered using complete-linkage hierarchical clustering with the Euclidian distance metric. Statistical analyses and data processing were performed in R 2.11.1 and Bioperl 1.6 (Stajich et al., 2002).

*Pathway analysis:* Enrichment was determined at the protein level by collapsing the mTOR-regulated phosphopeptides at the -2 MAD cutoff from both datasets into gene symbols. Analysis was performed using DAVID (Huang da et al., 2009a, b), and SP_PIR_KEYWORDS, the GO FAT categories, Interpro domains, and Biocarta and KEGG pathways. Terms were defined as enriched if they contained at least 2 hits from the screen and had p-values < 0.01 and a FDR < 10%.

**Positional scanning peptide library screening**

*PSPL screening:* mTORC1 purification from HEK-293T cells stably expressing FLAG-raptor and Rheb purification from transiently transfected HEK-293T cells were performed as described previously (Sancak et al., 2007; Yip et al.). PSPL screening was done according to the published protocol (Hutti et al., 2004) with the final reaction conditions as follows: 20 mM HEPES, pH 7.4, 10 mM $MgCl_2$, 4 mM $MnCl_2$, 1 mM DTT, 50 ng Rheb, 150 ng mTORC1, 50 μM biotinylated peptides, 50 μM ATP, 2 μCi [$\gamma$-$^{32}$P]ATP. Each reaction consists of purified mTORC1, Rheb, radiolabeled ATP, and a mixture of

peptides containing one fixed residue relative to the central phospho-acceptor and other residues randomized. After incubating for 6 hrs. at 30°C, aliquots of the reactions were spotted onto streptavidin membrane and analyzed by PhosphorImaging.

*Data analysis:* A position specific scoring matrix (PSSM) was generated based on the normalized average intensities of the spots in the PSPL plot. A PSSM entry $S_{ij}$ for residue *i* in position *j* was calculated using the formula

$$S_{ij} = e^{\left(I_{ij} - \bar{I}_j\right)\frac{s_{Ij}}{\bar{I}_j}}$$

where $I_{ij}$ is the normalized average intensity of the spot for residue *i* in position *j*, $\bar{I}_j$ is the mean of the average normalized intensities in position *j*, and $s_{Ij}$ is the standard deviation of the average normalized intensities in position *j*. The Scansite algorithm was used to predict likely mTOR phospho-acceptor sites (Obenauer et al., 2003). Confidence thresholds for predictions were set based on the 0.2$^{nd}$, 1.5$^{th}$, and 5$^{th}$ percentile of the empiric score distributions of all serine and threonine sites in NCBI human and mouse RefSeq databases (downloaded June 2008). This setting corresponds to high, medium, and low stringency, respectively, in the standard Scansite configuration. For the classification of the mTOR-regulated phosphopeptides, those phosphopeptides containing sites whose Scansite scores were below the 5$^{th}$ percentile were considered as possessing a putative mTOR motif. AGC kinase motifs were determined by querying the sites for an (R/K)X(R/K)XX(S*/T*) sequence.

## Acknowledgements

We thank members of the Sabatini Lab for helpful discussion and especially thank B. Joughin, G. Bell, H. Keys, D. Wagner, and C. Thoreen for assistance with technical or conceptual aspects of this project. This work was supported by the National Institutes of Health (CA103866 and AI47389 to D.M.S.; ES015339, GM68762, and CA112967 to M.B.Y.), Department of Defense (W81XWH-07-0448 to D.M.S.), the W.M. Keck Foundation (D.M.S.), LAM Foundation (D.M.S.), Dana Farber Cancer Institute (N.S.G, J.M), the International Fulbright Science and Technology Award (J. R.), and American Cancer Society (S.A.K.). D.M.S. is an investigator of the Howard Hughes Medical Institute.

## References


Alessi, D.R., Pearce, L.R., and Garcia-Martinez, J.M. (2009). New insights into mTOR signaling: mTORC2 and beyond. Science signaling *2*, pe27.

Ali, S.M., and Sabatini, D.M. (2005). Structure of S6 kinase 1 determines whether raptor-mTOR or rictor-mTOR phosphorylates its hydrophobic motif site. J Biol Chem *280*, 19445-19448.

Askenazi, M., Parikh, J.R., and Marto, J.A. (2009). mzAPI: a new strategy for efficiently sharing mass spectrometry data. Nat Methods *6*, 240-241.

Brown, N.R., Noble, M.E., Endicott, J.A., and Johnson, L.N. (1999). The structural basis for specificity of substrate and recruitment peptides for cyclin-dependent kinases. Nature cell biology *1*, 438-443.

Choi, J.H., Bertram, P.G., Drenan, R., Carvalho, J., Zhou, H.H., and Zheng, X.F. (2002). The FKBP12-rapamycin-associated protein (FRAP) is a CLIP-170 kinase. EMBO Rep *3*, 988-994.

Choo, A.Y., Yoon, S.O., Kim, S.G., Roux, P.P., and Blenis, J. (2008). Rapamycin differentially inhibits S6Ks and 4E-BP1 to mediate cell-type-specific repression of mRNA translation. Proc Natl Acad Sci U S A *105*, 17414-17419.

Coller, J., and Parker, R. (2005). General translational repression by activators of mRNA decapping. Cell *122*, 875-886.

Feldman, M.E., Apsel, B., Uotila, A., Loewith, R., Knight, Z.A., Ruggero, D., and Shokat, K.M. (2009). Active-site inhibitors of mTOR target rapamycin-resistant outputs of mTORC1 and mTORC2. PLoS Biol *7*, e38.

Ficarro, S.B., Adelmant, G., Tomar, M.N., Zhang, Y., Cheng, V.J., and Marto, J.A. (2009). Magnetic bead processor for rapid evaluation and optimization of parameters for phosphopeptide enrichment. Anal Chem *81*, 4566-4575.

Ganley, I.G., Lam du, H., Wang, J., Ding, X., Chen, S., and Jiang, X. (2009). ULK1.ATG13.FIP200 complex mediates mTOR signaling and is essential for autophagy. J Biol Chem *284*, 12297-12305.

Garcia-Martinez, J.M., Moran, J., Clarke, R.G., Gray, A., Cosulich, S.C., Chresta, C.M., and Alessi, D.R. (2009). Ku-0063794 is a specific inhibitor of the mammalian target of rapamycin (mTOR). Biochem J.

Garry, D.J., Meeson, A., Elterman, J., Zhao, Y., Yang, P., Bassel-Duby, R., and Williams, R.S. (2000). Myogenic stem cell function is impaired in mice lacking the forkhead/winged helix protein MNF. Proc Natl Acad Sci U S A *97*, 5416-5421.

Gold, M.G., Barford, D., and Komander, D. (2006). Lining the pockets of kinases and phosphatases. Curr Opin Struct Biol *16*, 693-701.

Gray, C.H., Good, V.M., Tonks, N.K., and Barford, D. (2003). The structure of the cell cycle protein Cdc14 reveals a proline-directed protein phosphatase. The EMBO journal *22*, 3524-3535.

Hosokawa, N., Hara, T., Kaizuka, T., Kishi, C., Takamura, A., Miura, Y., Iemura, S., Natsume, T., Takehana, K., Yamada, N., *et al.* (2009). Nutrient-dependent mTORC1 association with the ULK1-Atg13-FIP200 complex required for autophagy. Mol Biol Cell *20*, 1981-1991.

Huang da, W., Sherman, B.T., and Lempicki, R.A. (2009a). Bioinformatics enrichment tools: paths toward the comprehensive functional analysis of large gene lists. Nucleic Acids Res *37*, 1-13.

Huang da, W., Sherman, B.T., and Lempicki, R.A. (2009b). Systematic and integrative analysis of large gene lists using DAVID bioinformatics resources. Nature protocols *4*, 44-57.

Huber, A., Bodenmiller, B., Uotila, A., Stahl, M., Wanka, S., Gerrits, B., Aebersold, R., and Loewith, R. (2009). Characterization of the rapamycin-sensitive phosphoproteome reveals that Sch9 is a central coordinator of protein synthesis. Genes Dev *23*, 1929-1943.

Hutti, J.E., Jarrell, E.T., Chang, J.D., Abbott, D.W., Storz, P., Toker, A., Cantley, L.C., and Turk, B.E. (2004). A rapid method for determining protein kinase phosphorylation specificity. Nat Methods *1*, 27-29.

Jung, C.H., Jun, C.B., Ro, S.H., Kim, Y.M., Otto, N.M., Cao, J., Kundu, M., and Kim, D.H. (2009). ULK-Atg13-FIP200 complexes mediate mTOR signaling to the autophagy machinery. Mol Biol Cell *20*, 1992-2003.

Laplante, M., and Sabatini, D.M. (2009). mTOR signaling at a glance. J Cell Sci *122*, 3589-3594.

Matsuoka, S., Ballif, B.A., Smogorzewska, A., McDonald, E.R., 3rd, Hurov, K.E., Luo, J., Bakalarski, C.E., Zhao, Z., Solimini, N., Lerenthal, Y., *et al.* (2007). ATM and ATR substrate analysis reveals extensive protein networks responsive to DNA damage. Science *316*, 1160-1166.

Mok, J., Kim, P.M., Lam, H.Y., Piccirillo, S., Zhou, X., Jeschke, G.R., Sheridan, D.L., Parker, S.A., Desai, V., Jwa, M., *et al.* (2010). Deciphering protein kinase specificity through large-scale analysis of yeast phosphorylation site motifs. Sci Signal *3*, ra12.

Moritz, A., Li, Y., Guo, A., Villen, J., Wang, Y., MacNeill, J., Kornhauser, J., Sprott, K., Zhou, J., Possemato, A., *et al.* (2010). Akt-RSK-S6 kinase signaling networks activated by oncogenic receptor tyrosine kinases. Science signaling *3*, ra64.

Nykamp, K., Lee, M.H., and Kimble, J. (2008). C. elegans La-related protein, LARP-1, localizes to germline P bodies and attenuates Ras-MAPK signaling during oogenesis. RNA *14*, 1378-1389.

Obenauer, J.C., Cantley, L.C., and Yaffe, M.B. (2003). Scansite 2.0: Proteome-wide prediction of cell signaling interactions using short sequence motifs. Nucleic Acids Res *31*, 3635-3641.

Parikh, J.R., Askenazi, M., Ficarro, S.B., Cashorali, T., Webber, J.T., Blank, N.C., Zhang, Y., and Marto, J.A. (2009). multiplierz: an extensible API based desktop environment for proteomics data analysis. BMC Bioinformatics *10*, 364.

Parker, R., and Sheth, U. (2007). P bodies and the control of mRNA translation and degradation. Mol Cell *25*, 635-646.

Polson, H.E., de Lartigue, J., Rigden, D.J., Reedijk, M., Urbe, S., Clague, M.J., and Tooze, S.A. (2010). Mammalian Atg18 (WIPI2) localizes to omegasome-anchored phagophores and positively regulates LC3 lipidation. Autophagy *6*.

Ramirez-Valle, F., Braunstein, S., Zavadil, J., Formenti, S.C., and Schneider, R.J. (2008). eIF4GI links nutrient sensing by mTOR to cell proliferation and inhibition of autophagy. The Journal of cell biology *181*, 293-307.

Ross, P.L., Huang, Y.N., Marchese, J.N., Williamson, B., Parker, K., Hattan, S., Khain-

ovski, N., Pillai, S., Dey, S., Daniels, S., *et al.* (2004). Multiplexed protein quantitation in Saccharomyces cerevisiae using amine-reactive isobaric tagging reagents. Mol Cell Proteomics *3*, 1154-1169.

Rowe, H.M., Jakobsson, J., Mesnard, D., Rougemont, J., Reynard, S., Aktas, T., Maillard, P.V., Layard-Liesching, H., Verp, S., Marquis, J., *et al.* (2010). KAP1 controls endogenous retroviruses in embryonic stem cells. Nature *463*, 237-240.

Rush, J., Moritz, A., Lee, K.A., Guo, A., Goss, V.L., Spek, E.J., Zhang, H., Zha, X.M., Polakiewicz, R.D., and Comb, M.J. (2005). Immunoaffinity profiling of tyrosine phosphorylation in cancer cells. Nature biotechnology *23*, 94-101.

Sancak, Y., Thoreen, C.C., Peterson, T.R., Lindquist, R.A., Kang, S.A., Spooner, E., Carr, S.A., and Sabatini, D.M. (2007). PRAS40 is an insulin-regulated inhibitor of the mTORC1 protein kinase. Mol Cell *25*, 903-915.

Shah, O.J., Wang, Z., and Hunter, T. (2004). Inappropriate activation of the TSC/Rheb/mTOR/S6K cassette induces IRS1/2 depletion, insulin resistance, and cell survival deficiencies. Curr Biol *14*, 1650-1656.

Shaulian, E. (2010). AP-1--The Jun proteins: Oncogenes or tumor suppressors in disguise? Cell Signal *22*, 894-899.

Singh, S.K., Clarke, I.D., Hide, T., and Dirks, P.B. (2004). Cancer stem cells in nervous system tumors. Oncogene *23*, 7267-7273.

Stajich, J.E., Block, D., Boulez, K., Brenner, S.E., Chervitz, S.A., Dagdigian, C., Fuellen, G., Gilbert, J.G., Korf, I., Lapp, H., *et al.* (2002). The Bioperl toolkit: Perl modules for the life sciences. Genome Res *12*, 1611-1618.

Stokes, M.P., Rush, J., Macneill, J., Ren, J.M., Sprott, K., Nardone, J., Yang, V., Beausoleil, S.A., Gygi, S.P., Livingstone, M., *et al.* (2007). Profiling of UV-induced ATM/ATR signaling pathways. Proceedings of the National Academy of Sciences of the United States of America *104*, 19855-19860.

Thoreen, C.C., Kang, S.A., Chang, J.W., Liu, Q., Zhang, J., Gao, Y., Reichling, L.J., Sim, T., Sabatini, D.M., and Gray, N.S. (2009). An ATP-competitive mammalian target of rapamycin inhibitor reveals rapamycin-resistant functions of mTORC1. J Biol Chem *284*, 8023-8032.

Yip, C.K., Murata, K., Walz, T., Sabatini, D.M., and Kang, S.A. (2010). Structure of the human mTOR complex I and its implications for rapamycin inhibition. Mol Cell *38*, 768-774.

Yu, K., Toral-Barza, L., Shi, C., Zhang, W.G., Lucas, J., Shor, B., Kim, J., Verheijen, J., Curran, K., Malwitz, D.J., *et al.* (2009). Biochemical, cellular, and in vivo activity of novel ATP-competitive and selective inhibitors of the mammalian target of rapamycin. Cancer Res *69*, 6232-6240.

Zhang, H., Zha, X., Tan, Y., Hornbeck, P.V., Mastrangelo, A.J., Alessi, D.R., Polakiewicz, R.D., and Comb, M.J. (2002). Phosphoprotein analysis using antibodies broadly reactive against phosphorylated motifs. The Journal of biological chemistry *277*, 39379-39387.

Zoncu, R., Efeyan, A., and Sabatini, D.M. (2011). mTOR: from growth signal integration to cancer, diabetes and ageing. Nat Rev Mol Cell Biol *12*, 21-35.

# Chapter 3

## The mTORC1 substrate Grb10 mediates feedback inhibition to PI3K-Akt

Peggy P. Hsu [1,2], Kathleen A. Ottina [1,7], Yi Zhang [3,4], Seong A. Kang [1], Timothy R. Peterson [1,2], Jarrod A. Marto [3,4,5], David M. Sabatini [1,2,4,6,7]

1 Whitehead Institute for Biomedical Research, Nine Cambridge Center, Cambridge, MA 02142, USA

2 Department of Biology, Massachusetts Institute of Technology (MIT), Cambridge, MA 02139, USA

3 Department of Cancer Biology, Dana Farber Cancer Institute (DFCI), 250 Longwood Avenue, Boston, MA 02115, USA

4 Blais Proteomics Center, DFCI, 250 Longwood Avenue, Boston, MA 02115, USA

5 Department of Biological Chemistry and Molecular Pharmacology, Harvard Medical School, 250 Longwood Avenue, Boston, MA 02115, USA

6 David H. Koch Institute for Integrative Cancer Research at MIT, 77 Massachusetts Avenue, Cambridge, MA 02139, USA

7 Howard Hughes Medical Institute

The experiments shown in all figures were performed by PPH with technical assistance from KAO with the exception of Figure 3A which was performed by TRP, Figures 5A and 5B which were performed by KAO, and Figure 4A which was performed by SAK. Mapping of the Grb10 sites (Figure 2D and 2E) was performed by PPH and YZ.

## Summary

The mTORC1 serine-threonine kinase is a master regulator of cell growth and metabolism that phosphorylates the translational regulators, S6K1 and 4E-BP1. Cells without the TSC1 or TSC2 tumor suppressors exhibit hyperactive mTORC1 and repressed PI3K-Akt signaling. This connection from mTORC1 to Akt is referred to as the negative feedback loop, and its most well-accepted mechanism is the inhibitory phosphorylation by S6K1 of insulin-receptor substrate 1 (IRS1), leading to IRS1 destabilization. Here, we identify the adaptor protein and negative regulator of growth factor signaling Grb10 as a direct mTORC1 substrate that mediates the inhibition of PI3K typical of cells lacking TSC2 without affecting inhibitory phosphorylation of IRS1 or IRS1 protein levels. mTORC1 phosphorylation positively regulates Grb10 function and stability. Therefore, mTORC1 activates and stabilizes Grb10 while also inhibiting and destabilizing the IRS proteins. These findings clarify the nature of feedback inhibition to PI3K-Akt and confirm the primacy of mTORC1 in regulating growth factor signaling.

## Introduction

The mechanistic target of rapamycin (mTOR) is an evolutionarily conserved serine-threonine kinase which regulates a diverse array of cellular processes, including cell growth, translation, autophagy, proliferation, cell survival, and metabolism (Laplante and Sabatini, 2009; Zoncu et al., 2011). mTOR is the catalytic subunit of two distinct complexes, mTOR complex 1 (mTORC1) and mTORC2. Prototypical mTORC1 substrates include the translational regulators, eIF4E-binding protein 1 (4E-BP1) and ribosomal S6 Kinase 1 (S6K1) while mTORC2 phosphorylates Akt and serum and glucocorticoid-regulated kinase 1 (SGK1). Both complexes are regulated by growth factors while mTORC1 additionally senses amino acids, hypoxia, and energetic stress. Most of the signals to mTORC1 are integrated by the hamartin-tuberin complex, TSC1/2, which is a heterodimeric GTPase activating protein (GAP) for Ras homolog enriched in brain (Rheb), a direct activator of mTORC1.

Small molecules derived from rapamycin, an allosteric mTORC1 inhibitor, have been in many trials for anti-cancer uses. However, several explanations exist as to why rapamycin analogs have been disappointing clinically. First, while mTORC1 was traditionally considered the "rapamycin-sensitive" complex, it is now appreciated that rapamycin does not inhibit all phosphorylations downstream of mTORC1 (Choo et al., 2008; Feldman et al., 2009; Thoreen et al., 2009). Moreover, rapamycin at short treatment times does not inhibit mTORC2 (Jacinto et al., 2004; Sarbassov et al., 2004; Sarbassov et al., 2006). And perhaps most importantly, mTORC1 inhibition leads to feedback activation of the PI3K-Akt pathway which may promote cell survival and proliferation (Efeyan and Sabatini, 2010).

The most well-accepted mechanism by which mTORC1 inhibits PI3K is the phosphorylation of IRS1 on inhibitory serine sites by S6K1 leading to a destabilization of the protein and inhibition of signal transduction from the insulin and IGF-1 receptors to Akt (Harrington et al., 2004; Shah et al., 2004). S6K1-null mice are resistant to

diet-induced obesity and exhibit enhanced insulin sensitivity due to disinhibition of this negative feedback signaling and decreased inhibitory phosphorylation of IRS1 (Um et al., 2004). Akt phosphorylation has been shown to be activated in clinical tumor samples treated with rapamycin alone (Faivre et al., 2006; O'Reilly et al., 2006), and the addition of either Akt or IGF1R inhibition has shown to sensitize cells to rapamycin (O'Reilly et al., 2006; Sun et al., 2005; Takeuchi et al., 2005; Wan et al., 2007). A detailed molecular understanding of the signaling between mTORC1 and PI3K could potentially lead to more targeted use of rapamycin mono- or combination therapy.

Here, we identify Grb10 as a direct substrate of mTORC1 which, similar to 4E-BP1, contains both rapamycin-sensitive and -insensitive mTOR phosphorylation sites. Grb10 is important for the inhibition of growth factor signaling typical of cells with loss of TSC2 and phosphorylation is required for both its function and its stability. Grb10 inhibition of Akt is independent of effects on IRS1 serine phosphorylation or protein levels. We propose that S6K1-IRS1 and Grb10 comprise two parallel arms of feedback inhibition of PI3K-Akt signaling, both orchestrated by mTORC1.

## Results

### Grb10 phosphorylation is regulated in an mTORC1-dependent manner

In a phosphoproteomic screen to identify new downstream effectors of mTOR, one candidate mTOR substrate was the adaptor protein growth-receptor bound protein 10 (Grb10) (Chapter 2, Fig. 8). By quantitative mass spectrometry with isobaric mass tags (iTRAQ), the abundance of a Grb10 phosphopeptide with sites consistent with the consensus mTOR motif defined by positional scanning peptide library screening was increased in the absence of TSC2 and decreased after Torin1 treatment in both wild-type (TSC2+/+) and TSC2-null (TSC2-/-) mouse embryonic fibroblasts (MEFs) (Chapter 2, Fig. 8), patterns consistent with being in the mTORC1 pathway.

Conserved among vertebrates, Grb10 is an adaptor protein which negatively regulates growth factor signaling (Holt and Siddle, 2005). Grb10 is related by sequence and function to two other adaptor proteins, Grb7 and Grb14. While Grb10 was originally identified as an EGF receptor binding protein (Ooi et al., 1995) and can bind a variety of growth factor receptors, the interaction between Grb10 and the insulin and IGF-1 receptors seems to be the strongest as well as the most well-characterized (Holt and Siddle, 2005).

Grb7, Grb10, and Grb14 all share the same domain structure. The N-terminal proline-rich domain contains motifs corresponding to the minimal consensus for SH3 domain binding (Fig. 2C). Two proteins, Grb10 interacting GYF protein 1 (GYGYF1) and GIGYF2, bind the proline-rich domain of Grb10, but the functional consequence of this interaction is unknown (Giovannone et al., 2003). Grb10 also contains a putative pleckstrin homology (PH) domain and Ras-binding domain, but the lipids and small G-proteins bound by Grb10 in the cell have not been characterized. The SH2 domain of Grb10 is important for its binding of phosphorylated tyrosine residues on the activated insulin and IGF-1 receptor (Hansen et al., 1996). Uniquely shared by only Grb7, Grb10, and Grb14 (Kasus-Jacobi et al., 1998), the between PH and SH2 domain (BPS) of

Grb10 contributes to receptor binding (He et al., 1998).

In both mouse and human cells, Grb10 is expressed as multiple isoforms which mostly differ in their N-termini as a result of alternative splicing or translation initiation. (Holt and Siddle, 2005). The functional differences between isoforms are not known. With the exception of the human isoform b which is missing a small portion of the PH domain, all mouse and human Grb10 proteins contain the aforementioned domains. Grb10 mRNA expression is highest in insulin-responsive tissues. In the adult mouse, Grb10 is expressed most highly in skeletal muscle, adipose tissue, heart, and kidney (Laviola et al., 1997; Ooi et al., 1995). Human Grb10 mRNA is highly expressed in skeletal muscle, and pancreas, cardiac muscle, and brain (Frantz et al., 1997; Liu and Roth, 1995; O'Neill et al., 1996).

Mice without Grb10 are larger and exhibit enhanced insulin sensitivity (Charalambous et al., 2003; Smith et al., 2007; Wang et al., 2007a). Although the E3 ubiquitin ligase neural precursor cell expressed, developmentally down-regulated 4 (Nedd4) does not directly ubiquitinate Grb10 (Morrione et al., 1999), Nedd4-null mice have more Grb10 protein and are insulin- and IGF-resistant, a signaling phenotype reminiscent of cells lacking TSC1 or TSC2 (Cao et al., 2008). Therefore, we speculated that Grb10 might function downstream of mTORC1 to inhibit PI3K-Akt signaling.

In SDS-PAGE analyses, Grb10 exhibited an insulin-stimulated mobility shift that is partially sensitive to rapamycin (Fig. 1A), mirroring the mobility shift in the mTORC1 substrate, 4E-BP1. In vitro phosphatase treatment eliminated the shift, as did Torin1, indicating that the shift results from phosphorylation and is dependent on mTOR activity (Fig. 1A, 1B). Amino acids stimulated Grb10 phosphorylation and were required for the serum-dependent phosphorylation of Grb10, 4E-BP1, and S6K1 but not of Akt (Fig. 1C). Moreover, in TSC2-/- MEFs, Grb10 phosphorylation was retained in the absence of serum but lost upon acute rapamycin and Torin1 treatment (Fig. 1D). TSC2-null cells also have more Grb10 protein, an observation elaborated upon later. These data point to mTORC1, but not mTORC2, as the main regulator of Grb10. Consistent with this conclusion, the loss of rictor, a core component of mTORC2, did not affect Grb10

phosphorylation (Fig. 1E, 1F).

**Grb10 is an mTORC1 substrate with rapamycin-sensitive and -insensitive sites**

In cells lacking S6K1 and S6K2, Grb10 was still regulated in an mTOR-dependent manner (Fig. 2A), suggesting that it might be a direct substrate. Indeed, Grb10 was phosphorylated in vitro by mTORC1 to an extent comparable with known substrates (Fig. 2B).

The sites regulated by mTOR in vitro were mapped by mass spectrometry primarily to S476 and secondarily to T155 and S428 (Fig. 2D), and the sites regulated in cells were mapped to S104, S150, S428, and S476 (Fig. 2E). In cells, all identified sites were Torin1-sensitive, while S476 was also rapamycin-sensitive (Fig. 2E). Grb10 is therefore similar to 4E-BP1, an mTORC1 substrate with both rapamycin-sensitive and -insensitive sites (Fig. 2F). These sites are located either in or near the N-terminal proline-rich region or the BPS domain of Grb10 (Fig. 2C). Grb10 is highly related both at the primary sequence level and functionally to Grb14. However, the only phosphorylation site conserved between Grb10 and the related Grb14 is S428, and preliminary data suggests that Grb14 is not regulated in an mTOR-dependent manner (Peggy Hsu, unpublished data).

We verified our characterization of these sites with phospho-specific antibodies against S150, S428, and S476 (Fig. 2G), which confirmed their Torin1-sensitivity and the rapamycin-sensitivity of S476. Mutation of all identified sites along with a few neighboring residues (9A mutant) eliminated the mobility shift (Fig. 2H), indicating that most if not all mTOR-regulated sites were localized.

**Grb10 mediates the insulin and IGF-1 resistance of cells with TSC2 loss**

mTORC1 inhibits PI3K-Akt signaling, but the molecular connections involved are poorly understood. One mechanism is the destabilization of insulin receptor substrate 1 (IRS1) by S6K1 phosphorylation (Harrington et al., 2004; Shah et al., 2004). However, other mechanisms likely exist because loss of raptor, an essential mTORC1

component, in S6K1-/-S6K2-/- cells still activated Akt phosphorylation without affecting IRS1 abundance (Fig. 3A). Therefore, we tested whether mTORC1 might also inhibit the PI3K pathway through Grb10. Consistent with this possibility, the shRNA-mediated knockdown of Grb10 in HEK-293E and HeLa cells boosted Akt phosphorylation (Fig. 3B, 3C). This boost was increased with rapamycin treatment and, to a lesser extent, with S6K inhibition (Pearce et al., 2010), suggesting that Grb10 is important for feedback but that other mTOR-dependent mechanisms are also at play. In all cells tested, the Grb10 knockdown caused a stronger boost in Akt phosphorylation than the S6K inhibitor alone, suggesting that the contribution of Grb10 in feedback signaling is at least as important as that of S6K (Fig. 3B, 3C, unpublished data). Moreover, rapamycin treatment had an equal or greater effect than the S6K inhibitor, confirming that mTORC1 also mediates feedback inhibition through an S6K-independent component (Fig. 3B, 3C).

We then examined signaling in TSC2-null cells, which, due to mTORC1 hyperactivity, are sensitized to changes in feedback inhibition. At baseline, cells without TSC2 are insulin and IGF-1 resistant (Harrington et al., 2004; Shah et al., 2004). Strikingly, loss of Grb10 in TSC2-/- MEFs also restored insulin sensitivity to Akt phosphorylation without affecting total IRS1 levels or the phosphorylation of S636 and S639 on IRS1, thereby acting independently of known feedback mechanisms (Fig. 3D). While in TSC2-/- cells Grb10 suppression or acute rapamycin treatment each did not rescue insulin signaling to the same level as in wild-type cells, the two in combination approximated the wild-type level of Akt activation (Fig. 3E). This restoration in growth factor sensitivity also applied to increased autophosphorylation of the insulin and IGF receptors, Erk1/2 activation, and IGF-1, but not EGF or PDGF, stimulation (Fig. 3F, 3G). Finally, suppression of Grb10 also increased tyrosine phosphorylation of IRS1 and IRS2 and p85 PI3K recruitment by IRS, again independently of IRS protein levels (Fig. 3H).

**Grb10 phosphorylation is important for its function**

To examine the importance of the mTOR phosphorylation sites of Grb10 on feedback signaling to Akt, we generated TSC2-null cells in which we replaced

endogenous Grb10 with wild-type Grb10 or mutants lacking the phosphorylation sites. Compared to cells expressing wild-type Grb10, cells expressing an equivalent amount of non-phosphorylatable Grb10 had increased Akt phosphorylation, confirming that mTORC1 phosphorylation is necessary for its inhibitory function (Fig. 4A).

Given that some of the mTOR sites are located in the BPS domain important for binding to the activated insulin and IGF-1 receptors (He et al., 1998), we asked if Grb10 phosphorylation was important for this interaction. In cell lines overexpressing either the insulin or the IGF-1 receptor, we found that, consistent with the literature, growth factor stimulation increased binding of Grb10 to the receptors, presumably by inducing autophosphorylation of the receptors on tyrosine residues and recruitment of Grb10 by its SH2 domain (Fig. 4B). However, this interaction was not regulated by mTOR activity (Fig. 4B). We also found that Grb10 was both membrane associated and diffusely cytoplasmic, but we did not appreciate a significant change in Grb10 localization either with growth factor stimulation or with Torin1 treatment (Nora Kory, unpublished data).

**mTORC1 positively regulates the stability of Grb10**

Although we were not able to pinpoint the exact mechanism by which phosphorylation regulates Grb10 function, we also suspected that mTORC1-mediated phosphorylation of Grb10 might affect its stability. We found that the more sites we mutated to alanine, the more lentiviral expression construct was required to achieve expression levels equivalent to the wild-type protein. Grb10 is also highly abundant in the TSC2-/- cells with hyperactive mTORC1 signaling (Fig. 5A), and chronic mTOR inhibition decreased Grb10 protein abundance (Fig. 1D, 5B) without significantly affecting mRNA levels (Fig. 5B). Indeed, determination of Grb10 half-life by pulse-chase experiments revealed at least a two-fold decrease (~12 hrs. to ~5 hrs.) in stability with either mTOR inhibitor treatment (Fig. 5C) or mutation of the mTOR sites to alanines (Fig. 5D). Proteasome inhibition (Fig. 5E), suppression of Nedd4 (Fig. 5F), or phosphomimetic mutation of the mTOR sites (Fig. 5G) rescued the decrease in Grb10 protein caused by mTOR inhibition. Therefore, mTORC1 inhibits and destabilizes IRS1 and simultaneously

activates and stabilizes Grb10.

We compared the acute and chronic effects of the S6K1 inhibitor PF-4708671, rapamycin, and Torin1 treatment on Akt activation in TSC2-null cells. We serum deprived cells for either one or 24 hours in the presence of the inhibitors and then stimulated with 100 nM insulin for 15 minutes. After acute treatment, we found that the S6K inhibitor caused inhibition of S302 phosphorylation but did not have effects on S636 and S639 on IRS1 and, as expected, had no effect on Grb10 phosphorylation (Fig. 6). Rapamycin inhibited S302, S636, and S639 phosphorylation on IRS1 as well as S476 on Grb10 and rescued Akt activation to a greater extent than the S6K inhibitor. Torin1 treatment prevented phosphorylation of all the aforementioned sites as well as S150 on Grb10 but Akt phosphorylation was still inhibited due to its effects on hydrophobic motif phosphorylation. At longer treatment times, rapamycin and Torin1 led to effects on Grb10 and IRS levels (Grb10 being destabilized, IRS1 and IRS2 stabilized) while S6K inhibition, in accordance with similar results reported by Pearce et al., 2010, did not (Fig. 6). These effects on IRS and Grb10 stability caused by mTOR inhibition were correlated with full rescue in insulin sensitivity of TSC2-null cells comparable to the extent of Akt activation in wild-type cells. With chronic treatment of Torin1, despite residual inhibition of S473 phosphorylation of Akt, T308 phosphorylation was rescued presumably due to disinhibition of the negative feedback loop and incomplete inhibition of mTORC2 chronically, similar to the effects of DEPTOR overexpression (Fig. 6) (Peterson et al., 2009). Collectively, these results establish the primacy of mTORC1 itself in mediating feedback inhibition of PI3K-Akt through several parallel signaling arms involving S6K-IRS and Grb10.

**mTORC1 may regulate the trafficking of growth factor receptors through Grb10**

While it is now well established that Grb10 is a negative regulator of growth factor signaling, no consensus exists in the literature as to the mechanism of Grb10 action. One proposed mechanism is that Grb10 directly inhibits the kinase activity of the receptor (Stein et al., 2001). Another is that Grb10 prevents recruitment of IRS proteins

to the receptor (Wick et al., 2003). A third mechanism is that Grb10 binds the ubiquitin ligase Nedd4 which then subsequently targets the receptor for degradation (Vecchione et al., 2003). A fourth mechanism is that Grb10 regulates the trafficking of the receptor in a Nedd4-dependent mechanism (Monami et al., 2008; Vecchione et al., 2003).

Several of these mechanisms may be occurring simultaneously. We detected modest increases in receptor autophosphorylation upon Grb10 loss, consistent with Grb10 affecting the catalytic activity of the receptor (Fig. 3F). While we did not directly examine IRS recruitment to the receptor, as described above, tyrosine phosphorylation of IRS1 and IRS2 as well as consequent p85 PI3K activation were increased upon Grb10 loss, not inconsistent with Grb10 perhaps affecting the recruitment and phosphorylation of receptor substrates (Fig. 3H). We did not however detect any significant changes in insulin or IGF-1 receptor levels upon Grb10 suppression (Fig. 3F).

Nedd4 is a ubiquitin ligase originally thought to be responsible for PTEN degradation (Trotman et al., 2007; Wang et al., 2007b). Nedd4-null mice exhibit severe growth retardation and perinatal lethality (Cao et al., 2008). Nedd4-/- MEFs, similar to MEFs null for TSC1 or TSC2, are resistant to insulin and IGF-1 stimulation with decreased Akt T308 and S473 phosphorylation, IGF-1R autophosphorylation, and tyrosine phosphorylation of IRS-1. When the authors examined the levels of several putative Nedd4 targets, including PTEN, they also saw no differences between wild-type and Nedd4-null cells, with the exception of Grb10 whose protein levels were highly elevated. Of note, while Grb10 had previously been shown to bind Nedd4, it was determined not to be directly ubiquitinated by it (Morrione et al., 1999). Moreover, even though total receptor levels were similar to wild-type cells, Nedd4-/- MEFs had less IGF-1R at the cell surface. Finally, the perinatal lethality of the Nedd4-/- mice could be reversed with loss of one allele of Grb10, suggesting that Grb10 is the key growth factor signaling molecule downstream of Nedd4.

While TSC1 or TSC2 loss results in mTORC1 hyperactivation and overgrowth, rather than growth retardation, the PI3K-Akt signaling and insulin/IGF-1 resistance of TSC-null cells resembles that of Nedd4-null cells, with both perturbations correlated with

elevated levels of Grb10 protein. And in both TSC and Nedd4 loss, Grb10 suppression rescued growth factor signaling. Given the similarities, we wondered if the insulin or IGF-1 receptors might also be mislocalized in the TSC2-/- MEFs as they had been in the Nedd4-/- MEFs.

We biotinylated cell surface proteins and found that, while wild-type and TSC2 null cells both expressed similar levels of IGF-1 receptor, in TSC2-/- cells, the receptor was not at the plasma membrane (Fig. 7A). Surface localization was rescued either with rapamycin treatment or suppression of Grb10 (Fig. 7A), conditions which also lead to reactivation of Akt phosphorylation (Fig 3E).

As an alternative method to assess the amount of receptor at the surface, we modified a protease protection assay, taking advantage of the fact that the β chain of the IGF-1 receptor is 627 amino acids, 195 of which are extracellular. We kept either wild-type or TSC2-null cells on ice and treated the cells with Proteinase K. As the antibody to the β chain recognizes the intracellular domain, protease cleavage resulted in a ~20 kDa molecular weight shift in wild-type cells while the intracellular domain was protected (Fig. 7B). The IGF-1 receptor is initially synthesized as one long chain which is subsequently cleaved into an α and β chain. The precursor IGF1R protein was protected from the protease, as was S6K1 (Fig. 7B). Treatment of the cells with detergent led to increased access of the protease to intracellular compartments and degradation of the mature β chain, the pro-IGF1R, and S6K1 (Fig. 7B). Interestingly, in cells without TSC2, a fraction of the receptors was resistant to cleavage, suggesting that some of it is protected within the cell (Fig. 7B).

While these preliminary data suggest that mTORC1 may regulate the trafficking of insulin and IGF-1 receptors through Grb10 and that mTORC1 hyperactivation may result in a sequestration of receptors inside the cell, thereby partially explaining the insulin and IGF-1 resistance of TSC-null cells, additional experimental verification is required.

## Discussion

These results confirm the importance of the mTORC1 pathway in regulating growth factor signaling and clarify the nature of the feedback loop to PI3K-Akt. While acute mTORC1 inhibition leads to dephosphorylation of IRS1 and Grb10, chronic mTORC1 inhibition leads to changes in the levels of IRS and Grb10 proteins which are likely to be the most important effects of mTOR inhibitors to consider in their clinical use (Fig. 8).

While S636 and S639 on IRS1 are thought to be phosphorylated by S6K1 (Um et al., 2004), they do not correspond to the consensus AGC kinase motif. S302 (in mouse, S307 in human), however, does, and was the only IRS1 phosphorylation site which we found to be sensitive to S6K inhibition (Fig. 6). Given that mTORC1 has been shown to phosphorylate IRS1 directly (Tzatsos and Kandror, 2006), we propose that S6K1 and mTORC1 both phosphorylate IRS1 and perhaps also IRS2, and that mTORC1 inhibition prevents all of these phosphorylations from occurring while S6K inhibition only affects a subset. In accordance with this theory, chronic treatment with rapamycin or Torin1 affects IRS1 and IRS2 levels, while S6K inhibition does not under the conditions which we tested (Fig. 6) (Pearce et al., 2010).

Furthermore, mTORC1 inhibition has greater effects on Akt reactivation in TSC2-null cells due to its additional effects on Grb10. Rapamycin and Torin1 treatment destabilized Grb10 to similar extents (Fig. 5C), leading us to suspect that the rapamycin-sensitive site (S476) on Grb10 is likely to be responsible for regulating stability. However, upon addition of the inhibitors to cells, Torin1 has a greater effect on Grb10 stability than rapamycin (Fig. 5A), suggesting that mTOR may additionally regulate the synthesis of Grb10 protein.

Reintroduction of the platelet-derived growth factor receptor (PDGFR) has been shown to restore sensitivity of TSC2 null cells to other growth factors, including EGF and insulin (Zhang et al., 2003). Since Grb10 can in fact bind PDGFR (Frantz et al.,

1997; Wang et al., 1999), albeit with supposedly lower affinity than its binding to the insulin or IGF receptors, one possible explanation for this phenomenon in light of the results presented here is that overexpression of PDGFR titrates Grb10 away from other receptors, leading to enhanced signaling through the receptors normally bound to Grb10.

Nedd4 suppression profoundly suppresses insulin and IGF-1 signaling (Cao et al., 2008). While several groups had proposed that Nedd4 was responsible for PTEN degradation (Trotman et al., 2007; Wang et al., 2007b), we support the thought that the primary target of Nedd4 is Grb10. Mouse models of Nedd4 loss do not have increased PTEN protein (Cao et al., 2008; Fouladkou et al., 2008). Nedd4-null mice however, do have elevated Grb10 levels (Cao et al., 2008). Furthermore, one group reported no effect of Nedd4 loss on Akt signaling (Fouladkou et al., 2008), in contrast to Cao et al., or our own experiments with Nedd4 knockdown (Peggy Hsu, unpublished data). One reason for this discrepancy is that the authors of this work used serum to stimulate the cells, rather than specific growth factors. We hypothesize that had the authors attempted selective growth factor stimulation with insulin and IGF-1, the insulin and IGF receptors being most preferred by Grb10, a defect in growth factor signaling would have been apparent. How Nedd4 loss leads to an increase in Grb10 protein levels remains to be determined.

Interestingly, Grb10 is an imprinted gene. In mice, most tissues express the maternal copy, while the brain expresses the paternal copy (Garfield et al., 2011). Mice with loss of the maternal copy exhibit tissue overgrowth which does not affect the brain, while disruption of the paternal allele results in increased displays of social dominance (Garfield et al., 2011). In humans, Grb10 seems to be similarly imprinted with most tissues expressing the maternal copy (Abu-Amero et al., 2008; Holt and Siddle, 2005). Silver-Russell syndrome (SRS) is a genetic disorder characterized by intrauterine growth retardation, poor postnatal growth, craniofacial malformations, and difficulty feeding (Abu-Amero et al., 2008). A subset of SRS patients are maternal uniparental disomic for a region of chromosome 7 where GRB10 is located and would therefore express two doses of the gene and be expected to have increased Grb10 protein, similar to Nedd4

or TSC loss. One hypothesis that springs from the work presented here is that these SRS patients might, counterintuitively, benefit from treatment with rapamycin. While they do have difficulties in growth and therefore would not be expected to tolerate mTOR inhibition, rapamycin treatment might actually lead to the destabilization of Grb10 and a reduction in levels of the inhibitory protein.

## Figure 1

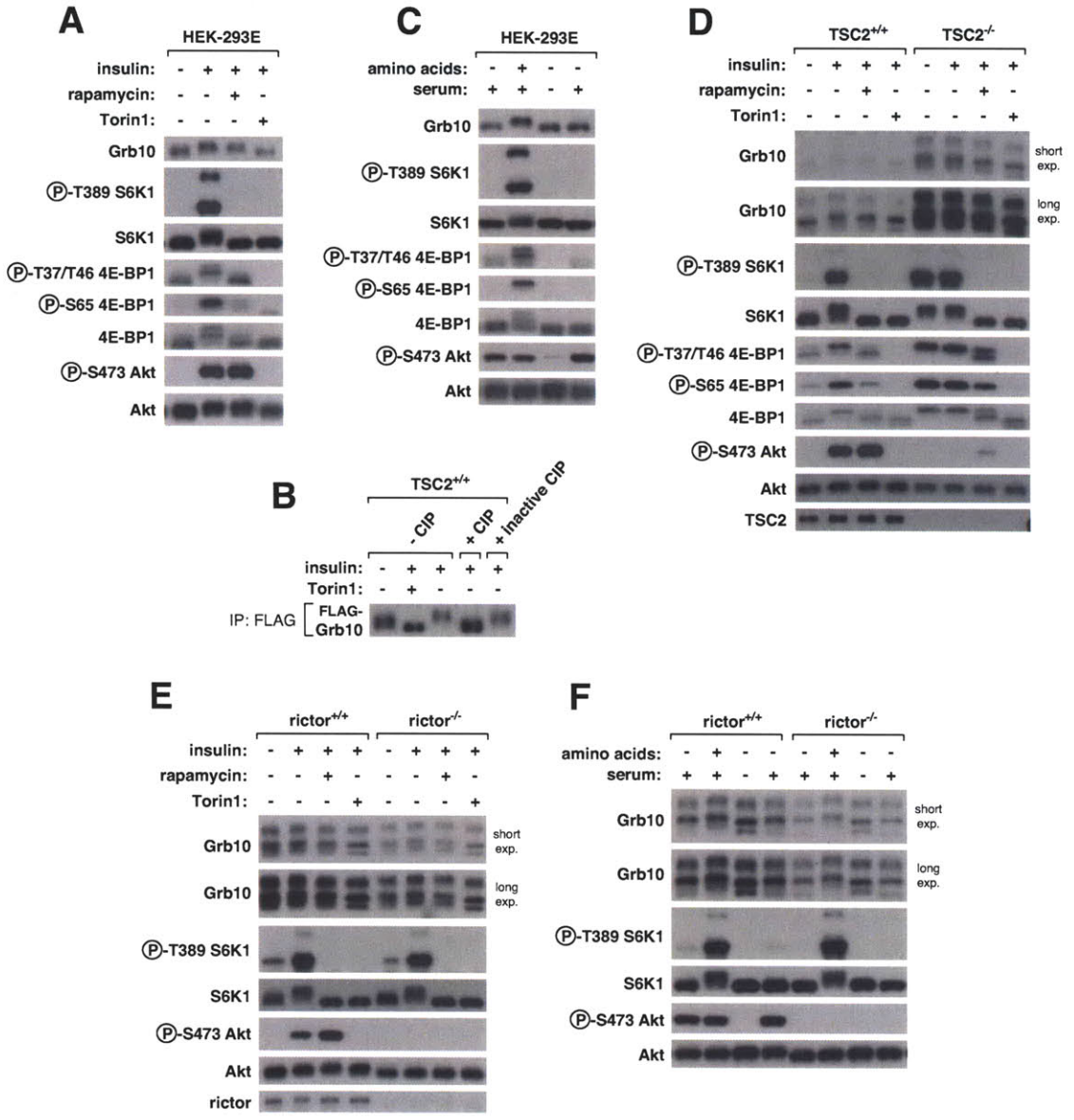
A
HEK-293E
insulin:
rapamycin:
Torin1:
Grb10
Ⓟ-T389 S6K1
S6K1
Ⓟ-T37/T46 4E-BP1
Ⓟ-S65 4E-BP1
4E-BP1
Ⓟ-S473 Akt
Akt
C
HEK-293E
amino acids:
serum:
Grb10
Ⓟ-T389 S6K1
S6K1
Ⓟ-T37/T46 4E-BP1
Ⓟ-S65 4E-BP1
4E-BP1
Ⓟ-S473 Akt
Akt
D
TSC2+/+
TSC2-/-
insulin:
rapamycin:
Torin1:
Grb10
short exp.
Grb10
long exp.
Ⓟ-T389 S6K1
S6K1
Ⓟ-T37/T46 4E-BP1
Ⓟ-S65 4E-BP1
4E-BP1
Ⓟ-S473 Akt
Akt
TSC2
B
TSC2+/+
- CIP
+ CIP
+ inactive CIP
insulin:
Torin1:
IP: FLAG
FLAG-Grb10
E
rictor+/+
rictor-/-
insulin:
rapamycin:
Torin1:
Grb10
short exp.
Grb10
long exp.
Ⓟ-T389 S6K1
S6K1
Ⓟ-S473 Akt
Akt
rictor
F
rictor+/+
rictor-/-
amino acids:
serum:
Grb10
short exp.
Grb10
long exp.
Ⓟ-T389 S6K1
S6K1
Ⓟ-S473 Akt
Akt

**Figure 1. Grb10 is regulated in an mTORC1-dependent manner.**

(A) HEK-293E cells were deprived of serum for 4 hrs, treated with 100 nM rapamycin or 250 nM Torin1 for 1 hr, and then stimulated with 150 nM insulin for 15 min. Cell lysates were analyzed by immunoblotting. (B) TSC2+/+ MEFs stably expressing FLAG-Grb10 were serum deprived for 4 hours, treated with 250 nM Torin1 for 1 hr, and then stimulated with 150 nM insulin for 15 min. All FLAG-tagged Grb10 constructs correspond to isoform c of human Grb10. FLAG-immunoprecipitates were incubated in buffer, CIP, or heat-inactivated CIP and analyzed by immunoblotting. (C) HEK-293E cells were deprived of amino acids or both amino acids and serum for 50 min, and then stimulated with either amino acids or serum for 10 min and analyzed by immunoblotting. (D) TSC2+/+ and TSC2-/- MEFs were treated and analyzed as in (A). (E) rictor+/+ and rictor-/- MEFs treated and analyzed as in (A). (F) rictor+/+ and rictor-/- MEFs were treated and analyzed as in (C).

**Figure 2**

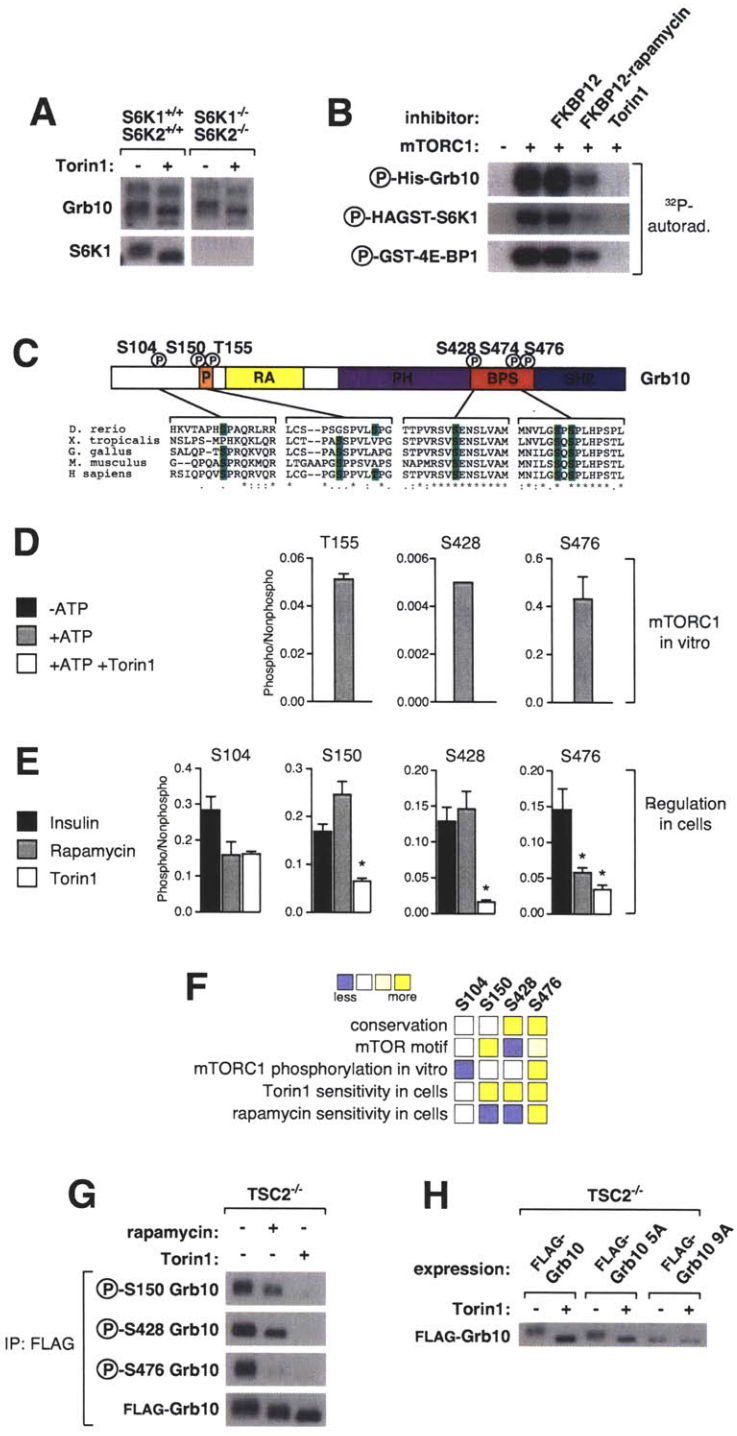
A
S6K1+/+ S6K2+/+
S6K1-/- S6K2-/-
Torin1: - + - +
Grb10
S6K1
B
inhibitor:
FKBP12
FKBP12-rapamycin
Torin1
mTORC1: - + + + +
Ⓟ-His-Grb10
Ⓟ-HAGST-S6K1
Ⓟ-GST-4E-BP1
32P-autorad.
C
S104 S150 T155
S428 S474 S476
RA
PH
BPS
SHD
Grb10
D. rerio
X. tropicalis
G. gallus
M. musculus
H sapiens
D
-ATP
+ATP
+ATP +Torin1
Phospho/Nonphospho
T155
S428
S476
mTORC1 in vitro
E
Insulin
Rapamycin
Torin1
S104
S150
S428
S476
Regulation in cells
F
less
more
S104 S150 S428 S476
conservation
mTOR motif
mTORC1 phosphorylation in vitro
Torin1 sensitivity in cells
rapamycin sensitivity in cells
G
TSC2-/-
rapamycin: - + -
Torin1: - - +
IP: FLAG
Ⓟ-S150 Grb10
Ⓟ-S428 Grb10
Ⓟ-S476 Grb10
FLAG-Grb10
H
TSC2-/-
expression:
FLAG-Grb10
FLAG-Grb10 5A
FLAG-Grb10 9A
Torin1: - + - + - +
FLAG-Grb10

**Figure 2. mTORC1 phosphorylates Grb10 on rapamycin-sensitive and -insensitive sites.**

(A) S6K1-/- S6K2-/- or control cells were treated with 250nM Torin1 or vehicle control for 1 hr and analyzed by immunoblotting. (B) mTORC1 in vitro kinase assays with substrates in the presence of the indicated inhibitors and radiolabeled ATP were analyzed by autoradiography. (C) Schematic representation of Grb10 protein structure with the phosphorylation sites from vertebrate orthologs aligned below. Numbering is according to human isoform a. (D) The phosphorylation state of Grb10 from kinase assays performed similarly to (B) were analyzed by targeted mass spectrometry (MS) and phosphorylation ratios determined from chromatographic peak intensities. (E) FLAG-immunoprecipitates from HEK-293E cells stably expressing FLAG-Grb10 treated as in (A) were analyzed as in (G). Data are means ± s.e.m (n=2-6). *Mann-Whitney t-test p-values $< 0.05$ for differences between stimulated and treated conditions. (F) A summary of (C), (D), and (E) for each Grb10 phosphorylation site. (G) FLAG-immunoprecipitates from TSC2-/- MEFs stably expressing FLAG-Grb10 treated with 100 nM rapamycin or 250 nM Torin1 for 1 hr were analyzed by immunoblotting with Grb10 phospho-specific antibodies. (H) TSC2-/- MEFs stably expressing FLAG-Grb10, 5A (S150A T155A S158A S474A S476A), or 9A (5A + S104A S426A S428A S431A) mutants treated with 250 nM Torin1 for 1 hr were analyzed by immunoblotting.

## Figure 3

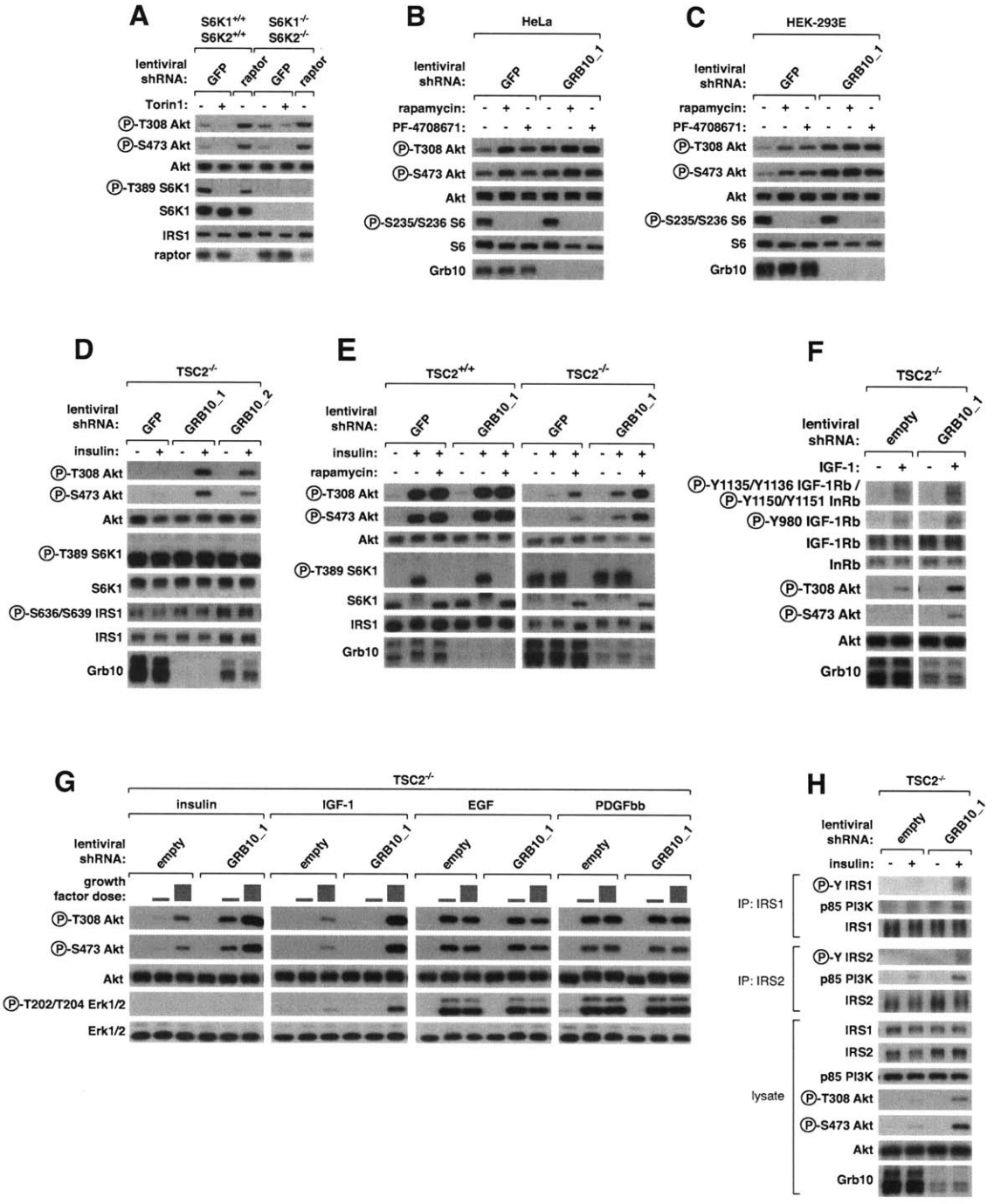
A
S6K1+/+ S6K2+/+
S6K1-/- S6K2-/-
lentiviral shRNA:
GFP
raptor
GFP
raptor
Torin1:
Ⓟ-T308 Akt
Ⓟ-S473 Akt
Akt
Ⓟ-T389 S6K1
S6K1
IRS1
raptor
B
HeLa
lentiviral shRNA:
GFP
GRB10_1
rapamycin:
PF-4708671:
Ⓟ-T308 Akt
Ⓟ-S473 Akt
Akt
Ⓟ-S235/S236 S6
S6
Grb10
C
HEK-293E
lentiviral shRNA:
GFP
GRB10_1
rapamycin:
PF-4708671:
Ⓟ-T308 Akt
Ⓟ-S473 Akt
Akt
Ⓟ-S235/S236 S6
S6
Grb10
D
TSC2-/-
lentiviral shRNA:
GFP
GRB10_1
GRB10_2
insulin:
Ⓟ-T308 Akt
Ⓟ-S473 Akt
Akt
Ⓟ-T389 S6K1
S6K1
Ⓟ-S636/S639 IRS1
IRS1
Grb10
E
TSC2+/+
TSC2-/-
lentiviral shRNA:
GFP
GRB10_1
GFP
GRB10_1
insulin:
rapamycin:
Ⓟ-T308 Akt
Ⓟ-S473 Akt
Akt
Ⓟ-T389 S6K1
S6K1
IRS1
Grb10
F
TSC2-/-
lentiviral shRNA:
empty
GRB10_1
IGF-1:
Ⓟ-Y1135/Y1136 IGF-1Rb /
Ⓟ-Y1150/Y1151 InRb
Ⓟ-Y980 IGF-1Rb
IGF-1Rb
InRb
Ⓟ-T308 Akt
Ⓟ-S473 Akt
Akt
Grb10
G
TSC2-/-
insulin
IGF-1
EGF
PDGFbb
lentiviral shRNA:
empty
GRB10_1
growth factor dose:
Ⓟ-T308 Akt
Ⓟ-S473 Akt
Akt
Ⓟ-T202/T204 Erk1/2
Erk1/2
H
TSC2-/-
lentiviral shRNA:
empty
GRB10_1
insulin:
IP: IRS1
Ⓟ-Y IRS1
p85 PI3K
IRS1
IP: IRS2
Ⓟ-Y IRS2
p85 PI3K
IRS2
lysate
IRS1
IRS2
p85 PI3K
Ⓟ-T308 Akt
Ⓟ-S473 Akt
Akt
Grb10

**Figure 3. Grb10 is important for feedback inhibition from mTORC1 to PI3K-Akt.**

(A) S6K1-/- S6K2-/- or control cells expressing short hairpin RNA (shRNA) constructs against GFP or raptor were treated with 250 nM Torin1 for 1 hr, and lysates were analyzed by immunoblotting. (B) HEK-293E and (C) HeLa cells expressing shRNAs against GFP or human Grb10 were treated for 100 nM rapamycin, 10 $\mu$M PF-4708671 (an S6K inhibitor), or vehicle control for 1 hr, and lysates were analyzed by immunoblotting. (D) TSC2+/+ and TSC2-/- MEFs expressing shRNAs against GFP or mouse Grb10 were starved for 4 hrs, treated with rapamycin or vehicle control for 1 hr, and then stimulated with 100nM insulin where indicated for 15 min and analyzed by immunoblotting. (E) TSC2+/+ and TSC2-/- MEFs expressing shRNAs against GFP or mouse Grb10 were starved for 4 hrs, treated with rapamycin or vehicle control for 1 hr, and then stimulated with 100nM insulin where indicated for 15 min and analyzed by immunoblotting. (F) TSC2-/- MEFs expressing either an empty vector or shRNA against Grb10 were starved for 4 hrs and then stimulated where indicated with 10 or 100 nM insulin, 10 or 100 ng/ml IGF-1, 10 or 100 ng/ml EGF, or 10 or 100 ng/ml PDGFbb for 15 minutes analyzed by immunoblotting. (G) TSC2-/- MEFs expressing shRNAs against GFP or mouse Grb10 were serum starved for 4 hrs and then stimulated where indicated with 100 ng/ml IGF-1 for 15 min and analyzed by immunoblotting. (H) TSC2-/- MEFs expressing a control shRNA or shRNA against Grb10 were treated as in (D). IRS1 and IRS2 immunoprecipitates and cell lysates were analyzed by immunoblotting.

**Figure 4**

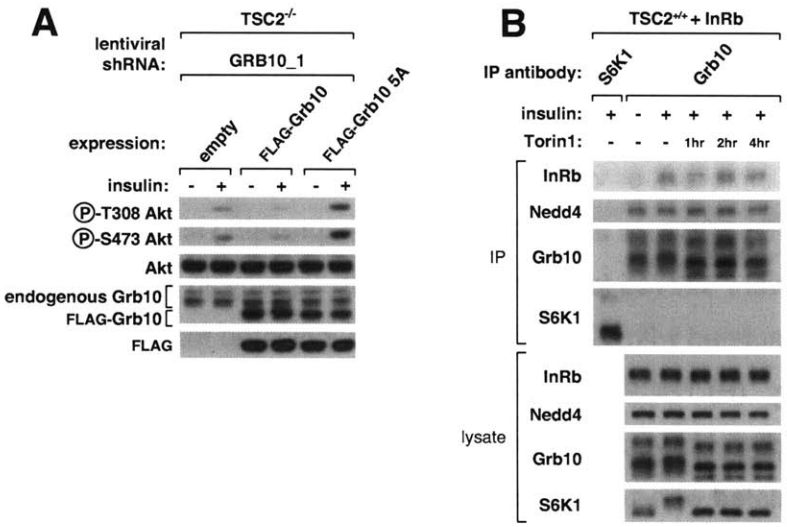
A
TSC2-/-
lentiviral shRNA:
GRB10_1
expression:
empty
FLAG-Grb10
FLAG-Grb10 5A
insulin: - + - + - +
Ⓟ-T308 Akt
Ⓟ-S473 Akt
Akt
endogenous Grb10
FLAG-Grb10
FLAG
B
TSC2+/+ + InRb
IP antibody:
S6K1
Grb10
insulin: + - + + + +
Torin1: - - - 1hr 2hr 4hr
IP
InRb
Nedd4
Grb10
S6K1
lysate
InRb
Nedd4
Grb10
S6K1

**Figure 4. Phosphorylation is important for Grb10 function, but not binding to the receptor.**

(A) TSC2-/- MEFs coexpressing an shRNA against the mouse Grb10 3'UTR and an empty vector, FLAG-Grb10, or 5A cDNA expression construct were starved for 4 hrs, treated with rapamycin or vehicle control for 1 hr, and then stimulated with 100 nM insulin where indicated for 15 min and analyzed by immunoblotting. (B) TSC2+/+ MEFs over-expressing the insulin receptor were starved overnight and then treated with 250 nM Torin1 for the indicated times and then stimulated with 100 nM insulin for 15 min. Endogenous Grb10 and control S6K1 immunoprecipitates and cell lysates were analyzed by immunoblotting.

## Figure 5

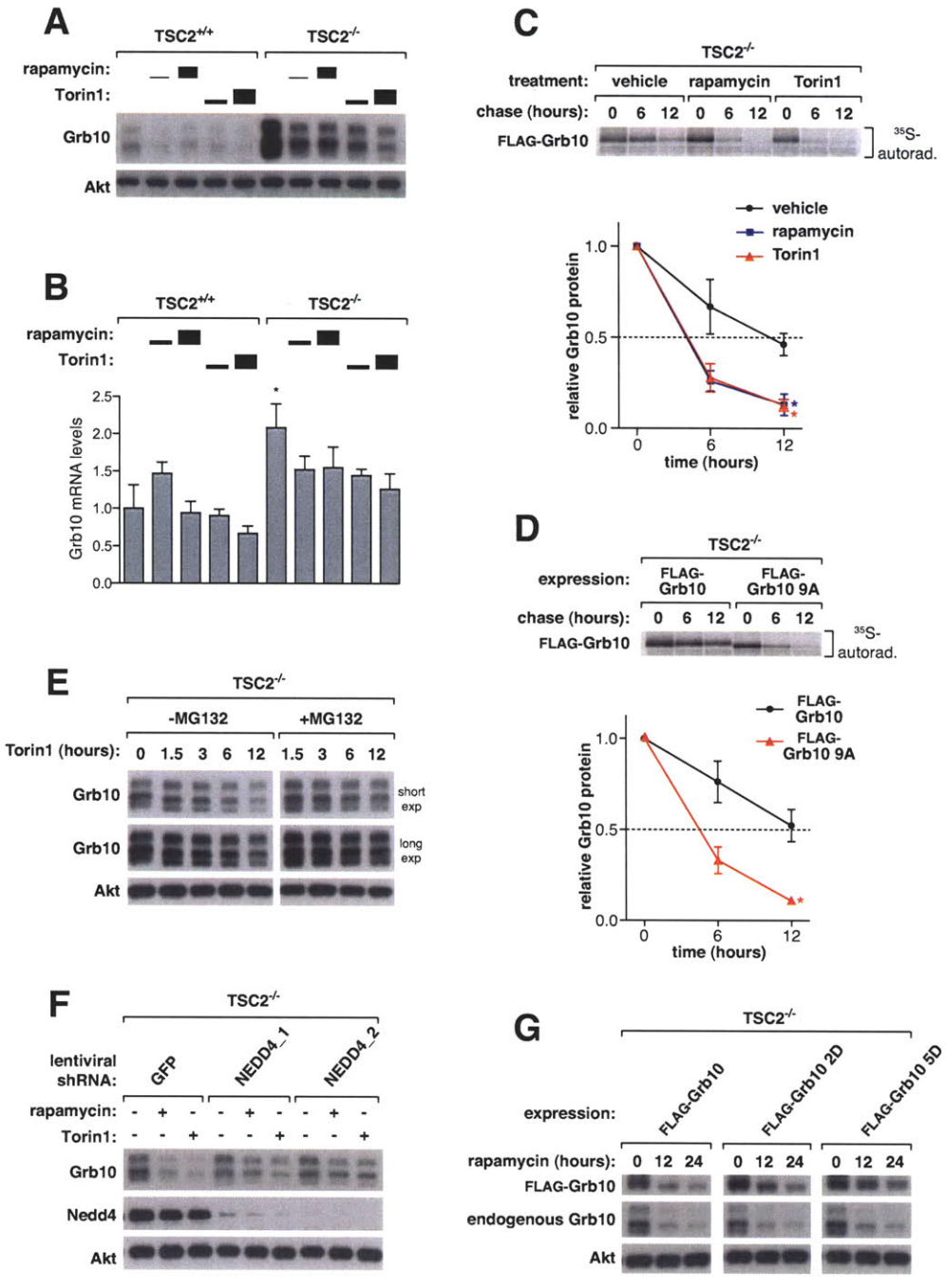
A
TSC2+/+
TSC2-/-
rapamycin:
Torin1:
Grb10
Akt
B
TSC2+/+
TSC2-/-
rapamycin:
Torin1:
Grb10 mRNA levels
2.5
2.0
1.5
1.0
0.5
0.0
C
TSC2-/-
treatment:
vehicle
rapamycin
Torin1
chase (hours):
0 6 12 0 6 12 0 6 12
FLAG-Grb10
35S-
autorad.
vehicle
rapamycin
Torin1
relative Grb10 protein
1.0
0.5
0.0
0
6
12
time (hours)
D
TSC2-/-
expression:
FLAG-Grb10
FLAG-Grb10 9A
chase (hours):
0 6 12 0 6 12
FLAG-Grb10
35S-
autorad.
FLAG-Grb10
FLAG-Grb10 9A
relative Grb10 protein
1.0
0.5
0.0
0
6
12
time (hours)
E
TSC2-/-
-MG132
+MG132
Torin1 (hours):
0 1.5 3 6 12 1.5 3 6 12
Grb10
short exp
Grb10
long exp
Akt
F
TSC2-/-
lentiviral shRNA:
GFP
NEDD4_1
NEDD4_2
rapamycin:
- + - - + - - + -
Torin1:
- - + - - + - - +
Grb10
Nedd4
Akt
G
TSC2-/-
expression:
FLAG-Grb10
FLAG-Grb10 2D
FLAG-Grb10 5D
rapamycin (hours):
0 12 24 0 12 24 0 12 24
FLAG-Grb10
endogenous Grb10
Akt

**Figure 5. mTORC1 phosphorylation stabilizes Grb10.**

(A) Abundance of Grb10 in TSC2+/+ and TSC2-/- MEFs treated with 10 or 100 nM rapamycin, Torin1, or vehicle control for 24 hrs. Cells were lysed and analyzed by immunoblotting. (B) RNA was isolated from TSC2+/+ and TSC2-/- MEFs treated as in (A). Grb10 mRNA was measured by qRT-PCR and normalized to the level of Rplp0 mRNA. Data are means ± s.e.m. (n=7); *Mann-Whitney t-test p-value < 0.05 for differences between vehicle treated TSC2+/+ and TSC2-/- MEFs. Other comparisons are not significant. (C) TSC2-/- MEFs stably expressing FLAG-Grb10 were labeled for 2 hours with [35S]cysteine and methionine and then chased for the indicated times in the presence of vehicle control, 100 nM rapamycin, or 100 nM Torin1. FLAG-immunoprecipitates were analyzed by autoradiography. Data are means ± s.e.m (n=3). *Two-way ANOVA p-values < 0.05 for differences between vehicle and inhibitor treatment. (D) TSC2-/- MEFs stably expressing FLAG-Grb10 or 9A mutant were treated and analyzed as in (C) but without inhibitor treatment. (E) Abundance of Grb10 in TSC2-/- MEFs treated with 100nM Torin1 or vehicle control for the indicated number of hrs in the absence or presence of 10 $\mu$M MG132. Cells were lysed and analyzed by immunoblotting. (F) Abundance of Grb10 in TSC2-/- MEFs expressing shRNAs against GFP or mouse Nedd4 and treated with 100 nM rapamycin, Torin1, or vehicle control for 24 hrs. Cells were lysed and analyzed by immunoblotting. (G) Abundance of endogenous Grb10 or exogenous FLAG-Grb10 in TSC2-/- stably expressing FLAG-Grb10, 2D (S474D S476 D), or 5D (S150D T155D S158D S474D S476D) mutants treated with 20 nM rapamycin or vehicle control for the indicated lengths of time. Cells were lysed and analyzed by immunoblotting.

**Figure 6**

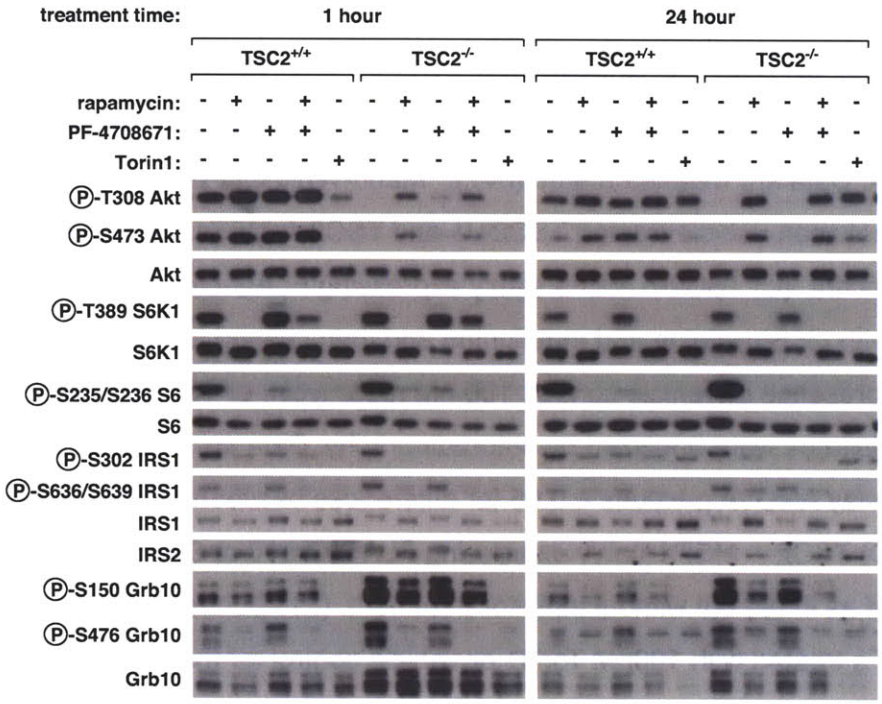
treatment time:
1 hour
24 hour
TSC2+/+
TSC2-/-
TSC2+/+
TSC2-/-
rapamycin: - + - + - - + - + - - + - + - - + - + -
PF-4708671: - - + + - - - + + - - - + + - - - + + -
Torin1: - - - - + - - - - + - - - - + - - - - +
Ⓟ-T308 Akt
Ⓟ-S473 Akt
Akt
Ⓟ-T389 S6K1
S6K1
Ⓟ-S235/S236 S6
S6
Ⓟ-S302 IRS1
Ⓟ-S636/S639 IRS1
IRS1
IRS2
Ⓟ-S150 Grb10
Ⓟ-S476 Grb10
Grb10

**Figure 6. mTORC1, but not S6K1, inhibition results in rescue of Akt signaling in TSC2-null cells.**

TSC2+/+ and TSC2-/- MEFs expressing shRNA constructs against GFP or Grb10 were starved for one or 24 hrs in the presence of 100 nM rapamycin, 10 $\mu$M PF-4708671, 100 nM Torin1, or vehicle control as indicated, and then all samples were stimulated with 100 nM insulin for 15 min and analyzed by immunoblotting.

**Figure 7**

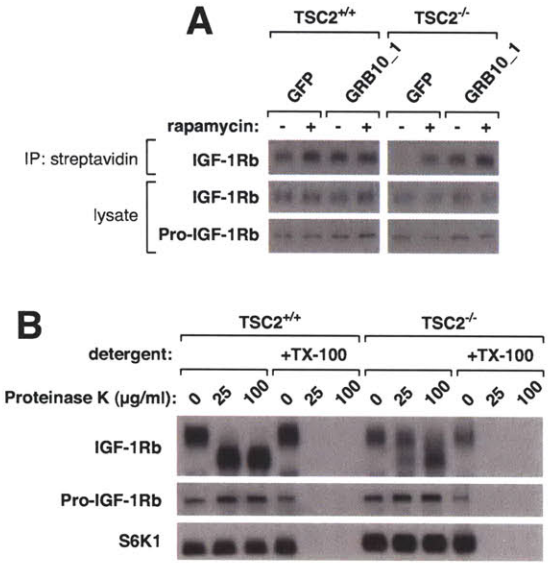
A
TSC2+/+
TSC2-/-
GFP
GRB10_1
GFP
GRB10_1
rapamycin: - + - + - + - +
IP: streptavidin
IGF-1Rb
lysate
IGF-1Rb
Pro-IGF-1Rb
B
TSC2+/+
TSC2-/-
detergent:
+TX-100
+TX-100
Proteinase K (µg/ml): 0 25 100 0 25 100 0 25 100 0 25 100
IGF-1Rb
Pro-IGF-1Rb
S6K1

**Figure 7. mTORC1 hyperactivation leads to Grb10-mediated sequestration of growth factor receptors inside the cell.**

(A) TSC2+/+ and TSC2-/- MEFs expressing shRNA constructs against GFP or Grb10 were treated for 1 hr with 100 nM rapamycin. Cell surface proteins were biotinylated, and then cells were lysed. Biotinylated proteins were isolated by affinity purification with streptavidin and analyzed, along with cell lysates, by immunoblotting. (B) TSC2+/+ and TSC2-/- MEFs growing in replete media were treated with Proteinase K at the indicated concentrations for 30 min, either in the presence or absence of 1% Triton X-100. Lysates were immediately boiled in sample buffer and analyzed by immunoblotting.

**Figure 8**

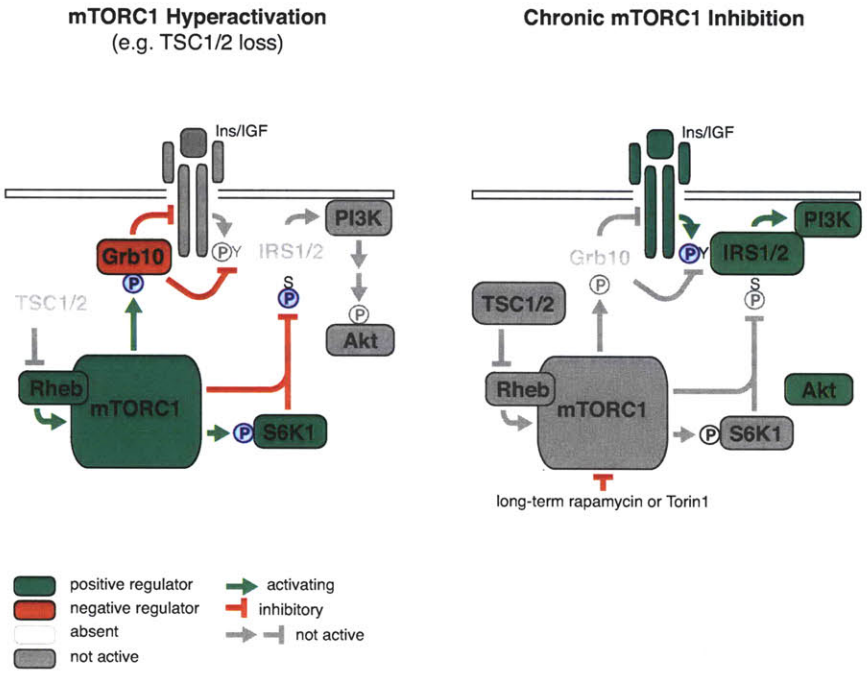
mTORC1 Hyperactivation
(e.g. TSC1/2 loss)
Chronic mTORC1 Inhibition
Ins/IGF
PI3K
Grb10
IRS1/2
TSC1/2
Rheb
mTORC1
S6K1
Akt
long-term rapamycin or Torin1
positive regulator
negative regulator
absent
not active
activating
inhibitory
not active

**Figure 8. mTORC1 inhibits PI3K-Akt signaling through effects on IRS and Grb10 function and stability.**

mTORC1 hyperactivation results in acute increases in IRS1, IRS2, and Grb10 phosphorylation which stabilize Grb10 and destabilize the IRS proteins, leading to insulin and IGF-1 resistance. Acute mTORC1 inhibition results decreased phosphorylation of IRS and Grb10 proteins while chronic mTORC1 inhibition, either by rapamycin or kinase domain inhibitors, result in IRS protein stabilization and Grb10 destabilization.

## Materials and Methods

### Materials

Reagents were obtained from the following sources: antibodies to phospho-T389 S6K1, phospho-S235/S236 S6, phospho-T37/T46 4E-BP1, phospho-S65 4E-BP1, phosho-T308 Akt, phospho-S473 Akt, phospho-S302 IRS1, phospho-S636/S639 IRS1, phospho-T202/T204 Erk1/2, phospho-tyrosine, phospho-Y1135/1136 IGF1-Rb/phospho-Y1150/Y1151 InRb, phospho-Y1131 IGF-1Rb/phospho-Y1146 InRb, phospho-Y980 IGF-1Rb, phospho-S150 Grb10, phospho-S428 Grb10, phospho-S476 Grb10, Akt, S6K1, 4E-BP1, TSC2, FLAG, rictor, IRS1, IRS2, Nedd4, Erk1/2, IGF-1R, InR, p85 PI3K, and human Grb10 from Cell Signaling Technology; an antibody to mouse Grb10 and HRP-labeled anti-mouse and anti-rabbit secondary antibodies from Santa Cruz Biotechnology; an antibody to IRS1 from Upstate/Millipore; FLAG M2 affinity gel, ATP, staurosporine, FKBP12, L-glutathione, amino acids, insulin, IGF-1, EGF, and PDGFbb from Sigma-Aldrich; CIP from New England Biolabs, MG-132 from Calbiochem; [[γ-32P]ATP and [35S]cysteine and methionine from Perkin-Elmer; FuGENE 6, PhosSTOP, and Complete Protease Cocktail from Roche; rapamycin from LC Laboratories, PF-4708671 from Tocris Bioscienes, Proteinase K from EMD Chemicals, DMEM from SAFC Biosciences; Inactivated Fetal Calf Serum (IFS), MagicMedia E. coli expression medium and SimplyBlue Coomassie G from Invitrogen, amino acid-free RPMI from US Biological, Superose 6 10/300 GL and HiLoad 16/60 Superdex 200 from GE Healthcare; sulfo-NHS-LC-Biotin, BCA assay reagent, protein G-sepharose, streptavidin-agarose, and immobilized glutathione beads from Pierce; Ni-NTA agarose from Qiagen; QuikChange XLII mutagenesis kit and BL21(DE3) Competent Cells from Stratagene. Torin1 was provided by Nathanael Gray (Harvard Medical School) (Thoreen et al., 2009).

**cDNA manipulations and mutagenesis**

The cDNA for human GRB10 (NCBI NM_001001550.2 isoform c) in the pOTB7vector was obtained from OpenBiosystems. The GRB10 cDNA was amplified by PCR, and the product was subcloned into the Sal1 and Not1 sites of FLAG-pRK5 for transient expression, the XhoI and NotI sites of the pMSCV retroviral vector for stable expression, or the Xba1 and Xho1 sites of pET303/CT-His vectors for bacterial expression. The INR and IGF1R cDNAs were also cloned by a multi-step process into the MCS of pMSCV. The HA-GST-S6K1-pRK5 and GST-4E-BP1-pGEX-4T constructs were described previously (Burnett et al., 1998; Sancak et al., 2007).

The Grb10-pMSCV and HA-GST-S6K1-pRK5 were mutagenized with the QuikChange XLII mutagenesis kit with oligonucleotides obtained from Integrated DNA Technologies. The Grb10 mutants used in our experiments are (amino acid numbering according to NCBI NM_005311.4 isoform a although all clones used in this study are the human isoform c): 5A = S150A T155A S158A S474A S476A Grb10, 9A = S104A S150A T155A S158A S426A S428A S431A S474A S476A, 2D = S474D S476, and 5D = S150D T155D S158D S474D S476D. T229 of S6K1 in the HA-GST-pRK5 vector was mutated to an alanine to attenuate its catalytic activity. All constructs were sequenced verified.

**Cell treatments, lysis, immunoprecipitations, and phosphatase treatment**

For growth factor stimulation, almost confluent cells were rinsed once and incubated in serum-free DMEM for times as indicated in figure legends, and then stimulated for 15 or 20 minutes. Inhibitors and doses of growth factors were added as indicated. Insulin and IGF-1 were most commonly used at 100 or 150nM and 100ng/ml, respectively. Amino acid starvation was done as described previously (Sancak et al., 2010).

Cells rinsed once with ice-cold PBS and lysed in ice-cold lysis buffer (50 mM HEPES [pH 7.4], 40 mM NaCl, 2 mM EDTA, 1 mM orthovanadate, 50 mM NaF, 10 mM pyrophosphate, 10 mM glycerophosphate, and 1% Triton X-100 or 0.3% CHAPS (for immunoprecipitations), and one tablet of EDTA-free protease inhibitors per 25ml. The

soluble fractions of cell lysates were isolated by centrifugation at 13,000 rpm for 10 minutes by centrifugation in a microfuge. For immunoprecipitations, one PhosSTOP tablet was added per 25 ml of CHAPS lysis buffer, and primary antibodies were added and the lysates and incubated with rotation overnight at 4°C. 50% slurry of protein G-sepharose was then added and the incubation continued for an additional 1 hour. Immunoprecipitates were washed three times with lysis buffer containing 150mM NaCl. Immunoprecipitated proteins were denatured by the addition of sample buffer, boiled for 5 minutes, resolved by SDS-PAGE, and analyzed by immunoblotting as previously described (Kim et al., 2002).

For FLAG purification, FLAG M2 affinity resins were washed 2 times in lysis buffer, added to pre-cleared lysates, and incubated with rotation for 2 hours at 4°C. FLAG-Grb10 purified from a 10cm plate of insulin stimulated TSC2+/+ MEFs stably expressing FLAG-Grb10 was phosphatase treated while still bound to FLAG resin. The resin-bound FLAG-Grb10 washed once in 1X NEBuffer 3, divided among the reaction tubes, and incubated in 20µl of buffer alone, buffer with 20 units of CIP, or 20 units of CIP previously inactivated by boiling for 10 minutes for 60 minutes at 37°C. FLAG-Grb10 from serum starved or Torin1-treated cells was incubated in buffer alone. The reactions were stopped with the addition of sample buffer, boiled, and analyzed by immunoblotting.

**mTORC1 kinase assays**

HA-GST-S6K1 (T229A) was purified from transiently transfected HEK-293T cells treated with 250nM Torin1 for one hour and lysed in Triton lysis buffer. The cleared lysates were incubated with glutathione resin for 2 hours at 4°C, eluted as described previously (Sancak et al., 2007), concentrated, quantified, and stored in 50% glycerol at -20°C. BL21(DE3) cells carrying GST-4E-BP1-pGEX-4T were grown in MagicMedia for 24 hours, and lysed by sonication in ice-cold Triton lysis. GST-4E-BP1 purification proceeded as detailed for HA-GST-S6K1, but was further purified by gel filtration using a HiLoad 16/60 Superdex 200 column and stored at -80°C. BL21 (DE3) cells carrying

pET303-Grb10 were grown in MagicMedia for 24 hours, and lysed by sonication in ice-cold His-tag lysis buffer (25 mM Hepes [pH 7.4], 500 mM NaCl, 5 mM Imidazole, 1% Triton + protease inhibitor tablets). The cleared lysate was incubated with Ni-NTA agarose, incubated for 20 minutes at 4°C, washed, eluted in 150 mM imidazole-containing buffer, and further purified by gel filtration using a HiLoad 16/60 Superdex 200 column and stored at -80°C.

mTORC1 was purified from HEK-293T cells stably-expressing FLAG-raptor as described (Yip et al.). Kinase assays were preincubated for 10 minutes at 4°C before addition of ATP, and then for 30 minutes at 30°C in a final volume of 20µl consisting of: kinase buffer (25 mM HEPES, pH 7.4, 50 mM KCl, 10 mM MgCl2, 1uM staurosporine), active mTORC1, 500 nM substrate, 50 uM ATP, 2 µCi [[γ-32P]ATP, and when indicated 250 nM Torin1 or 250nM rapamycin/FKBP12. Samples were stopped by the addition of 10 µl of sample buffer, boiled for 5 minutes, and analyzed by SDS-PAGE followed by autoradiography.

**Grb10 phosphorylation site mapping**

mTORC1 kinase assays were performed as detailed above, except with a one hour reaction time and in the presence of 500 µM cold ATP. For the in vitro kinase assay samples, urea was added to a final concentration of 1.6M. Proteins were reduced with 10 mM DTT at 56 °C for 30 min., alkylated with 55 mM iodoacetamide for 1hr at room temperature in the dark, then digested with trypsin at 37 °C overnight. The solution was then acidified with 10% TFA. Peptides were extracted using c18 ZipTip, were lyophilized to dryness, and were stored at -80 °C until needed. A third of each sample was analyzed by LC/MS/MS on an orbitrap velos mass spectrometer in data-dependent mode. Identified phosphopeptides were manually validated and combined into a single list. A targeted MS method was then created to perform MS/MS on those selected phosphopeptides, as well as the top 5 most abundant precursors in each cycle. The in vitro kinase samples were then re-analyzed with the targeted MS method. Peak intensity values of extract ion chromatogram were obtained for both the

phosphorylated and unphosphorylated forms. Their ratios were used to compare the phosphorylation level in different samples. FLAG-Grb10 immunoprecipitates from HEK-293E cells stably expressing Grb10 were separated on SDS-PAGE and stained with Coomassie. The bands corresponding to Grb10 were excised and digested in situ. Peptides were extracted and analyzed using the targeted MS method. Phosphorylation levels on identified phosphopeptides were estimated as described above. p-values were determined by a one-tailed Mann-Whitney t-test.

**Antibody detection of Grb10**

The human Grb10 antibody (CST) detects one isoform of Grb10 while the mouse Grb10 antibody detects multiple isoforms (Santa Cruz). Phosphospecific antibodies against S150, S428, and S476 of Grb10 were provided as bleeds from Cell Signaling Technology. All work well on immunoprecipitated proteins, and the antibodies against S150 and S476 work well on mouse lysates.

**Lentiviral shRNAs**

TRC lentiviral shRNAs targeting Grb10 and Nedd4 were obtained from the RNAi consortium (Broad Institute of MIT and Harvard) (Moffat et al., 2006). The TRC identifications for each shRNA are as follows:

Human GRB10 shRNA #1: TRCN0000063686; NM_001001549.1-1459s1c1
Human GRB10 shRNA #2: TRCN0000063687; NM_001001549.1-524s1c1
Mouse Grb10 shRNA #1: TRCN0000109915; NM_010345.2-2392s1c1
Mouse Grb10 shRNA #2: TRCN0000109917; NM_010345.2-1841s1c1
Mouse Nedd4 shRNA #1: TRCN000009235; XM_486230.1-2082s1c1
Mouse Nedd4 shRNA #2: TRCN0000092436; XM_486230.1-1319s1c1

The shGFP control shRNA and the shRNA targeting mouse raptor were previously described and validated (Sarbassov et al., 2005; Thoreen et al., 2009). The

mouse Grb10 shRNAs were also additionally cloned into a pLKO.1 derivative, pLKO_TRC016, obtained from the RNAi consortium (Broad Institute of MIT and Harvard) with a blasticidin resistance gene. Virus production was performed as previously described (Sarbassov et al., 2005). Virus-containing supernatants were collected 48 hours after transfection, filtered to eliminated cells, and target cells were infected in the presence of 8 µg/ml polybrene. 24 hours later, cells were selected with puromycin or blasticidin and analyzed starting at the 3rd day after infection. Grb10 knockdown cells were passaged with persistent antibiotic selection.

For replacement of endogenous murine Grb10 with human Grb10 isoform c, TSC2-/- p53-/- MEFs were infected with retroviruses (pMSCV) expressing empty vector, FLAG-Grb10, FLAG-Grb10 5A, or FLAG-Grb10 9A mutants, and selected for 4 days in puromycin. The resulting stable cell lines were subsequently infected with lentiviruses expressing either the control hairpin or mouse Grb10 shRNA #1 that recognizes the mouse Grb10 3' untranslated region, but not the human cDNA. Cells were then kept in puromycin and additionally selected in blasticidin, and analyzed starting at the 7th day after lentiviral infection. Grb10 replacement cells were passaged with persistent dual antibiotic selection.

**Pulse chase**

Cells were labeled with 1 mCi [35S]methionine/cysteine (1175 Ci/mmol; PerkinElmer Life Sciences) in 15ml methionine- and cysteine-free DMEM at 37 °C for 2 hours and chased with DMEM and 10% IFS supplemented with nonradiolabeled methionine (2.5 mM) and cysteine (0.5 mM) at 37 °C for the indicated times. mTOR inhibitors were added to the chase as indicated. Cells were lysed in 1% SDS in PBS. Immunoprecipitations were performed in Nonidet P-40 lysis buffer (50 mM Tris [pH 7.5], 150 mM NaCl, 5 mM EDTA, 0.5% NP-40, and protease inhibitors) with 0.1% SDS and 30 µl of anti-FLAG M2-agarose for 3 hr at 4 °C. Immunoprecipitates were boiled in sample buffer, subjected to 10% SDS-PAGE, and visualized by autoradiography or quantified by PhosphorImaging. p-values were determined by a two-way ANOVA.

**Grb10 mRNA expression analysis**

For quantification of Grb10 mRNA expression, total RNA was isolated from cells grown in the indicated conditions and reverse-transcription was performed. The resulting cDNA was diluted in DNase-free water (1:100) before quantification by real-time PCR. Data are expressed as the ratio between the expression of Grb10 and the housekeeping gene Rplp0. p-values were determined by a two-tailed Mann-Whitney t-test.

The following primers were used for quantitative real-time PCR:
Grb10 (M. musculus):
Forward: ACAGGATCATCAAGCAACAA
Reverse: TCTTTGTGAAGTCCAATAAC
Rplp0 (M. musculus):
Forward: TAAAGACTGGAGACAAGGTG
Reverse: GTGTACTCAGTCTCCACAGA

**Cell-surface biotinylation and proteinase K cleavage assays**

For cell surface biotinylation, cells in 6 cm plates were put on ice and then washed two times in cold PBS+. They were then incubated in PBS containing 1 mg/ml sulfo-NHS-LC-Biotin for 30 min at 4°C. The cells were then washed three times in cold PBS containing 100mM glycine, once with PBS, and then lysed in 1% Triton lysis buffer. The cleared lysates were incubated with strepatividin-agarose beads for at least 1 hr at 4°C. The beads were washed in lysis buffer and then boiled in sample buffer.

For protease cleavage and protection assays, cells in 6-well dishes were put on ice and then washed once in cold PBS+. Cells were then covered in 250 µl of cold PBS + with proteinase K (25 or 100 µg/ml) and incubated with rocking for 30 min at 4°C. 5 mM PMSF was added for 5 min to stop the reaction. The cell/PBS mixture was then transferred to microcentrifuge tubes (either by scraping or pipetting if cells had detached) and then boiled with sample buffer supplemented with PMSF.

## Acknowledgments

We thank members of the Sabatini Lab for helpful discussion and especially thank H. Keys, K. Birsoy, N. Kory, C. Thoreen, D. Wagner , and J. Claessen for assistance with technical or conceptual aspects of this project. This work was supported by the National Institutes of Health (CA103866 and AI47389 to D.M.S.), Department of Defense (W81XWH-07-0448 to D.M.S.), the W.M. Keck Foundation (D.M.S.), LAM Foundation (D.M.S.), and the American Cancer Society (S.A.K.). D.M.S. is an investigator of the Howard Hughes Medical Institute.

## References

Abu-Amero, S., Monk, D., Frost, J., Preece, M., Stanier, P., and Moore, G.E. (2008). The genetic aetiology of Silver-Russell syndrome. J Med Genet 45, 193-199.

Burnett, P.E., Barrow, R.K., Cohen, N.A., Snyder, S.H., and Sabatini, D.M. (1998). RAFT1 phosphorylation of the translational regulators p70 S6 kinase and 4E-BP1. Proc Natl Acad Sci U S A 95, 1432-1437.

Cao, X.R., Lill, N.L., Boase, N., Shi, P.P., Croucher, D.R., Shan, H., Qu, J., Sweezer, E.M., Place, T., Kirby, P.A., et al. (2008). Nedd4 controls animal growth by regulating IGF-1 signaling. Sci Signal 1, ra5.

Charalambous, M., Smith, F.M., Bennett, W.R., Crew, T.E., Mackenzie, F., and Ward, A. (2003). Disruption of the imprinted Grb10 gene leads to disproportionate overgrowth by an Igf2-independent mechanism. Proc Natl Acad Sci U S A 100, 8292-8297.

Choo, A.Y., Yoon, S.O., Kim, S.G., Roux, P.P., and Blenis, J. (2008). Rapamycin differentially inhibits S6Ks and 4E-BP1 to mediate cell-type-specific repression of mRNA translation. Proc Natl Acad Sci U S A 105, 17414-17419.

Efeyan, A., and Sabatini, D.M. (2010). mTOR and cancer: many loops in one pathway. Curr Opin Cell Biol 22, 169-176.

Faivre, S., Kroemer, G., and Raymond, E. (2006). Current development of mTOR inhibitors as anticancer agents. Nat Rev Drug Discov 5, 671-688.

Feldman, M.E., Apsel, B., Uotila, A., Loewith, R., Knight, Z.A., Ruggero, D., and Shokat, K.M. (2009). Active-site inhibitors of mTOR target rapamycin-resistant outputs of mTORC1 and mTORC2. PLoS Biol 7, e38.

Fouladkou, F., Landry, T., Kawabe, H., Neeb, A., Lu, C., Brose, N., Stambolic, V., and Rotin, D. (2008). The ubiquitin ligase Nedd4-1 is dispensable for the regulation of PTEN stability and localization. Proceedings of the National Academy of Sciences of the United States of America 105, 8585-8590.

Frantz, J.D., Giorgetti-Peraldi, S., Ottinger, E.A., and Shoelson, S.E. (1997). Human GRB-IRbeta/GRB10. Splice variants of an insulin and growth factor receptor-binding

protein with PH and SH2 domains. The Journal of biological chemistry 272, 2659-2667.

Garfield, A.S., Cowley, M., Smith, F.M., Moorwood, K., Stewart-Cox, J.E., Gilroy, K., Baker, S., Xia, J., Dalley, J.W., Hurst, L.D., et al. (2011). Distinct physiological and behavioural functions for parental alleles of imprinted Grb10. Nature 469, 534-538.

Giovannone, B., Lee, E., Laviola, L., Giorgino, F., Cleveland, K.A., and Smith, R.J. (2003). Two novel proteins that are linked to insulin-like growth factor (IGF-I) receptors by the Grb10 adapter and modulate IGF-I signaling. The Journal of biological chemistry 278, 31564-31573.

Hansen, H., Svensson, U., Zhu, J., Laviola, L., Giorgino, F., Wolf, G., Smith, R.J., and Riedel, H. (1996). Interaction between the Grb10 SH2 domain and the insulin receptor carboxyl terminus. The Journal of biological chemistry 271, 8882-8886.

Harrington, L.S., Findlay, G.M., Gray, A., Tolkacheva, T., Wigfield, S., Rebholz, H., Barnett, J., Leslie, N.R., Cheng, S., Shepherd, P.R., et al. (2004). The TSC1-2 tumor suppressor controls insulin-PI3K signaling via regulation of IRS proteins. J Cell Biol 166, 213-223.

He, W., Rose, D.W., Olefsky, J.M., and Gustafson, T.A. (1998). Grb10 interacts differentially with the insulin receptor, insulin-like growth factor I receptor, and epidermal growth factor receptor via the Grb10 Src homology 2 (SH2) domain and a second novel domain located between the pleckstrin homology and SH2 domains. The Journal of biological chemistry 273, 6860-6867.

Holt, L.J., and Siddle, K. (2005). Grb10 and Grb14: enigmatic regulators of insulin action--and more? Biochem J 388, 393-406.

Jacinto, E., Loewith, R., Schmidt, A., Lin, S., Ruegg, M.A., Hall, A., and Hall, M.N. (2004). Mammalian TOR complex 2 controls the actin cytoskeleton and is rapamycin insensitive. Nat Cell Biol 6, 1122-1128.

Kasus-Jacobi, A., Perdereau, D., Auzan, C., Clauser, E., Van Obberghen, E., Mauvais-Jarvis, F., Girard, J., and Burnol, A.F. (1998). Identification of the rat adapter Grb14 as an inhibitor of insulin actions. The Journal of biological chemistry 273, 26026-26035.

Kim, D.H., Sarbassov, D.D., Ali, S.M., King, J.E., Latek, R.R., Erdjument-Bromage, H., Tempst, P., and Sabatini, D.M. (2002). mTOR interacts with raptor to form a nutrient-sensitive complex that signals to the cell growth machinery. Cell 110, 163-175.

Laplante, M., and Sabatini, D.M. (2009). mTOR signaling at a glance. J Cell Sci 122, 3589-3594.

Laviola, L., Giorgino, F., Chow, J.C., Baquero, J.A., Hansen, H., Ooi, J., Zhu, J., Riedel, H., and Smith, R.J. (1997). The adapter protein Grb10 associates preferentially with the insulin receptor as compared with the IGF-I receptor in mouse fibroblasts. The Journal of clinical investigation 99, 830-837.

Liu, F., and Roth, R.A. (1995). Grb-IR: a SH2-domain-containing protein that binds to the insulin receptor and inhibits its function. Proceedings of the National Academy of Sciences of the United States of America 92, 10287-10291.

Moffat, J., Grueneberg, D.A., Yang, X., Kim, S.Y., Kloepfer, A.M., Hinkle, G., Piqani, B., Eisenhaure, T.M., Luo, B., Grenier, J.K., et al. (2006). A lentiviral RNAi library for human and mouse genes applied to an arrayed viral high-content screen. Cell 124, 1283-1298.

Monami, G., Emiliozzi, V., and Morrione, A. (2008). Grb10/Nedd4-mediated multiubiquitination of the insulin-like growth factor receptor regulates receptor internalization. Journal of cellular physiology 216, 426-437.

Morrione, A., Plant, P., Valentinis, B., Staub, O., Kumar, S., Rotin, D., and Baserga, R. (1999). mGrb10 interacts with Nedd4. The Journal of biological chemistry 274, 24094-24099.

O'Neill, T.J., Rose, D.W., Pillay, T.S., Hotta, K., Olefsky, J.M., and Gustafson, T.A. (1996). Interaction of a GRB-IR splice variant (a human GRB10 homolog) with the insulin and insulin-like growth factor I receptors. Evidence for a role in mitogenic signaling. The Journal of biological chemistry 271, 22506-22513.

O'Reilly, K.E., Rojo, F., She, Q.B., Solit, D., Mills, G.B., Smith, D., Lane, H., Hofmann, F., Hicklin, D.J., Ludwig, D.L., et al. (2006). mTOR inhibition induces upstream receptor tyrosine kinase signaling and activates Akt. Cancer Res 66, 1500-1508.

Ooi, J., Yajnik, V., Immanuel, D., Gordon, M., Moskow, J.J., Buchberg, A.M., and Margolis, B. (1995). The cloning of Grb10 reveals a new family of SH2 domain proteins. Oncogene 10, 1621-1630.

Pearce, L.R., Alton, G.R., Richter, D.T., Kath, J.C., Lingardo, L., Chapman, J., Hwang, C., and Alessi, D.R. (2010). Characterization of PF-4708671, a novel and highly specific inhibitor of p70 ribosomal S6 kinase (S6K1). Biochem J 431, 245-255.

Peterson, T.R., Laplante, M., Thoreen, C.C., Sancak, Y., Kang, S.A., Kuehl, W.M., Gray, N.S., and Sabatini, D.M. (2009). DEPTOR is an mTOR inhibitor frequently overexpressed in multiple myeloma cells and required for their survival. Cell 137, 873-886.

Sancak, Y., Bar-Peled, L., Zoncu, R., Markhard, A.L., Nada, S., and Sabatini, D.M. (2010). Ragulator-Rag complex targets mTORC1 to the lysosomal surface and is necessary for its activation by amino acids. Cell 141, 290-303.

Sancak, Y., Thoreen, C.C., Peterson, T.R., Lindquist, R.A., Kang, S.A., Spooner, E., Carr, S.A., and Sabatini, D.M. (2007). PRAS40 is an insulin-regulated inhibitor of the mTORC1 protein kinase. Mol Cell 25, 903-915.

Sarbassov, D.D., Ali, S.M., Kim, D.H., Guertin, D.A., Latek, R.R., Erdjument-Bromage, H., Tempst, P., and Sabatini, D.M. (2004). Rictor, a novel binding partner of mTOR, defines a rapamycin-insensitive and raptor-independent pathway that regulates the cytoskeleton. Curr Biol 14, 1296-1302.

Sarbassov, D.D., Ali, S.M., Sengupta, S., Sheen, J.H., Hsu, P.P., Bagley, A.F., Markhard, A.L., and Sabatini, D.M. (2006). Prolonged rapamycin treatment inhibits mTORC2 assembly and Akt/PKB. Mol Cell 22, 159-168.

Sarbassov, D.D., Guertin, D.A., Ali, S.M., and Sabatini, D.M. (2005). Phosphorylation and regulation of Akt/PKB by the rictor-mTOR complex. Science 307, 1098-1101.

Shah, O.J., Wang, Z., and Hunter, T. (2004). Inappropriate activation of the TSC/Rheb/mTOR/S6K cassette induces IRS1/2 depletion, insulin resistance, and cell survival deficiencies. Curr Biol 14, 1650-1656.

Smith, F.M., Holt, L.J., Garfield, A.S., Charalambous, M., Koumanov, F., Perry, M., Bazzani, R., Sheardown, S.A., Hegarty, B.D., Lyons, R.J., et al. (2007). Mice with a disruption of the imprinted Grb10 gene exhibit altered body composition, glucose homeostasis, and insulin signaling during postnatal life. Mol Cell Biol 27, 5871-5886.

Stein, E.G., Gustafson, T.A., and Hubbard, S.R. (2001). The BPS domain of Grb10 inhibits the catalytic activity of the insulin and IGF1 receptors. FEBS Letters 493, 106-111.

Sun, S.Y., Rosenberg, L.M., Wang, X., Zhou, Z., Yue, P., Fu, H., and Khuri, F.R. (2005). Activation of Akt and eIF4E survival pathways by rapamycin-mediated mammalian target of rapamycin inhibition. Cancer Res 65, 7052-7058.

Takeuchi, H., Kondo, Y., Fujiwara, K., Kanzawa, T., Aoki, H., Mills, G.B., and Kondo, S. (2005). Synergistic augmentation of rapamycin-induced autophagy in malignant glioma cells by phosphatidylinositol 3-kinase/protein kinase B inhibitors. Cancer Res 65, 3336-3346.

Thoreen, C.C., Kang, S.A., Chang, J.W., Liu, Q., Zhang, J., Gao, Y., Reichling, L.J., Sim, T., Sabatini, D.M., and Gray, N.S. (2009). An ATP-competitive mammalian target of rapamycin inhibitor reveals rapamycin-resistant functions of mTORC1. J Biol Chem 284, 8023-8032.

Trotman, L.C., Wang, X., Alimonti, A., Chen, Z., Teruya-Feldstein, J., Yang, H., Pavletich, N.P., Carver, B.S., Cordon-Cardo, C., Erdjument-Bromage, H., et al. (2007). Ubiquitination regulates PTEN nuclear import and tumor suppression. Cell 128, 141-156.

Tzatsos, A., and Kandror, K.V. (2006). Nutrients suppress phosphatidylinositol 3-kinase/Akt signaling via raptor-dependent mTOR-mediated insulin receptor substrate 1 phosphorylation. Molecular and Cellular Biology 26, 63-76.

Um, S.H., Frigerio, F., Watanabe, M., Picard, F., Joaquin, M., Sticker, M., Fumagalli, S., Allegrini, P.R., Kozma, S.C., Auwerx, J., et al. (2004). Absence of S6K1 protects against age- and diet-induced obesity while enhancing insulin sensitivity. Nature 431, 200-205.

Vecchione, A., Marchese, A., Henry, P., Rotin, D., and Morrione, A. (2003). The Grb10/Nedd4 complex regulates ligand-induced ubiquitination and stability of the insulin-like growth factor I receptor. Molecular and Cellular Biology 23, 3363-3372.

Wan, X., Harkavy, B., Shen, N., Grohar, P., and Helman, L.J. (2007). Rapamycin induces feedback activation of Akt signaling through an IGF-1R-dependent mechanism. Oncogene 26, 1932-1940.

Wang, J., Dai, H., Yousaf, N., Moussaif, M., Deng, Y., Boufelliga, A., Swamy, O.R., Leone, M.E., and Riedel, H. (1999). Grb10, a positive, stimulatory signaling adapter in platelet-derived growth factor BB-, insulin-like growth factor I-, and insulin-mediated mitogenesis. Molecular and Cellular Biology 19, 6217-6228.

Wang, L., Balas, B., Christ-Roberts, C.Y., Kim, R.Y., Ramos, F.J., Kikani, C.K., Li, C., Deng, C., Reyna, S., Musi, N., et al. (2007a). Peripheral disruption of the Grb10 gene enhances insulin signaling and sensitivity in vivo. Mol Cell Biol 27, 6497-6505.

Wang, X., Trotman, L.C., Koppie, T., Alimonti, A., Chen, Z., Gao, Z., Wang, J., Erdju-

ment-Bromage, H., Tempst, P., Cordon-Cardo, C., et al. (2007b). NEDD4-1 is a proto-oncogenic ubiquitin ligase for PTEN. Cell 128, 129-139.

Wick, K.R., Werner, E.D., Langlais, P., Ramos, F.J., Dong, L.Q., Shoelson, S.E., and Liu, F. (2003). Grb10 inhibits insulin-stimulated insulin receptor substrate (IRS)-phosphatidylinositol 3-kinase/Akt signaling pathway by disrupting the association of IRS-1/IRS-2 with the insulin receptor. The Journal of biological chemistry 278, 8460-8467.

Yip, C.K., Murata, K., Walz, T., Sabatini, D.M., and Kang, S.A. (2010). Structure of the human mTOR complex I and its implications for rapamycin inhibition. Mol Cell 38, 768-774.

Zhang, H., Cicchetti, G., Onda, H., Koon, H.B., Asrican, K., Bajraszewski, N., Vazquez, F., Carpenter, C.L., and Kwiatkowski, D.J. (2003). Loss of Tsc1/Tsc2 activates mTOR and disrupts PI3K-Akt signaling through downregulation of PDGFR. J Clin Invest 112, 1223-1233.

Zoncu, R., Efeyan, A., and Sabatini, D.M. (2011). mTOR: from growth signal integration to cancer, diabetes and ageing. Nat Rev Mol Cell Biol 12, 21-35.

# Chapter 4

# Future Directions and Conclusions

## Summary

mTOR is a serine-threonine kinase which plays a conserved role in cell growth, proliferation, homeostasis, and metabolism and whose activity is dysregulated in diabetes, genetic hamartoma syndromes, and cancer. Although the understanding of the mechanisms by which various cellular and environmental cues regulate mTOR has accelerated, in contrast, the number of direct substrates has remained a small handful and a mechanistic appreciation of how mTOR executes its functions has often been lacking.

We believe that the work presented in this thesis makes three contributions to the field. First, what is potentially the most exciting advance, is a catalogue of mTOR-regulated phosphorylations, some of which point to processes known to be downstream of mTOR, and many more of which implicate mTOR in processes not presently associated with the pathway. Second, we defined a consensus motif that may aid in the identification of direct substrates and serve as a starting point for understanding how mTOR recognizes its substrates. Finally, we clarified the nature of feedback inhibition, which is often discussed, but poorly understood. In the following chapter, we discuss several questions to emerge from this work.

## Discussion

### How many more mTOR substrates remain to be discovered?

It is a provocative question with an unclear answer. If the complexity of upstream regulation is an indication of a similar complexity of downstream effector pathways, then it is likely that the number of known substrates could be a small fraction of the total. Given that mTOR senses many intracellular and extracellular cues, it would not be surprising if mTOR controls a large number of homeostatic functions. Our results show that mTOR regulates the majority of insulin-stimulated phosphorylations, and so is likely to have additional substrates. Preliminary experiments have indicated that several additional candidate substrates (e.g. LARP1, FOXK1) from our iTRAQ dataset are indeed mTOR-regulated (Peggy Hsu, unpublished results). The significance and function of these mTOR phosphorylations, however, must still be tested.

Besides the phosphorylation sites directly detected through our proteomic efforts, it may be possible to bioinformatically mine our datasets to identify additional downstream effectors. For example, one could examine the remaining phosphorylation sites which were not predicted to be AGC or mTOR sites, and based on known kinase motifs predict which kinases may be activated or inhibitied by mTOR.

It is becoming increasingly clear that even for processes known to be regulated by mTOR, mTOR does so through multiple mechanisms. For example, mTOR is a central regulator of cell growth and size, through the phosphorylation of the inhibitors of the eIF-4E cap-binding protein, 4E-BP1 and 4E-BP2 as well as through S6K1. mTOR also regulates the activity of eEF2K, as well as possibly eIF4G1, both of which we confirmed to be mTOR-regulated in our phosphoproteomic screen. Furthermore, our identification of PATL1 as a putative substrate indicates that mTOR may also regulate the dynamics of P-body formation and mRNA decapping and therefore indirectly the rates at which mRNAs are translated. Turning to autophagy, while the molecular mechanisms are just beginning to be characterized, mTOR phosphorylates both

ULK1 and ATG13. Our data also suggests that the Atg18 homologue WIPI2 may also be a possible substrate. mTORC2 is an important regulator of cell survival and phosphorylates both Akt and SGK, each of which has multiple substrates implicated in apoptosis and cell proliferation. Finally, the identification of Grb10 as an mTORC1 substrate indicates that feedback inhibition occurs through multiple mechanisms: mTORC1 activates S6K1 which inhibits and destabilizes IRS1, and mTORC1 may directly phosphorylate IRS and Grb10 proteins. mTORC1 thereby inhibits an activator and activates an inhibitor of growth factor signaling. Even among processes in which mTOR is already known to play a role, it is likely that mTOR does so through multiple substrates, some of which have yet to be discovered.

**Is the consensus mTOR motif one motif or two?**

It was a great surprise to us to find that mTOR recognizes hydrophobic and aromatic residues at the +1 position, in addition to proline. The structures of known proline-directed kinases and phosphatases are distinct beause the active sites cannot satisfy the hydrogen bonding requirements of other amino acids besides proline (Brown et al., 1999; Gray et al., 2003). Therefore, how mTOR phosphorylates these proline-directed sites in addition to sites with hydrophobic and aromatic residues at the +1 is still a mystery. While others have proposed that mTOR regulates an intermediate proline-directed kinase or phosphatase our in vitro results suggest that mTOR directly phosphorylates these sites. One possible explanation is that the motif is a conflation of two (or more) motifs and that mTOR can exist in two different conformations, one which prefers proline-directed sites, and the other which prefers aromatic and hydrophobic residues. We speculate that basal mTOR activity allows it to phosphorylate +1 hydrophobic residues but fully activated mTOR can act on proline directed sites. One mechanism by which Rheb acts may be to cause a motif switch in the mTOR kinase. Rheb addition in vitro leads to a profound mobility shift in S6K1 (Sancak et al., 2007). These mobility shifts are usually due to proline-directed phosphorylations. It would therefore be interesting to repeat the PSPL screening with mTORC1 purified from cells

grown from replete media but without in vitro Rheb addition. It would also be interesting to see how the presence of FKBP12-rapamycin would affect the mTOR motif. Based on our consensus motif, one could design model peptides to further characterize the motif preference of mTOR. Ultimately, however, structural studies of the kinase domain will be required to fully understand how mTOR phosphorylation occurs.

**What factors determine the sites and proteins phosphorylated by mTOR?**

The definition of a consensus motif for mTOR now allows us to rule-in and rule-out phosphorylation sites from being direct substrates. However, the motif is not restricted enough to allows us to bioinformatically predict mTOR substrates without additional information. mTOR, therefore, must utilize additional "information" to select its substrates. Raptor has already been shown to be important in recognizing the TOR signaling (TOS) motif present in some of its substrates. The other members of the mTOR complexes are likely to play a role. One could potentially mine the sequences of those proteins which we determined to be mTOR-regulated by quantitative mass spectrometry in order to refine the TOS signaling motif. Colocalization and/or compartmentalization are also likely to be factors in determining the accessibility of mTOR to various substrates.

**Does mTORC1 regulate the trafficking of growth factor receptors?**

Our preliminary results indicate that mTORC1 may regulate the localization of the insulin and IGF-1 receptors through Grb10. Additional experiments are required to verify this finding. We had previously tried to directly visualize the receptors by immunofluorescence, but the results were inconclusive. We found that the antibodies to the insulin and IGF-receptors mostly recognized the intracellular portion of the β chain, and therefore the cells needed to be permeabilized before staining. Because the TSC2-null cells are very flat and had been permeabilized, it was difficult to differentiate plasma membranes from internal membranes. To address these problems, we have created different receptor constructs, tagging them on both extracellular and intracellular

domains. These constructs would allow us to use anti-epitope antibodies on cells with and without permeabilization to track the amount of receptor at the surface and total receptor by immunofluorescence or flow cytometry.

mTORC1 is localized to the lysosome, which serves as a signaling platform. mTORC1 is recruited to the lysosome upon amino acid stimulation by the Rag GTPases where it is then activated by Rheb (Sancak et al., 2010; Sancak et al., 2008). One explanation as to why mTORC1 requires lysosomal localization is that amino acid sensing occurs at the lysosome. An alternative idea is that mTORC1 requires membrane localization in order to execute its downstream functions. mTORC1 regulates autophagy, and recent work has shown that mTORC1 localization at the lysosome is coordinated with its regulation of autophagosome-lysosome fusion (Korolchuk et al., 2011). In addition, mTORC1 may also be membrane-localized to regulate the trafficking of growth factors. It would be interesting to test which of mTORC1's substrates or functions require membrane approximation. One could localize mTORC1 and Rheb in Ragulator-null cells to other compartments and assess if some substrates, like S6K1, which are soluble inside the cytoplasm, would therefore still be activated, while other substrates would require mTORC1 localization specifically on the lysosome.

**Will mTOR catalytic domain inhibitors be effective anti-cancer agents?**

Dysregulated growth factor signaling is a hallmark of cancer (Hanahan and Weinberg, 2011). Several anti-cancer therapies target this signaling at the level of the receptor, either through anti-receptor antibodies or catalytic domain inhibition. While we had expected that mTOR might regulate some insulin-stimulated phosphorylations, we were quite surprised to find that a majority of the insulin-stimulated phosphorylation program is mTOR-dependent. Similar kinds of quantitative phosphoproteomic experiments could be performed with additional growth factors or with activation of different growth factor receptors to examine the extent of mTOR involvement in other signaling contexts. Our work with insulin stimulation suggests that mTOR, if fully inhibited, is an effective mimetic of serum deprivation. Our results also confirm that

mTOR catalytic domain inhibitors, at least globally, are better inhibitors of mTOR than rapamycin, as a significant fraction of Torin1-sensitive sites are rapamycin-insensitive.

One thing to keep in mind, however, is that the pathway has ways in which to reactivate signaling under conditions of mTOR inhibition. The feedback loop to PI3K-Akt is one example, as are effects on DEPTOR expression or PDGFR downregulation. While our phosphoproteomic data suggested that acute mTOR inhibition is a mimetic of serum deprivation, our data on Grb10 suggests that chronic mTOR inhibition leads to Grb10 degradation and IRS protein stabilization, effects which lead to reactivation of insulin and IGF-1 pathway signaling and increased phosphorylation of Akt on T308 by PDK1. S473 phosphorylation may also increase if mTORC2 is not sufficiently inhibited. Our data therefore supports the existing idea that mTOR inhibitors in combination with IGF1R inhibition would be more effective as an anti-cancer regimen (O'Reilly et al., 2006; Wan et al., 2007). It would be interesting to define the phosphoproteomic changes which occur with chronic mTOR inhibition. While acute inhibitor treatment is required to identify direct substrates and immediate phosphorylation changes, the effects of chronic mTOR inhibition are likely to be more relevant clinically.

**What determines how cells respond to chronic mTOR inhibition?**

Given that mTOR signaling is upregulated across cancer types, consistent with it being regulated by a diverse array of oncogenes and tumor suppressors, it might be expected that mTOR inhibition could be a universal anti-cancer strategy. However, not all cell types behave similarly when treated with rapamyin or with kinase domain inhibitors. Determining the context in which to employ mTOR inhibitors is the next major hurdle for the field.

Several factors could contribute to the heterogeneity of signaling responses. First, different tissues express varying levels of Grb10, Nedd4, and DEPTOR. The relative contributions of the different components of the feedback loop (i.e. S6K1, IRS1, IRS2, Grb10, mTORC1) may also vary across different cell types. While acute mTOR inhibition leads to dephosphorylation of its substrates, including Grb10 and IRS, not

all cells activate Akt with chronic treatment. Moreover, we found that Torin1 treatment caused a decrease in Grb10 and an increase in IRS proteins (Chapter 3, Fig. 6 and Peggy Hsu, unpublished data), however the magnitude of these abundance changes varied depending on cell type. Cells even have varying amounts of the two complexes basally, and mTORC2 assembly is affected by rapamycin treatment in some cell types but not others. Finally, the combination of oncogenes activated and tumor suppressors lost (e.g. the PTEN/PI3K status of the cell) may determine the effect of mTOR inhibitors on the cell. Ultimately, a systems level approach will be required to tease apart the complexity of the mTOR signaling pathway and to assess which markers may be predictive of response to mTOR inhibitors.

## References

Brown, N.R., Noble, M.E., Endicott, J.A., and Johnson, L.N. (1999). The structural basis for specificity of substrate and recruitment peptides for cyclin-dependent kinases. Nat Cell Biol 1, 438-443.

Gray, C.H., Good, V.M., Tonks, N.K., and Barford, D. (2003). The structure of the cell cycle protein Cdc14 reveals a proline-directed protein phosphatase. EMBO J 22, 3524-3535.

Hanahan, D., and Weinberg, R.A. (2011). Hallmarks of cancer: the next generation. Cell 144, 646-674.

Korolchuk, V.I., Saiki, S., Lichtenberg, M., Siddiqi, F.H., Roberts, E.A., Imarisio, S., Jahreiss, L., Sarkar, S., Futter, M., Menzies, F.M., et al. (2011). Lysosomal positioning coordinates cellular nutrient responses. Nature cell biology.

O'Reilly, K.E., Rojo, F., She, Q.B., Solit, D., Mills, G.B., Smith, D., Lane, H., Hofmann, F., Hicklin, D.J., Ludwig, D.L., et al. (2006). mTOR inhibition induces upstream receptor tyrosine kinase signaling and activates Akt. Cancer Res 66, 1500-1508.

Sancak, Y., Bar-Peled, L., Zoncu, R., Markhard, A.L., Nada, S., and Sabatini, D.M. (2010). Ragulator-Rag complex targets mTORC1 to the lysosomal surface and is necessary for its activation by amino acids. Cell 141, 290-303.

Sancak, Y., Peterson, T.R., Shaul, Y.D., Lindquist, R.A., Thoreen, C.C., Bar-Peled, L., and Sabatini, D.M. (2008). The Rag GTPases bind raptor and mediate amino acid signaling to mTORC1. Science 320, 1496-1501.

Sancak, Y., Thoreen, C.C., Peterson, T.R., Lindquist, R.A., Kang, S.A., Spooner, E., Carr, S.A., and Sabatini, D.M. (2007). PRAS40 is an insulin-regulated inhibitor of the mTORC1 protein kinase. Mol Cell 25, 903-915.

Wan, X., Harkavy, B., Shen, N., Grohar, P., and Helman, L.J. (2007). Rapamycin induces feedback activation of Akt signaling through an IGF-1R-dependent mechanism. Oncogene 26, 1932-1940.

# Appendix

## Cancer Cell Metabolism: Warburg and Beyond

Peggy P. Hsu [1,2] and David M. Sabatini [1,2,3,4]

1 Whitehead Institute for Biomedical Research, Nine Cambridge Center, Cambridge, MA 02142, USA
2 Department of Biology, Massachusetts Institute of Technology (MIT), Cambridge, MA 02139, USA
3 Broad Institute, Cambridge, MA 02142, USA
4 Koch Institute for Integrative Cancer Research at MIT, Cambridge, MA 02139, USA

This work was published in:
Hsu, P.P., and Sabatini, D.M. (2008). Cancer cell metabolism: Warburg and beyond. Cell 134, 703-707.

## Introduction

It is hard to begin a discussion of cancer cell metabolism without first mentioning Otto Warburg. A pioneer in the study of respiration, Warburg made a striking discovery in the 1920s. He found that, even in the presence of ample oxygen, cancer cells prefer to metabolize glucose by glycolysis, a seeming paradox as glycolysis, when compared to oxidative phosphorylation, is a less efficient pathway for producing ATP (Warburg, 1956). The Warburg effect has since been demonstrated in different cancer types and the concomitant increase in glucose uptake has been exploited clinically for the detection of tumors by fluorodeoxyglucose positron emission tomography (FDG-PET). Although aerobic glycolysis has now been generally accepted as a metabolic hallmark of cancer, its causal relationship with cancer progression is still unclear.

In this essay, we discuss the possible drivers, advantages, and potential liabilities of the altered metabolism of cancer cells (Fig. 1). Although our emphasis on the Warburg effect reflects the focus of the field, we would also like to encourage a broader approach to the study of cancer metabolism that takes into account the contributions of all interconnected small molecule pathways of the cell.

## The tumor microenvironment selects for altered metabolism

One compelling idea to explain the Warburg effect is that the altered metabolism of cancer cells confers a selective advantage for survival and proliferation in the unique tumor microenvironment. As the early tumor expands, it outgrows the diffusion limits of its local blood supply, leading to hypoxia and stabilization of the hypoxia-inducible transcription factor, HIF. HIF initiates a transcriptional program that provides multiple solutions to hypoxic stress (reviewed in Kaelin and Ratcliffe, 2008). Because a decreased dependence on aerobic respiration becomes advantageous, cell metabolism is shifted towards glycolysis by the increased expression of glycolytic enzymes, glucose transporters, and inhibitors of mitochondrial metabolism. In addition, HIF stimulates angiogenesis (the formation of new blood vessels) by upregulating several factors,

including most prominently vascular endothelial growth factor (VEGF).

Blood vessels recruited to the tumor microenvironment, however, are disorganized, may not deliver blood effectively, and therefore do not completely alleviate hypoxia (reviewed in Gatenby and Gillies, 2004). The oxygen levels within a tumor vary both spatially and temporally, and the resulting rounds of fluctuating oxygen levels potentially select for tumors that constitutively upregulate glycolysis. Interestingly, with the possible exception of tumors that have lost the von Hippel-Lindau protein (VHL), which normally mediates degradation of HIF, HIF is still coupled to oxygen levels, as evident from the heterogeneity of HIF expression within the tumor microenvironment (Wiesener et al., 2001; Zhong et al., 1999). Therefore, the Warburg effect---that is, an uncoupling of glycolysis from oxygen levels---cannot be explained solely by upregulation of HIF expression. Other molecular mechanisms are likely to be important, such as the metabolic changes induced by oncogene activation and tumor suppressor loss.

**Oncogene activation drives changes in metabolism**

Not only may the tumor microenvironment select for a deranged metabolism, but oncogene status can also drive metabolic changes. Since Warburg's time, the biochemical study of cancer metabolism has been overshadowed by efforts to identify the mutations that contribute to cancer initiation and progression. Recent work, however, has demonstrated that the key components of the Warburg effect---increased glucose consumption, decreased oxidative phosphorylation, and accompanying lactate production---are also distinguishing features of oncogene activation. The signaling molecule Ras, a powerful oncogene when mutated, promotes glycolysis (reviewed in Dang and Semenza, 1999; Ramanathan et al., 2005). Akt kinase, a well-characterized downstream effector of insulin signaling, reprises its role in glucose uptake and utilization in the cancer setting (reviewed in Manning and Cantley, 2007), whereas the Myc transcription factor upregulates the expression of various metabolic genes (reviewed in Gordan et al., 2007). The most parsimonious route to tumorigenesis may be activation of key oncogenic nodes that execute a proliferative program, of which metabolism

may be one important arm. Moreover, regulation of metabolism is not exclusive to oncogenes. Loss of the tumor suppressor protein p53 prevents expression of the gene encoding SCO2 (the synthesis of cytochrome c oxidase protein), which interferes with the function of the mitochondrial respiratory chain (Matoba et al., 2006). A second p53 effector, TIGAR (TP53-induced glycolysis and apoptosis regulator), inhibits glycolysis by decreasing levels of fructose-2,6-bisphosphate, a potent stimulator of glycolysis and inhibitor of gluconeogenesis (Bensaad et al., 2006). Other work also suggests that p53-mediated regulation of glucose metabolism may be dependent on the master transcription factor NF-□B (Kawauchi et al., 2008).

It has been shown that inhibition of lactate dehydrogenase A (LDH-A) prevents the Warburg effect and forces cancer cells to revert to oxidative phosphorylation in order to reoxidize NADH and produce ATP (Fantin et al., 2006; Shim et al., 1997). While the cells are respiratory-competent, they exhibit attenuated tumor growth, suggesting that aerobic glycolysis might be essential for cancer progression. In a primary fibroblast cell culture model of stepwise malignant transformation through overexpression of telomerase, large and small T antigen, and the H-Ras oncogene, increasing tumorigenicity correlates with sensitivity to glycolytic inhibition. This finding suggests that the Warburg effect might be inherent to the molecular events of transformation (Ramanathan et al., 2005). However, the introduction of similar defined factors into human mesenchymal stem cells (MSCs) revealed that transformation can be associated with increased dependence on oxidative phosphorylation (Funes et al., 2007). Interestingly, when introduced in vivo these transformed MSCs do upregulate glycolytic genes, an effect that is reversed when the cells are explanted and cultured under normoxic conditions. These contrasting models suggest that the Warburg effect may be context-dependent, in some cases driven by genetic changes and in others by the demands of the microenvironment. Regardless of whether the tumor microenvironment or oncogene activation plays a more important role in driving the development of a distinct cancer metabolism, it is likely that the resulting alterations confer adaptive, proliferative, and survival advantages on the cancer cell.

**Altered metabolism provides substrates for biosynthetic pathways**

Although studies in cancer metabolism have largely been energy-centric, rapidly dividing cells have diverse requirements. Proliferating cells not only require ATP, but also nucleotides, fatty acids, membrane lipids, and proteins, and a reprogrammed metabolism may serve to support synthesis of macromolecules. Recent studies have shown that several steps in lipid synthesis are required for and may even actively promote tumorigenesis. Inhibition of ATP citrate lyase, the distal enzyme that converts mitochondrial-derived citrate into cytosolic acetyl coenzyme A, the precursor for many lipid species, prevents cancer cell proliferation and tumor growth (Hatzivassiliou et al., 2005). Fatty acid synthase, expressed at low levels in normal tissues, is upregulated in cancer and may also be required for tumorigenesis (reviewed in Menendez and Lupu, 2007). Furthermore, cancer cells may also enhance their biosynthetic capabilities by expressing a tumor-specific form of pyruvate kinase (PK), M2-PK. Pyruvate kinase catalyzes the third irreversible reaction of glycolysis, the conversion of phosphoenolpyruvate (PEP) to pyruvate. Surprisingly, the M2-PK of cancer cells is thought to be less active in the conversion of PEP to pyruvate and thus less efficient at ATP production (reviewed in Mazurek et al., 2005). A major advantage to the cancer cell, however, is that the glycolytic intermediates upstream of PEP might be shunted into synthetic processes. Recent work has found that the cancer-specific M2-PK causes an increase in the incorporation of glucose carbons into lipids and, expanding the connection between growth factor signaling and cancer metabolism, may be regulated by phosphotyrosine binding (Christofk et al., 2008a, b).

Making the building blocks of the cell, however, incurs an energetic cost and cannot fully explain the Warburg effect. Biosynthesis, in addition to causing an inherent increase in ATP demand in order to execute synthetic reactions, also causes a decrease in ATP supply as various glycolytic and Krebs cycle intermediates are diverted. Lipid synthesis, for example, requires the cooperation of glycolysis, the Krebs cycle, and the pentose phosphate shunt. Pyruvate must enter the mitochondria, avoid

conversion to lactate and then contribute to glycolysis-derived ATP. In addition, whereas increased biosynthesis may explain the glucose hunger of cancer cells, it cannot explain the increase in lactic acid production originally described by Warburg, suggesting that lactate must also result from the metabolism of non-glucose substrates. Recently, it has been demonstrated again that glutamine may be metabolized by the citric acid cycle in cancer cells and converted into lactate, producing NADPH for lipid biosynthesis and oxaloacetate for anaplerosis (DeBerardinis et al., 2007).

**Metabolic pathways regulate apoptosis**

In addition to involvement in proliferation, altered metabolism may promote another cancer-essential function: the avoidance of apoptosis. Loss of the p53 target TIGAR sensitizes cancer cells to apoptosis, most likely by causing an increase in reactive oxygen species (Bensaad et al., 2006). On the other hand, overexpression of glyceraldehyde-3-phosphate dehydrogenase (GAPDH) prevents caspase-independent cell death, presumably by stimulating glycolysis, increasing cellular ATP levels, and promoting autophagy (Colell et al., 2007). Whether or not GAPDH plays a physiological role in the regulation of cell death remains to be determined.

Intriguingly, Bonnet et al. (2007) have reported that treating cancer cells with dichloroacetate (DCA), a small molecule inhibitor of pyruvate dehydrogenase kinase, has striking effects on their survival and on xenograft tumor growth. DCA, a currently approved treatment for congenital lactic acidosis, activates oxidative phosphorylation and promotes apoptosis by two mechanisms. First, increased flux through the electron transport chain causes depolarization of the mitochondrial membrane potential (which the authors found to be hyperpolarized specifically in cancer cells) and release of the apoptotic effector cytochrome c. Second, an increase in reactive oxygen species generated by oxidative phosphorylation upregulates the voltage-gated K+ channel, leading to potassium ion efflux and caspase activation. Their work suggests that cancer cells may shift their metabolism to glycolysis in order to prevent cell death and that forcing cancer cells to respire aerobically can counteract this adaptation. Although

this preliminary work has prompted some cancer patients to self-medicate with DCA, a controlled clinical trial will be essential to demonstrate unequivocally the safety and efficacy of DCA as an anti-cancer agent.

**Cancer cells may signal locally in the tumor microenvironment**

Cancer cells may rewire metabolic pathways to exploit the tumor microenvironment and to support cancer-specific signaling. Without access to the central circulation, it is possible that metabolites can be concentrated locally and reach suprasystemic levels, allowing cancer cells to engage in metabolite-mediated autocrine and paracrine signaling that does not occur in normal tissues. So-called androgen-independent prostate cancers may only be independent from exogenous, adrenal-synthesized androgens. Androgen-independent prostate cancer cells still express the androgen receptor and may be capable of autonomously synthesizing their own androgens (Stanbrough et al., 2006).

Perhaps the more provocative but as yet untested idea is that metabolites in the diffusion-limited tumor microenvironment could be acting as paracrine signaling molecules. Traditionally thought of as a glycolytic waste product, lactate may be one such signal. As noted above, it has been found that inhibition of lactate dehydrogenase can block tumor growth, most likely by multiple mechanisms. Much of the evidence for lactate as a multifunctional metabolite comes from work in exercise physiology and muscle metabolism (reviewed in Philp et al., 2005). Transported by several monocarboxylate transporters, lactate may be shared and metabolized among cells, although the idea is still controversial (Hashimoto et al., 2006; Yoshida et al., 2007). The interconversion of lactate and pyruvate might alter the NAD+/NADH ratio in cells, and lactate exchange may serve to coordinate the metabolism of a group of cells. The tumor-stroma interaction may therefore have a metabolic component to it (Koukourakis et al., 2006). Cancer cells respond cell-autonomously to hypoxia to initiate angiogenesis, and so it would be exciting if a metabolite such as lactate could positively amplify this angiogenic program, a process that requires a semi-coordinated effort among multiple

cells. Indeed, acidosis often precedes angiogenesis, and lactate may stimulate HIF expression independently of hypoxia (Fukumura et al., 2001; Lu et al., 2002; Shi et al., 2001). Cancer cells, by participating in a kind of quorum sensing and coordinating their metabolism, may therefore act as a pseudo-organ.

**Metabolism as an upstream modulator of signaling pathways**

Not only is metabolism downstream of oncogenic pathways, but an altered upstream metabolism may affect the activity of signaling pathways that normally sense the state of the cell. Individuals with inherited mutations in succinate dehydrogenase and fumarate hydratase develop highly angiogenic tumors, not unlike those exhibiting loss of the VHL tumor suppressor protein that acts upstream of HIF (reviewed in Kaelin and Ratcliffe, 2008). The mechanism of tumorigenesis in these cancer syndromes is still contentious. However, it has been proposed that loss of succinate dehydrogenase and fumarate hydratase causes an accumulation of succinate or fumarate, respectively, leading to inhibition of the prolyl hydroxylases that mark HIF for VHL-mediated degradation (Isaacs et al., 2005; Pollard et al., 2005; Selak et al., 2005). In this rare case, succinate dehydrogenase and fumarate hydratase are acting as bona fide tumor suppressors.

Mutations in metabolic genes, however, need not be a cancer-causing event. More subtly, the activation of various metabolic pathways might modulate the activity of downstream pro-cancer factors. Whereas it is well-accepted that growth factor signaling is commonly dysregulated in cancer, the involvement of nutrient or energy signaling in cancer remains unclear. In prokaryotes, various metabolites are sensed directly by the signaling machinery. The mammalian pathways that respond to energy and nutrient status may also interface with metabolites directly. It is well established that AMP-kinase senses the ATP/AMP ratio, and it has been proposed that mTOR (the mammalian target of rapamycin) may sense amino acid concentrations through an as yet unclear mechanism (reviewed in Guertin and Sabatini, 2007; reviewed in Hardie, 2007). Both AMP-kinase and mTOR have been linked to tumor syndromes. It is possible that one

way to upregulate these pro-growth signaling pathways is to increase the levels of the normal metabolites that they sense.

**Metabolism upregulation generates toxic byproducts**

Although altered metabolism confers several advantages on the cancer cell, it does not come without disadvantages. As a consequence of a deranged or simply overactive metabolism, cancer cells may be burdened with toxic byproducts that require disposal. So far, there is relatively little evidence for this hypothesis in the existing literature, but a few examples do suggest that cancer cells require detoxification mechanisms to maintain survival. Although there are enzymes that detoxify exogenous toxins, several "house-cleaning" enzymes, a term coined from studies in bacteria, deal with endogenous toxic metabolites (reviewed in Galperin et al., 2006). The best example of "house-cleaning" enzymes are the NUDIX (non-canonical nucleoside diphosphate linked to some other moiety X) hydrolases, a family of enzymes that act on the nucleotide pool and remove non-canonical nucleoside triphosphates. When incorporated into the DNA, these aberrant nucleotides can lead to mismatches, mutations, and eventually cell death. The dUTP pyrophosphatase (DUT), which hydrolyzes dUTP to dUMP and prevents the incorporation of uracils into DNA, may play a role in resistance to thymidylate synthase inhibitors. Suppression of DUT sensitizes some cancer cells to pyrimidine antimetabolites, suggesting that inhibition of these cellular house-cleaning enzymes may be an effective adjunct chemotherapeutic strategy (Koehler and Ladner, 2004).

The lactate production associated with the shift to a glycolytic metabolism is thought to contribute to the acidification of the microenvironment. Able to adapt to and even benefit from an acidic environment, cancer cells have been shown to upregulate vacuolar H+-ATPases, Na+-H+ antiporters, and H+-linked monocarboxylate transporters (reviewed in Gatenby and Gillies, 2004). Inhibition of these adaptive mechanisms leads to decreased viability of cancer cells and increased sensitivity to chemotherapeutic agents (reviewed in Fais et al., 2007; Fang et al., 2006).

**Uncharted territory**

Many mysteries remain unsolved in our understanding of even normal human metabolism let alone that of cancer cells. The metabolic pathways of the mammalian cell and their many interconnections are incomplete, as many enzymes remain unannotated in the human genome. Although we have guesses by homology, the identities of the human enzymes that catalyze reactions we know must occur are still elusive. In addition to annotating all human metabolic genes, the "ins" and the "outs" (i.e. the metabolites that enter and exit cells) should be measured and catalogued. It is also entirely unclear what percentage of the cellular fuel is normally used for ATP generation, biosynthesis, or other processes. And with few exceptions surprisingly little is known about intercellular metabolism. Much of our understanding of metabolism has been inherited from work in simple organisms; the compartmental nature of human metabolism is an exciting area of potential exploration.

Although aerobic glycolysis is the most characterized, although still puzzling, metabolic phenomenon in cancer, many other aspects of cancer metabolism are likely to be derangements of normal metabolism and ought to be elucidated. The nutrient conditions of the tumor microenvironment have not yet been carefully examined. Cancer cells, despite engaging in energy-costly processes, must still be able to maintain ATP levels, by relying either on increased flux through glycolysis or utilizing a diversity of fuel sources. Several explanations exist as to why a fraction of tumors are refractory to imaging by FDG-PET. One possibility is that certain cancer cells may not be primarily glucose-metabolizers but may rely on alternative fuel sources, the detailed characterization of which may lead to the detection and inhibition of "PET-negative" tumors. Furthermore, there are more complex questions to be answered: Is it possible that cancer cells exhibit "metabolite addiction?" Are there unique cancer-specific metabolic pathways, or combinations of pathways, utilized by the cancer cell but not by normal cells? Are different stages of metabolic adaptations required for the cancer cell to progress from the primary tumor stage to invasion to metastasis? How malleable is

cancer metabolism?

From a therapeutic perspective, knowledge of the causes, benefits, and vulnerabilities of cancer cell metabolism will enable the identification of new drug targets and will facilitate the design of metabolite mimetics that are uniquely taken up by a cancer cell or converted into the active form by enzymes upregulated in cancer cells. Profiling of either metabolites or enzymatic activities may allow us to develop diagnostic tests of cancer, and metabolite derivatives can be used for the molecular imaging of cancer, as exemplified by FDG-PET. We find the possibility of a new class of cancer therapeutics and diagnostic tools especially exciting. Therefore, we emphasize the need to explore beyond a glucose and energy-centric driven model of cancer metabolism to a broader one that encompasses all of the metabolic needs of a cancer cell. Perhaps it is time to step out from under Warburg's shadow.

**Figure 1**

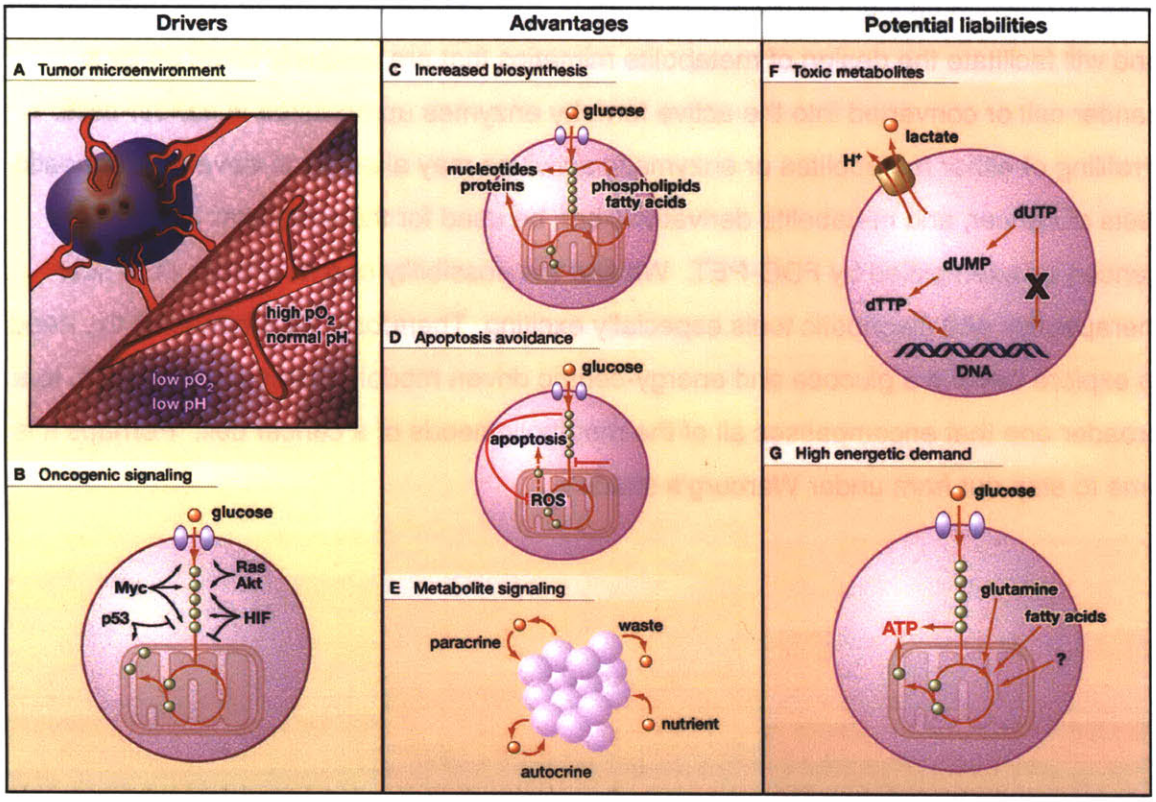
Drivers
Advantages
Potential liabilities
A Tumor microenvironment
high $pO_2$
normal pH
low $pO_2$
low pH
B Oncogenic signaling
glucose
Ras
Akt
Myc
p53
HIF
C Increased biosynthesis
glucose
nucleotides
proteins
phospholipids
fatty acids
D Apoptosis avoidance
glucose
apoptosis
ROS
E Metabolite signaling
paracrine
waste
nutrient
autocrine
F Toxic metabolites
lactate
$H^+$
dUTP
dUMP
dTTP
X
DNA
G High energetic demand
glucose
glutamine
fatty acids
ATP
?

**Figure 1. The altered metabolism of cancer cells.**

Drivers (A, B). Metabolic derangements in cancer cells may arise either from the selection of cells that have adapted to the tumor microenvironment or from aberrant signaling due to oncogene activation. The tumor microenvironment is spatially and temporally heterogeneous, containing regions of low oxygen and low pH (purple). Moreover, many canonical cancer-associated signaling pathways induce metabolic reprogramming. Target genes activated by hypoxia-inducible factor (HIF) decrease the dependence of the cell on oxygen, whereas Ras, Myc, and Akt increase glucose consumption and glycolysis. Loss of p53 may also recapitulate the features of the Warburg effect, that is, the uncoupling of glycolysis from oxygen levels.

Advantages (C-E). The altered metabolism of cancer cells is likely to imbue them with several proliferative and survival advantages, such as enabling cancer cells to execute the biosynthesis of macromolecules (C), to avoid apoptosis (D), and to engage in local metabolite-based paracrine and autocrine signaling (E).

Potential Liabilities (F-G). This altered metabolism, however, may also confer several vulnerabilities on cancer cells. For example, an upregulated metabolism may result in the build up of toxic metabolites, including lactate and non-canonical nucleotides, which must be disposed of (F). Moreover, cancer cells may also exhibit a high energetic demand, for which they must either increase flux through normal ATP-generating processes, or else rely on an increased diversity of fuel sources (G).

## References

Bensaad, K., Tsuruta, A., Selak, M. A., Vidal, M. N., Nakano, K., Bartrons, R., Gottlieb, E., and Vousden, K. H. (2006). Cell 126, 107-120.

Bonnet, S., Archer, S. L., Allalunis-Turner, J., Haromy, A., Beaulieu, C., Thompson, R., Lee, C. T., Lopaschuk, G. D., Puttagunta, L., Harry, G., et al. (2007). Cancer Cell 11, 37-51.

Christofk, H. R., Vander Heiden, M. G., Harris, M. H., Ramanathan, A., Gerszten, R. E., Wei, R., Fleming, M. D., Schreiber, S. L., and Cantley, L. C. (2008a). Nature 452, 230-233.

Christofk, H. R., Vander Heiden, M. G., Wu, N., Asara, J. M., and Cantley, L. C. (2008b). Nature 452, 181-186.

Colell, A., Ricci, J. E., Tait, S., Milasta, S., Maurer, U., Bouchier-Hayes, L., Fitzgerald, P., Guio-Carrion, A., Waterhouse, N. J., Li, C. W., et al. (2007). Cell 129, 983-997.

Dang, C. V., and Semenza, G. L. (1999). Trends Biochem Sci 24, 68-72.

DeBerardinis, R. J., Mancuso, A., Daikhin, E., Nissim, I., Yudkoff, M., Wehrli, S., and Thompson, C. B. (2007). Proc Natl Acad Sci U S A 104, 19345-19350.

Fais, S., De Milito, A., You, H., and Qin, W. (2007). Cancer Res 67, 10627-10630.

Fang, J., Quinones, Q. J., Holman, T. L., Morowitz, M. J., Wang, Q., Zhao, H., Sivo, F., Maris, J. M., and Wahl, M. L. (2006). Mol Pharmacol 70, 2108-2115.

Fantin, V. R., St-Pierre, J., and Leder, P. (2006). Cancer Cell 9, 425-434.

Fukumura, D., Xu, L., Chen, Y., Gohongi, T., Seed, B., and Jain, R. K. (2001). Cancer Res 61, 6020-6024.

Funes, J. M., Quintero, M., Henderson, S., Martinez, D., Qureshi, U., Westwood, C., Clements, M. O., Bourboulia, D., Pedley, R. B., Moncada, S., and Boshoff, C. (2007). Proc Natl Acad Sci U S A 104, 6223-6228.

Galperin, M. Y., Moroz, O. V., Wilson, K. S., and Murzin, A. G. (2006). Mol Microbiol 59, 5-19.

Gatenby, R. A., and Gillies, R. J. (2004). Nat Rev Cancer 4, 891-899.

Gordan, J. D., Thompson, C. B., and Simon, M. C. (2007). Cancer Cell 12, 108-113.

Guertin, D. A., and Sabatini, D. M. (2007). Cancer Cell 12, 9-22.

Hardie, D. G. (2007). Nat Rev Mol Cell Biol 8, 774-785.

Hashimoto, T., Hussien, R., and Brooks, G. A. (2006). Am J Physiol Endocrinol Metab 290, E1237-1244.

Hatzivassiliou, G., Zhao, F., Bauer, D. E., Andreadis, C., Shaw, A. N., Dhanak, D., Hingorani, S. R., Tuveson, D. A., and Thompson, C. B. (2005). Cancer Cell 8, 311-321.

Isaacs, J. S., Jung, Y. J., Mole, D. R., Lee, S., Torres-Cabala, C., Chung, Y. L., Merino, M., Trepel, J., Zbar, B., Toro, J., et al. (2005). Cancer Cell 8, 143-153.

Kaelin, W. G., Jr., and Ratcliffe, P. J. (2008). Mol Cell 30, 393-402.

Kawauchi, K., Araki, K., Tobiume, K., and Tanaka, N. (2008). Nat Cell Biol 10, 611-618.

Koehler, S. E., and Ladner, R. D. (2004). Mol Pharmacol 66, 620-626.

Koukourakis, M. I., Giatromanolaki, A., Harris, A. L., and Sivridis, E. (2006). Cancer Res 66, 632-637.

Lu, H., Forbes, R. A., and Verma, A. (2002). J Biol Chem 277, 23111-23115.

Manning, B. D., and Cantley, L. C. (2007). Cell 129, 1261-1274.

Matoba, S., Kang, J. G., Patino, W. D., Wragg, A., Boehm, M., Gavrilova, O., Hurley, P. J., Bunz, F., and Hwang, P. M. (2006). Science 312, 1650-1653.

Mazurek, S., Boschek, C. B., Hugo, F., and Eigenbrodt, E. (2005). Semin Cancer Biol 15, 300-308.

Menendez, J. A., and Lupu, R. (2007). Nat Rev Cancer 7, 763-777.

Philp, A., Macdonald, A. L., and Watt, P. W. (2005). J Exp Biol 208, 4561-4575.

Pollard, P. J., Briere, J. J., Alam, N. A., Barwell, J., Barclay, E., Wortham, N. C., Hunt, T., Mitchell, M., Olpin, S., Moat, S. J., et al. (2005). Hum Mol Genet 14, 2231-2239.

Ramanathan, A., Wang, C., and Schreiber, S. L. (2005). Proc Natl Acad Sci U S A 102, 5992-5997.

Selak, M. A., Armour, S. M., MacKenzie, E. D., Boulahbel, H., Watson, D. G., Mansfield, K. D., Pan, Y., Simon, M. C., Thompson, C. B., and Gottlieb, E. (2005). Cancer Cell 7, 77-85.

Shi, Q., Le, X., Wang, B., Abbruzzese, J. L., Xiong, Q., He, Y., and Xie, K. (2001). Oncogene 20, 3751-3756.

Shim, H., Dolde, C., Lewis, B. C., Wu, C. S., Dang, G., Jungmann, R. A., Dalla-Favera, R., and Dang, C. V. (1997). Proc Natl Acad Sci U S A 94, 6658-6663.

Stanbrough, M., Bubley, G. J., Ross, K., Golub, T. R., Rubin, M. A., Penning, T. M., Febbo, P. G., and Balk, S. P. (2006). Cancer Res 66, 2815-2825.

Warburg, O. (1956). Science 124, 269-270.

Wiesener, M. S., Munchenhagen, P. M., Berger, I., Morgan, N. V., Roigas, J., Schwiertz, A., Jurgensen, J. S., Gruber, G., Maxwell, P. H., Loning, S. A., et al. (2001). Cancer Res 61, 5215-5222.

Yoshida, Y., Holloway, G. P., Ljubicic, V., Hatta, H., Spriet, L. L., Hood, D. A., and Bonen, A. (2007). J Physiol 582, 1317-1335.

Zhong, H., De Marzo, A. M., Laughner, E., Lim, M., Hilton, D. A., Zagzag, D., Buechler, P., Isaacs, W. B., Semenza, G. L., and Simons, J. W. (1999). Cancer Res 59, 5830-5835.